THE EVALUATION OF NOVEL ANTI-INFLAMMATORY COMPOUNDS IN CELL CULTURE AND EXPERIMENTAL ARTHRITIS AND IDENTIFICATION OF AN INHIBITOR TO EARLY-STAGE LOBLOLLY PINE SOMATIC EMBRYO GROWTH

A Thesis
Presented to
The Academic Faculty

by

Jacob Lucrezi

In Partial Fulfillment
of the Requirements for the Degree
Doctor of Philosophy in the
School of Chemistry and Biochemistry

Georgia Institute of Technology
December 2013

THE EVALUATION OF NOVEL ANTI-INFLAMMATORY COMPOUNDS IN CELL CULTURE AND EXPERIMENTAL ARTHRITIS AND IDENTIFICATION OF AN INHIBITOR TO EARLY-STAGE LOBLOLLY PINE SOMATIC EMBRYO GROWTH

Approved by:

Dr. Sheldon W. May, Advisor
School of Chemistry and Biochemistry
Georgia Institute of Technology

Dr. James C. Powers
School of Chemistry and Biochemistry
Georgia Institute of Technology

Dr. Donald Doyle
School of Chemistry and Biochemistry
Georgia Institute of Technology

Dr. Stanley H. Pollock
College of Pharmacy and Heath Sciences
Mercer University

Dr. Nicholas V. Hud
School of Chemistry and Biochemistry
Georgia Institute of Technology

Date Approved: 11-5-2013

For my parents, who instilled in me a love of reading and taught me to ask questions.

ACKNOWLEDGEMENTS

I wish to thank Dr. Sheldon W. May for his patience and encouragement during my time as a graduate student. I also wish to thank the other members of the May group, Dr. Elizabeth Cowan, Dr. Mike Foster, Dr. Charlie Oldham, and Dr. Di Wu, that I had the opportunity to meet and collaborate with. I would also like to thank Ms. Nadia Boguslavsky for her advice and help in the use of IBB core equipment. I wish to thank Mr. Thejas Hiremath and Ms. Mijung Om for putting their trust into me as a mentor.

I wish to thank my collaborators at Mercer University, Dr. Stanley Pollock, Dr. Diane Matesic, and Mr. Tim Burns for their help with animals and Western blots. I also wish to thank my collaborators from IPST, Dr. Jerry Pullman and Ms. Kylie Bucalo for their help with plant cell culture. I wish to thank my collaborators from BME, Dr. Niren Murthy, Dr. Chen-Yu Kao and Dr. Sungmun Lee, and Dr. David Wilson for their help with nanoparticles and especially Dr. David Wilson for introducing me to cell culture techniques. All of you contributed to this work and I am grateful for it. I would also like to thank my family and friends for their support.

TABLE OF CONTENTS

PART 2:

LIST OF TABLES

LIST OF FIGURES

LIST OF SYMBOLS AND ABBREVIATIONS

AOPHA	5-(Acetylamino)-4-oxo-6-phenyl-2-hexenoic acid
ASK1	Apoptosis signal-regulating kinase 1
CD4	Cluster of differentiation 4
COX	Cyclooxygenase
DMARDs	Disease-modifying antirheumatic drugs
DMEM	Dulbecco's modified Eagle's medium
DMSO	Dimethylsulfoxide
ERK	Extracellular signal-regulated kinases
ELISA	Enzyme-linked immunosorbent assay
FBS	Fetal bovine serum
FCA	Freund's complete adjuvant
FG	Female gametophyte
GPC	Gel permeation chromatography
HPLC	High performance liquid chromatography
HSP65	Heat shock protein 65
IL-1β	Interleukin 1 beta
IL-10	Interleukin 10
IL-12	Interleukin 12
Ins	*myo*-inositol
myo-$InsP_6$	*myo*-inositol-1,2,3,4,5,6-hexakisphosphate
muco-$InsP_6$	*muco*-inositol-1,2,3,4,5,6-hexakisphosphate
IRAK1	Interleukin-1 receptor-associated kinase-1

IRAK4	Interleukin-1 receptor-associated kinase-4
JAKs	Janus kinases
JNKs	c-Jun N-terminal kinases
LPS	Lipopolysaccharide
MAPKs	Mitogen-activated protein kinases
MTT	Dimethyl thiazolyl diphenyl tetrazolium salt
MTX	Methotrexate
NK	Neurokinin
NKA	Neurokinin A
NKB	Neurokinin B
NMR	Nuclear magnetic resonance
NSAIDs	Non-steroidal anti-inflammatory drugs
NO	Nitric oxide
PAI-1	Plasminogen activator inhibitor 1
PAM	Peptidylglycine β-monooxygenase
PBA	4-phenyl-3-butenoic acid
PCADK	Poly(cyclohexane-1,4-diyl acetone dimethylene ketal)
PKMs	PCADK microparticles
PGL	Peptidylamidoglycolate lyase
PLGA	Poly(lactic-co-glycolic acid)
PGE_2	Prostaglandin E2
PGI_2	Prostacyclin
PVDF	Polyvinylidene difluoride
RNA	Ribonucleic acid
SDS	Sodium lauryl sulfate

SE	Somatic embryogenesis
SEM	Scanning electron microscopy
SP	Substance P
SP-Gly	Substance P glycine-extended precursor
TXA_2	Thromboxane
TGF-β	Transforming growth factor beta
TNF-α	Tumor necrosis factor alpha
TLR4	Toll-like receptor 4
TRAF6	Tumor necrosis factor-receptor-associated factor-6

SUMMARY

The interactions between the immune and nervous systems play an important role in immune and inflammatory conditions. Substance P (SP), the unidecapeptide RPKPQQFFGLM-NH_2, is known to upregulate the production of pro-inflammatory cytokines such as tumor necrosis factor (TNF)-α. We report here that 5-(Acetylamino)-4-oxo-6-phenyl-2-hexenoic acid methyl ester (AOPHA-Me) and 4-phenyl-3-butenoic acid **(**PBA), two anti-inflammatory compounds developed in our laboratory, reduce SP-stimulated TNF-α expression in RAW 264.7 macrophages. We also show that AOPHA-Me and PBA both inhibit SP-stimulated phosphorylation of JNK and p38 MAPK. Furthermore, molecular modeling studies indicate that both AOPHA-Me and PBA dock at the ATP binding site of apoptosis signal-regulating kinase 1 (ASK1) with predicted docking energies of -7.0 kcal/mol and -5.9 kcal/mol, respectively; this binding overlaps with that of staurosporine, a known inhibitor of ASK1. Taken together, these findings support the conclusion that AOPHA-Me and PBA inhibition of TNF-α expression in SP-stimulated RAW 264.7 macrophages is a consequence of the inhibition JNK and p38 MAPK phosphorylation. We have previously shown that AOPHA-Me and PBA inhibit the amidative bioactivation of SP, which also would be expected to decrease formation of pro-inflammatory cytokines. It is conceivable that this dual action of inhibiting amidation and MAPK phosphorylation may be of some advantage in enhancing the anti-inflammatory activity of a therapeutic molecule.

We also encapsulated AOPHA-Me separately in polyketal and poly(lactic-co-glycolic acid) microparticles. The *in-vitro* release profiles of AOPHA-Me from these particles were characterized. We have also shown that AOPHA-Me, when encapsulated in PCADK microparticles, is an effective treatment for edema induced by adjuvant arthritis in rats.

In separate work, it was determined that *myo*-inositol-1,2,3,4,5,6-hexakisphosphate is an inhibitor to early-stage Loblolly pine somatic embryo growth. In addition, it was determined that *muco*-inositol-1,2,3,4,5,6-hexakisphosphate is not an inhibitor to early-stage Loblolly pine somatic embryo growth. These experiments demonstrate the stereochemical dependence of *myo*-inositol-1,2,3,4,5,6-hexakisphosphates inhibitory activity.

PART 1: EVALUATION OF NOVEL ANTI-INFLAMMATORY COMPOUNDS IN CELL CULTURE AND EXPERIMENTAL ARTHRITIS

CHAPTER 1

INTRODUCTION

General Aspects of Inflammation

Inflammation is an essential function of a healthy organism's immune system. During the inflammatory response the immune system becomes activated through toxic agents, injury or infection. By a complicated series of events, the pathogen and injured tissue is destroyed, and the immune system returns to its normal state (Serhan, Chiang et al. 2008).

The initial series of inflammatory events following invasion by a pathogen is depicted in Figure 1. Platelets begin to close the wound while mast cells release vasodilators which promote the recruitment of circulating neutrophils from the blood stream. Recognition of the pathogen by neutrophils and macrophages stimulates them to release cytokine signaling molecules which both promote the inflammatory response and signal for tissue repair. Neutrophils and macrophages also destroy pathogens by phagocytosis. Inflammation is associated with a set of symptoms whereby an affected area of the body becomes warm, red, swollen and painful. Although primarily beneficial, inflammation can become a life threatening condition and chronic inflammatory diseases can increase the severity of other diseases such as cancer (Shacter and Weitzman 2002).

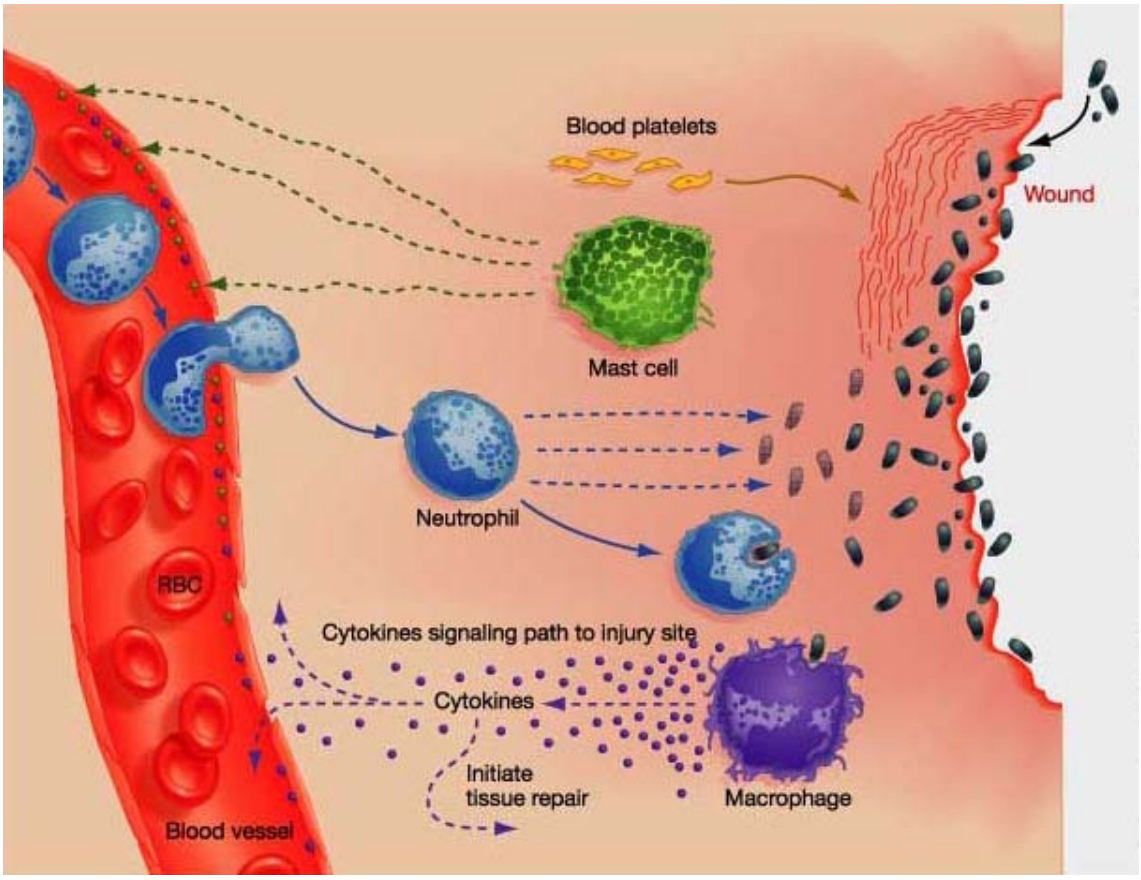

Figure 1. The initial responses of the immune system to invading pathogens as illustrated by http://www.uic.edu/classes/bios/bios100/lecturesf04am/lect23.htm.

Acute Inflammation

Acute inflammation is the temporary rapid response of the immune system to a stimulating agent, usually a pathogen. It is characterized by an increased presence of leukocytes (mainly macrophages and neutrophils), fluid, and plasma proteins at the site of stimulation (Serhan, Chiang *et al*. 2008). The movement of fluid, cells and proteins is facilitated by vasodilatation which is triggered by signaling molecules such as histamine and nitric oxide (Greaves and Sabroe 1996). Vascular permeability, allowing circulating cells to reach the site of stimulation, is stimulated by many signaling molecules including histamine and cytokines (Greaves and Sabroe 1996). Elimination of invading pathogens is achieved by phagocytosis and release of digestive enzymes and reactive oxygen species by leukocytes, such as macrophages and neutrophils (Serhan, Chiang *et al*. 2008). Digestive enzymes and reactive oxygen species are short-lived and their release only continues as long as the stimulation continues (Serhan, Chiang *et al*. 2008).

Resolution of acute inflammation occurs when the invading pathogen is eliminated, thereby removing stimulation. In addition the endogenous production of anti-inflammatory signaling molecules such as anti-inflammatory lipoxins, cytokines (IL-10), and growth factors (TGF-β) also contribute to the return to a non-inflammatory state (Serhan, Chiang *et al*. 2008). Resolution results in a return to normal vascular flow and permeability, termination of leukocyte migration, apoptosis of migrated neutrophils and removal of necrotic debris, accumulated fluid, and proteins (Serhan, Chiang *et al*. 2008).

Chronic Inflammation

When the inflammatory response persists for months or even years it becomes chronic. This is often either because an antigen cannot be cleared from the organism in a short period of time, such as in cancer, or from an improperly functioning immune system. Chronic inflammation is characterized by ongoing inflammation, tissue destruction and tissue repair (Buckley, Pilling *et al*. 2001).

Healthy normal tissue can be replaced by fibrous material during chronic inflammation. This occurs when healthy tissue is destroyed by the immune response. Growth factors and other stimulators for angiogenesis and fibroblasts are released resulting in scarring (Leask, Holmes et al. 2002; Auerbach, Lewis et al. 2003).

Lymphocytes are involved in a prolonged inflammatory state and they have a complex interaction with macrophages wherein both cell types activate each other (Macatonia, Hsieh *et al*. 1993). Antigen presenting cells, such as macrophages, display antigens on their surface after phagocytosis of foreign bodies. Macrophages produce and release IL-12 after antigen display thereby activating naïve T lymphocytes (Hsieh, Macatonia *et al*. 1993). Activated T lymphocytes activate macrophages by binding an antigen-displaying macrophage and releasing interferon gamma (Macatonia, Hsieh *et al*. 1993). Activated macrophages in turn release additional cytokines, which further activate T lymphocytes (Fearon and Locksley 1996).

Activated T helper lymphocytes induce antibody production by activating B lymphocytes which then produce antibodies. Antibodies then mark foreign bodies for phagocytosis. They also interfere with a bound pathogen's ability to function.

Inflammatory Diseases and Treatment

Inflammatory diseases are serious conditions in humans which often lead to a diminished quality of life and mortality. Among the most common and disabling diseases that are associated with chronic inflammation are atherosclerosis, tuberculosis, chronic lung diseases, and rheumatoid arthritis. Rheumatoid arthritis is responsible for affecting the lives of approximately 46 million adults in the United States (Cheng, Imperatore *et al*. 2012). The two most common classes of pharmaceuticals used to treat rheumatoid arthritis are non-steroidal anti-inflammatory drugs (NSAIDs) and disease-modifying antirheumatic drugs (DMARDs). Both classes of drugs are associated with sometimes fatal side effects. Therefore, there is a great need to develop new anti-inflammatory treatments.

NSAIDs, when taken chronically, are known to cause gastrointestinal and cardiovascular toxicity. The mortality rate in the United States from chronic use of NSAIDs is greater than the individual number of deaths resulting from multiple myeloma, asthma, cervical cancer, or Hodgkin's disease (Singh and Triadafilopoulos 1999). NSAIDs selective for COX-2 do not have the associated gastrointestinal toxicity that non-selective NSAIDs exhibit. However, due to their cardiovascular toxicity, the selective COX-2 inhibitors Vioxx and Bextra were removed from the US drug market. The FDA has issued a black box warning regarding the increased heart attack and stroke risk associated with the selective COX-2 inhibitors that remain on the market.

DMARDs are a diverse set of drugs that differ from NSAIDs in that they have the ability to modify the long-term progression of the disease. There are two main types of DMARDs: small molecules and biologicals. DMARDs are now the preferred treatment

for rheumatoid arthritis over the use of NSAIDs. Among the small molecule DMARDs, methotrexate, is the most widely used. Originally designed as a chemotherapy drug which inhibits the synthesis of folate, methotrexate was found to be effective in treatment of rheumatoid arthritis at lower doses. Methotrexate suppresses T-cell activation and adhesion molecule upregulation, and these effects are thought to explain its anti-inflammatory activity (Johnston, Gudjonsson *et al*. 2005).

Biological DMARDs are anti-inflammatory proteins made through genetic engineering that are synthesized by cells and harvested. For the treatment of rheumatoid arthritis, the most commonly prescribed class of biological agents are inhibitors of tumor necrosis factor alpha (TNF-α), a potent endogenous pro-inflammatory signaling molecule. There are two types of biological TNF-α inhibitor DMARDs. One type is composed of a monoclonal antibody against TNF-α and the other is composed of a circulating TNF-α receptor fusion protein. These drugs must be injected and are also associated with patients having severe susceptibility to infection, especially tuberculosis (Dixon, Hyrich *et al*. 2010). In addition, DMARDs are associated with a severe set of side effects which include hepatotoxicity, blood dyscrasias and interstitial lung disease (By, Scott *et al*. 2010).

Substance P

Substance P (SP), the unidecapeptide RPKPQQFFGLM-NH_2, is stored in nerve terminals and is a member of the tachykinin family of peptides, see Figure 2 (O'Connor, O'Connell *et al*. 2004).

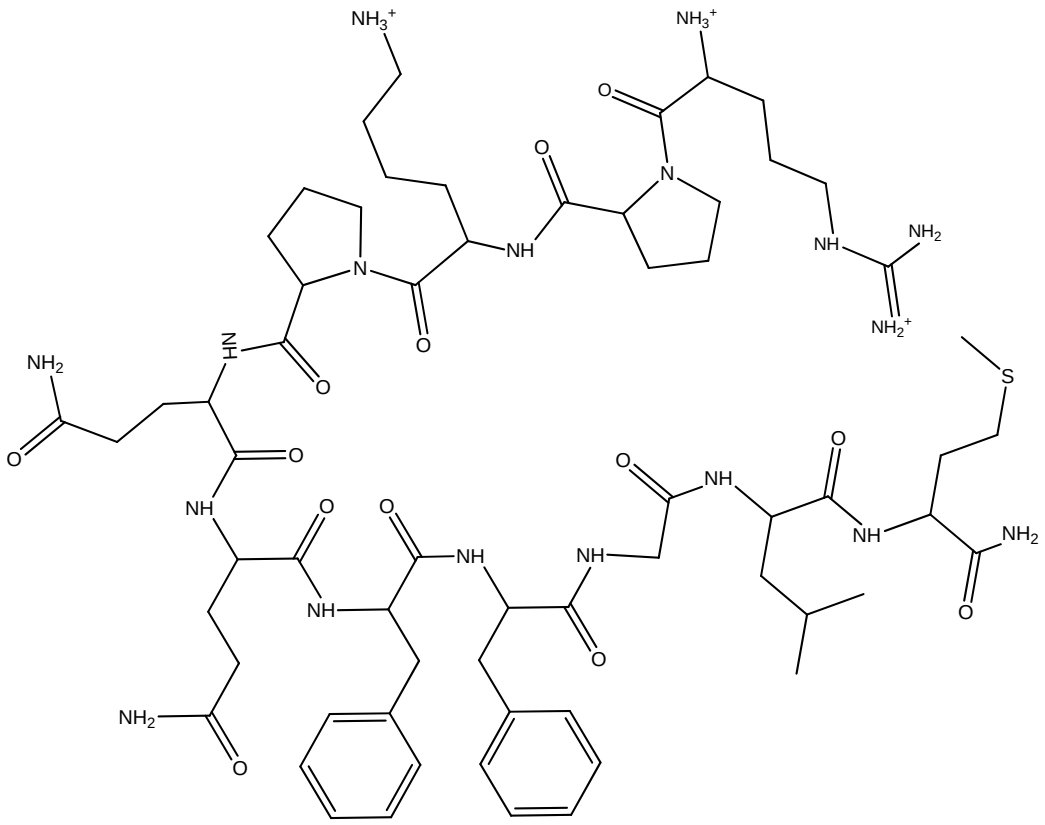

Figure 2. Structure of substance P.

Tachykinins are a group of structurally related peptide hormones found in invertebrates, fish, reptiles, amphibians, birds and mammals. Although once thought to be found exclusively in the nervous system, tachykinins and their receptors have now been reported in many cell types, such as human endothelial cells, human epithelial cells, and several human, mouse and rat immune cells (Pennefather, Lecci *et al*. 2004). The most studied mammalian tachykinins are SP, neurokinin A (NKA), and substance K (NKK). These peptides share the common C-terminal amino acid sequence Phe-X-Gly-Leu-Met-NH_2 (Chang, Leeman et al. 1971; Kangawa, Minamino et al. 1983; Nawa, Kotani et al. 1984; Tatemoto, Lundberg et al. 1985). However, the recently-discovered endokinin

tachykinins possess the C-terminal amino acid sequence of Phe-X-Gly-Leu-Leu-NH_2 (Zhang, Lu et al. 2000; Page, Bell et al. 2003).

Tachykinins transmit signals by binding to the neurokinin (NK) family of G protein-coupled cell surface receptors denoted NK-1R, NK-2R, and NK-3R. These NK receptors are characterized as possessing seven transmembrane helical domains, an intracellular C-terminal loop and an extracellular N-terminal loop. In mammals, SP is encoded by the preprotachykinin I gene which, through alternative splicing, also encodes NKA, NKK and the N-terminally extended forms of NKA (Nawa, Kotani et al. 1984; Carter and Krause 1990).

SP is released upon injury and mediates a number of functions relating to the inflammatory response. SP activity is relayed via binding to one of the three neurokinin receptors, with a preference for NK-1R. SP upregulates the production of nitric oxide, thereby increasing vasodilatation. SP also activates immune cells to produce pro-inflammatory cytokines such as TNF-α. Finally, SP also serves as a neurotransmitter for pain.

Amidation

SP requires an essential post-translational amidation modification to be able to interact with its NK receptors. Amidation is a common post-translational modification, and more than half of peptide hormones must be amidated in order to exhibit full biological activity (Yun, Johnson *et al*. 1993). This enzymatic process has been well characterized by our laboratory and by others.

As shown in Figure 3, amidation is a two step process whereby the SP glycine-extended precursor (SP-Gly) is first acted on by peptidylglycine β-monooxygenase (PAM), the rate-limiting enzyme in the pathway, to form an α-hydroxyglycine intermediate (Katopodis and May 1990). This step requires ascorbate, oxygen and copper as co-factors (Bradbury, Mistry *et al*. 1990). PAM activity is found in the serum and several tissues, such as the pituitary, the hypothalamus, the submandibular glands, and as well as in other parts of the brain (Eipper, Myers *et al*. 1985). Subsequently, peptidylamidoglycolate lyase (PGL) catalyzes the dealkylation of the α-hydroxyglycine intermediate to form the amidated peptide plus glyoxylic acid (Katopodis, Ping et al. 1990; Katopodis, Ping et al. 1991).

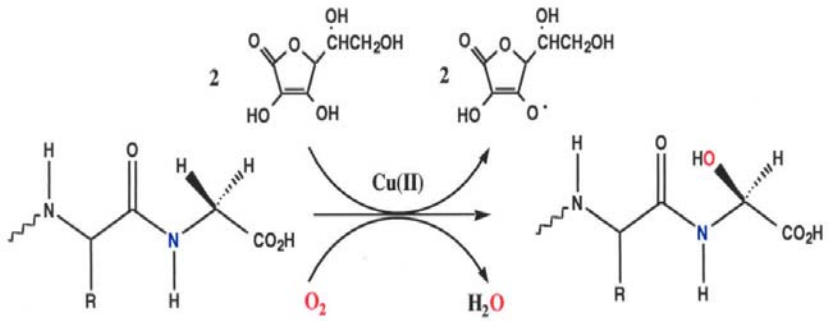

Peptidylglycine Monooxygenase
(PAM)

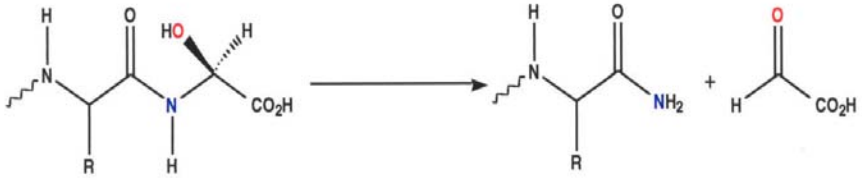

Peptidylamidoglycolate Lyase
(PGL)

Figure 3. The two sequential reactions of amidation are illustrated acting on a glycine-extended peptide.

Cytokines and Chemokines

Inflammation is controlled by a variety of signaling molecules often in a paracrine or autocrine fashion, as illustrated in Figure 4. Paracrine signaling is when a cell induces changes in nearby cells while autocrine signaling is when a cell induces changes in itself. These signaling molecules are found as precursors in the plasma and are both stored in cells and synthesized during inflammation. Signaling molecules exert their effect by binding cell surface receptors which can result in release of additional signaling molecules, production of cytotoxic compounds such as nitric oxide and changes in gene expression relating to host defense. Cytokines are a family of protein signaling molecules that modify the activity of other cells. During the inflammatory response they are most notably produced by activated immune cells such as macrophages and lymphocytes (Liles and Van Voorhis 1995). Pro-inflammatory cytokines activate leukocytes and induce the production and release of addition cytokines. Examples of proinflammatory cytokines include TNF-alpha and IL-12. Chemokines are a sub-family of cytokines that mainly act as chemoattractants for immune cells such as macrophages, mast cells, neutrophils, T-lymphocytes and eosinophils.

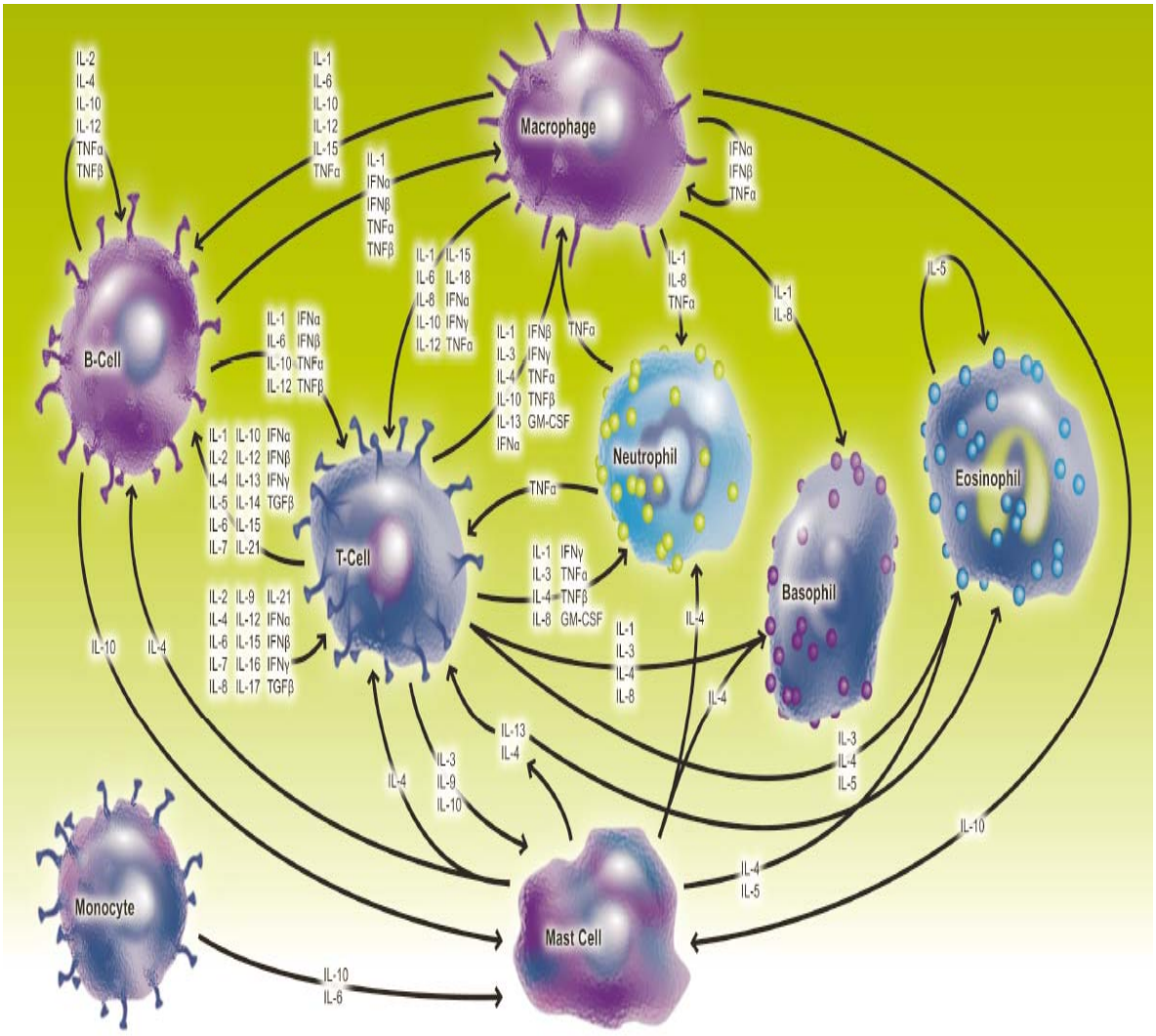

Figure 4. The autocrine and paracrine signaling network between immune cells with cytokines as illustrated by www.abcam.com.

TNF-α Signaling

TNF-α is a cytokine that produces complex and varied effects on cells. It regulates activities relating to lipid metabolism, coagulation, insulin resistance, and endothelial function (Baud and Karin 2001). TNF-α is a key signaling molecule in the inflammatory response and has been implicated in autoimmune diseases such as rheumatoid arthritis (Maini, Elliott *et al*. 1995), ankylosing spondylitis (Brandt, Haibel *et al*. 2000), and Crohn's disease (Derkx, Taminiau *et al*. 1993). TNF-α exerts its influence by binding to its receptor resulting in multiple signaling pathways being activated. Depending on what other signaling molecules a cell has interacted with, the binding of TNF-α can result in either cell death or cell proliferation. In the inflammatory state TNF-α usually does not signal for cell death because of the activation of the mitogen-activated protein kinase families (MAPKs) which suppress apoptosis through their downstream effectors.

MAPK Signaling

SP, LPS and cytokines such as TNF-α activate cytokine production via MAPK signaling (Azzolina, Guarneri *et al*. 2002). MAPKs are a family of proline-directed protein serine/threonine kinases which transmit signals from the surface of the cell to the nucleus via a cascade of intracellular phosphorylation events (Raman, Chen *et al*. 2007). There are four families of MAPKs, the most studied being extracellular signal-regulated kinases (ERKs), c-Jun N-terminal kinases (JNKs), and p38 MAPK; each family consists of three tiers of kinases where the MAPK is phosphorylated by a MAPK kinase (MKK)

which was phosphorylated by a MAPKK kinase (Raman, Chen *et al*. 2007). This process activates transcription factors such as NF-κB (Lieb, Fiebich *et al*. 1997), which in turn upregulates production of cytokines, such as TNF-α. A more detailed description of MAPK signaling is presented in the Discussion section.

SP Upregulation in Chronic Inflammation

There is a need to further understand the pro-inflammatory effects of SP in inflammatory diseases. It has been found that the SP concentration is raised in the synovial fluid of individuals with rheumatoid arthritis. Conversely, the SP concentration is depleted in the synovial tissue of these individuals. This raises the possibility that SP may be transferred from the tissue to the fluid during inflammation.

Elevated levels of SP have been observed in animal models of inflammation. The "gold standard" model for chronic inflammation in rats is adjuvant arthritis which has many similarities to human rheumatoid arthritis (Waksman 2002). Adjuvant arthritis is brought on by use of Freund's complete adjuvant (FCA), which consists of heat killed *Mycobaterium butyricum* suspended in mineral oil. A key antigen present in the mycobacterium is heat shock protein 65 (HSP65) (Van 1990). It is hypothesized that due to the conserved nature of heat shock proteins, the antibodies produced against HSP65 are cross-reactive with proteins found in the host, leading to spontaneous autoimmune arthritis. FCA is injected into one hindpaw in the subplantar region (Szekanecz, Halloran *et al*. 2000). This results in a three-phase response to the antigen HSP65 . The first phase is comprised of acute inflammation of the injected hindpaw, which reaches a maximum on day 2. During this phase T-lymphocytes recognize, and are activated by,

the presence of HSP65. The second phase occurs during days 2 through 10, where swelling remains constant but the population of activated lymphocytes for HSP65 grows. After day 10, the third phase begins with a massive cell-mediated response that causes further swelling of the injected hindpaw in addition to systemic inflammation of the other three limbs. SP is upregulated during this process, with increased levels being found in the dorsal root ganglia and in the sciatic nerves (Kar, Gibson et al. 1991; Donnerer, Schuligoi et al. 1992).

LPS Signaling

In bacterial infections, endotoxins are released when bacteria die. Large quantities of endotoxins can induce septic shock in patients by triggering a massive inflammatory response. Lipospollysacharide (LPS) is the prototypical endotoxin since it is also a component of the cell walls of gram negative bacteria. Cells exposed to LPS generate NO and cytokines such at TNF-α following a complicated series of events where cell signaling pathways are activated. LPS first complexes with LPS-binding protein which delivers LPS to the CD14 receptor, and this receptor then ultimately delivers LPS to the cell surface toll-like receptor 4 (TLR4) (Beutler 2004). LPS binding to TLR4 activates the myeloid differentiation primary-response protein-88 to recruit interleukin-1 receptor-associated kinase-1 (IRAK1) and IRAK4. IRAK4 then phosphorylates IRAK1. Phosphorylated IRAK1 then associates with tumor necrosis factor-receptor-associated factor-6 (TRAF6), TGF-β-activated kinase-1, TAK1-binding protein-1 and TAK1-binding protein-2. The complex of IRAK1, TRAF6, TGF-β-activated kinase-1, TAK1-binding protein-1 and TAK1-binding protein-2 phosphorylates TGF-β-activated

kinase-1 and TAK1-binding protein-2. This complex then associates with ubiquitin ligases UbC13 leading to ubiquitylation of TRAF6. This leads to TAK1-binding protein-2 being activated which then activates the JNK and p38 MAPK families leading to cytokine and NO upregulation.

Nanoparticle Drug Delivery

The delivery of a drug via encapsulation in nanoparticles composed of polymers can offer many advantages compared to traditional drug delivery methods (Heifts 2005). Nanoparticles can exhibit high stability, the ability to accept drugs of varying polarity, and the ability to be delivered by various types of administration. Nanoparticles can also exhibit sustained release of an encapsulated drug. Furthermore by incorporating ligands, such as peptides or RNA, on the surface of the nanoparticles it is possible to target nanoparticles to specific cells that interact with these ligands.

Poly(cyclohexane-1,4-diyl acetone dimethylene ketal) (PCADK) is a new polymer for nanoparticle formation, (Lee, Yang *et al*. 2007). PCADK is notable for being acid liable due to ketal linkages forming part of the polymer backbone. PCADK nanoparticles are hypothesized to be readily taken up by macrophages where they will rapidly hydrolyzed when exposed to the acidic environment of the phagosome. This hydrolysis releases the encapsulated drug within the PCADK, thus effectively delivering the drug to macrophages. When treating an inflammatory disease the ability to target a drug to macrophages is advantageous because of the key role macrophages play in the inflammatory process.

PBA and AOPHA

Both rationally designed substrates and inhibitors of PAM have been designed in this laboratory (see Figure 5). 5-(Acetylamino)-4-oxo-6-phenyl-2-hexenoic acid (AOPHA) and 4-phenyl-3-butenoic acid (PBA) are turnover-dependent inhibitors of amidating enzyme (Bradbury, Mistry et al. 1990; Katopodis and May 1990; Feng, Shi et al. 2000). In-vivo inhibition of PAM should inhibit the conversation of SP-Gly to the amidated product, SP. By inhibiting the synthesis of SP, it is hypothesized that these compounds will exhibit anti-inflammatory activity.

Indeed, work in our laboratory has established that AOPHA-Me and PBA both exhibit anti-inflammatory activity. In animal models of acute and chronic inflammation, these compounds reduced edema via a non-COX inhibitory pathway (Ogonowski, May et al. 1997; Bauer, Sunman et al. 2007). AOPHA-Me, when dosed via intraperitoneal injection, completely inhibits edema resulting from carrageenan-induced acute inflammation in rats (Figure 6). In addition, PBA inhibits JNK and activates p38 MAPK in both ras transformed WB and human lung carcinoma cells (Matesic, Sidorova *et al*. 2011).

However, results from the animal work also suggested that these compounds may possess anti-inflammatory activity not related to their function as amidation inhibitors. To gain further understanding of their activities we investigated the effect of AOPHA-Me and PBA in RAW 264.7 macrophage cell culture on pro-inflammatory signaling pathways.

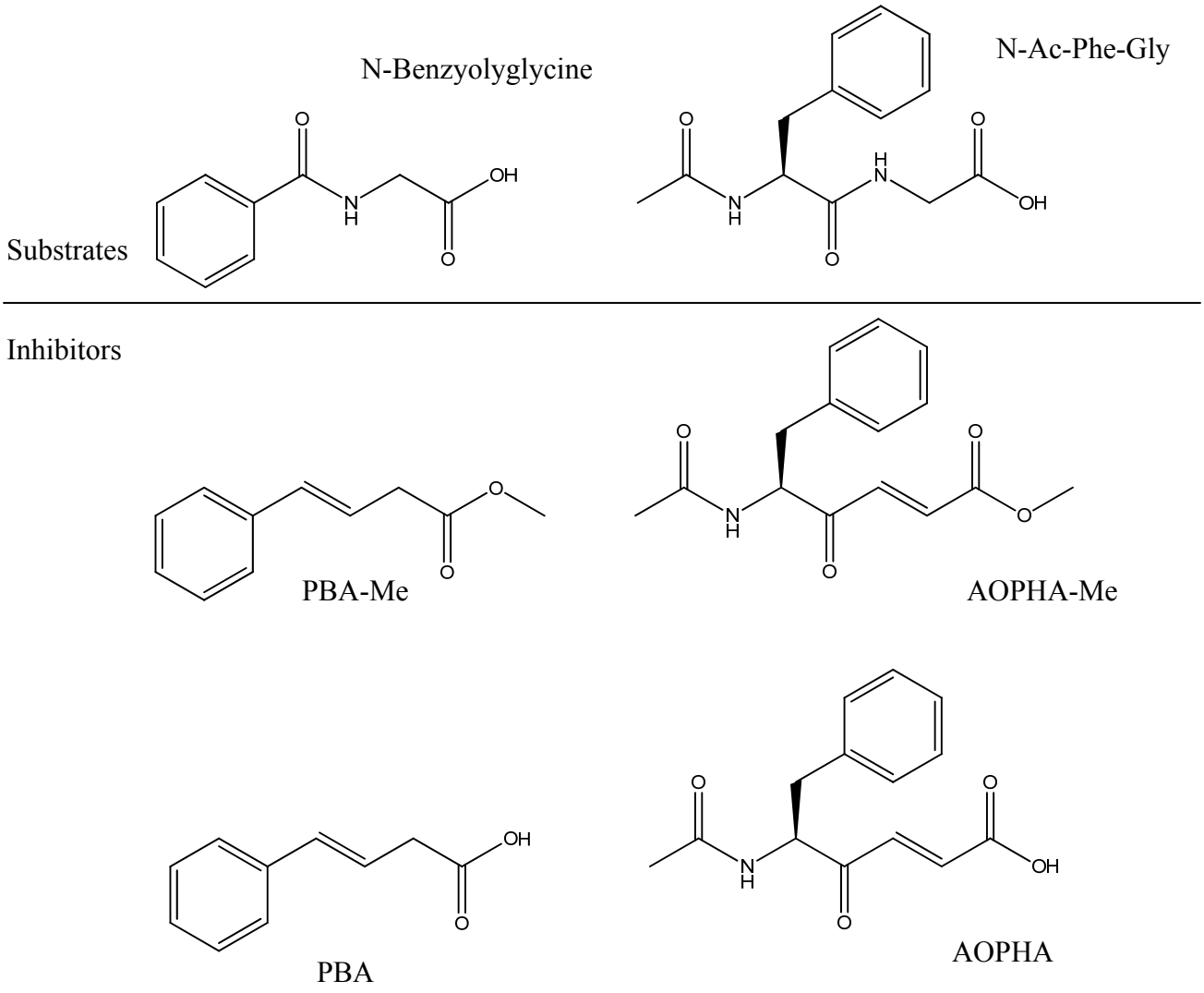

Figure 5. Molecular structures of N- benzyolyglycine, N-Ac-Phe-Gly, PBA, PBA-Me, AOPHA and AOPHA-Me.

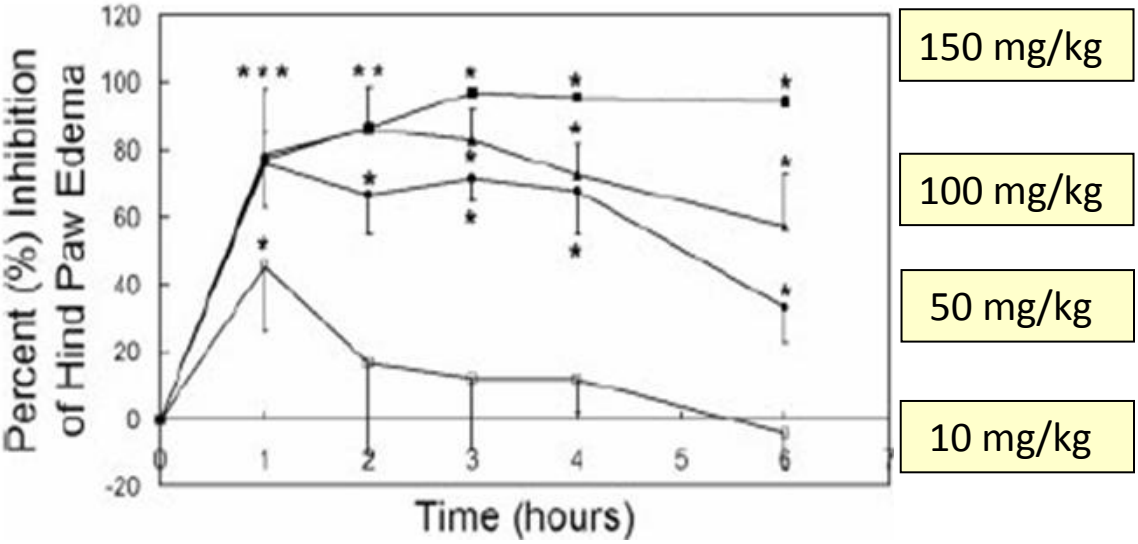

Figure 6. AOPHA-Me reduces carrageenan-induced edema in rats in a dose dependent manner. Rats were injected with 10-150 mg/kg of AOPHA-Me and the hind paw volumes were recorded at the indicated times after injection with carrageenan.

CHAPTER 2

MATERIALS AND METHODS

Instruments

Experiments were performed with a Shimadzu HPLC system (Kyoto, Japan), a HITACHI S-800 scanning electron microscope (Tokyo, Japan), a LEO-1530 scanning electron microscope (Tokyo, Japan), a Varian Mercury VX 400 MHz NMR spectrometer (Palo Alto, CA) and a Micromass Quattro mass spectrometer (Milford, MA).

Materials

RAW 264.7 cells were purchased from ATCC (Bethesda, MD). SP, PBA, cell culture grade quality MTT and DMSO were purchased from Sigma-Aldrich (St. Louis, MO). Cell culture quality Pen/Strep, DMEM, PBS and bicarbonate were purchased from Cellgro. FBS (≤ 5 EU/mL) was purchased from Gibco (Grant Island, NY). TNF-α ELISA kits were purchased from e-Bioscience (San Diego,CA). Phospho-p38 MAP kinase (Thr180/Tyr182) polyclonal antibody, p38 MAP kinase polyclonal antibody, JNK polyclonal antibody, phospho-JNK (Thr183/Tyr185) polyclonal antibody, and anti-rabbit IgG alkaline phosphataseconjugated antibody were purchased from Cell Signaling Technology (Beverly, MA). Tween-20, TRIS–HCl, DC Protein Assay, SDS, nonfat dry milk, 25X alkaline phosphatase color development buffer, 5-bromo-4-chloro-3-indolyl phosphate/nitroblue tetrazolium (BCIP/NBT), protein molecular mass standards, and all electrophoresis and transfer buffer components were from Bio-Rad (Hercules, CA).

Syntheses

AOPHA-Me was synthesized by the established multi-step synthesis developed in our laboratory (see Figure 7). (L)-Phe-OEt is converted to N-Ac-(L)-Phe-OEt which is converted to N-Ac-(L)-Phe-α-ketophosphonate which is reacted with methyl gloxylate to form AOPHA-Me (Feng 2000; Foster 2010). The individual reactions are described below.

N-Ac-(L)-Phe-OEt

11.0 mL of acetic anhydride and 9.5 mL of pyridine were used to dissolve 5 g of (L)-Phe-OEt and 100 mg p-toluenesulfonic acid. After running overnight the reaction was quenched with 100 mL of cold water and ice. This reaction mixture was extracted four times with 25 mL of methylene chloride. The pooled organic extracts were rinsed three times each with 25 mL of 0.1 HCl, water and then saturated sodium bicarbonate. The rinsed organic extracts were then dried over magnesium sulfate, filtered and evaporated to dryness under reduced pressure yielding 4.8 g of N-Ac-(l)-Phe-OEt as a white solid. ^{1}H NMR ([^{2}H]chloroform): δ 1.25 (t, 3H), δ 1.97 (s, 3H), δ 3.13 (q, 2H), δ 4.16 (q, 2H), δ 4.87 (m, 1H), δ 5.90 (broad, 1H), δ 7.09 (m, 2H), δ 7.27 (m, 3H).

N-Ac-(L)-Phe-α-ketophosphonate

50 mL of tetrahydrofuran, dried over sodium metal, was used to dissolve 4.7 g of N-Ac-(L)-Phe-OEt. In a separate three-neck flask, kept under argon at -78° C in a dry ice and acetone bath, 4.4 mL dimethylmethylphosphante was dissolved in 50 mL of

tetrahydrofuran that had been dried over sodium metal. Through the use of an addition funnel, 16.5 mL of 2.5 M n-BuLi in hexanes was added dropwise over 30 minutes to the dimethylmethylphosphante. A white precipitate appeared during the addition and then disappeared after 15-30 minutes. After the precipitate disappeared, the dissolved N-Ac-(l)-Phe-OEt was added to the reaction mixture. The reaction was allowed to proceed overnight and gradually come to room temperature. The next morning 100 mL of cold water was used to quench the reaction. The solution was then rinsed twice with 50 mL of diethyl ether. The aqueous phase was retained, and its pH was lowered to 1.0 by the addition of dilute HCl, and it was extracted four times with 25 mL methylene chloride. The organic extracts were combined and dried over magnesium sulfate, filtered, and then evaporated under reduced pressure yielding yellow oil. The oil was purified via silica gel chromatography using a solvent of chloroform and methanol (20:1 v/v), ultimately yielding 6.0 g of yellow oil. ^{1}H NMR ([$_{2}$H]chloroform): δ 1.98 (s, 3H), δ 2.99-3.15 (m, 4H), δ 3.75 (m, 6H), δ 4.85 (q, 1H), δ 6.53 (d, 1H), δ 7.25 (m, 5H).

Methyl Glyoxylate

4.6 mL methyl dimethoxyacetone was used to dissolve 0.6 g of glyoxylic acid monohydrate and 100 mg p-toluenesulfonic acid. The reaction was heated overnight while refluxing. The next day, after the reaction had cooled to room temperature, 4 g of phosphorous pentoxide were gradually added. The reaction was heated to reflux at 80º C for four hours and then distilled under reduced pressure at 70º C, to produce 3.0 mL of a yellow oil. ^{1}H NMR ([$_{2}$H]chloroform) δ 3.76 (singlet).

AOPHA-Me

6.0 g N-Ac-(L)-α-ketophosphonate and 2.5 mL methyl glyoxylate were dissolved in 10 mL of water in a flask in an ice bath. After 5 minutes 20 mL potassium carbonate was added, upon which a white precipitate formed. After 30 minutes the precipitate was collected by vacuum filtration and washed with cold ethyl ether. The product was then recrystalized from water and ethanol before being dried over phosphorous pentoxide to yield 1.3 g of a white powder. ^{1}H NMR ([^{2}H]chloroform): δ 1.99 (s, 3H), δ 3.00-3.24 (o, 2H), δ 3.81 (s, 3H), δ 5.09 (q, 1H), δ 6.03 (d, 1H), δ 6.78 (d, 1H, J = 15.9 Hz), δ 7.06 (m, 2H, J = 15.9 Hz), δ 7.15 (m, 2H), δ 7.25 (m, 3H). Mass spectrum (electrospray ionization) m/e = 262.1 (M + 1).

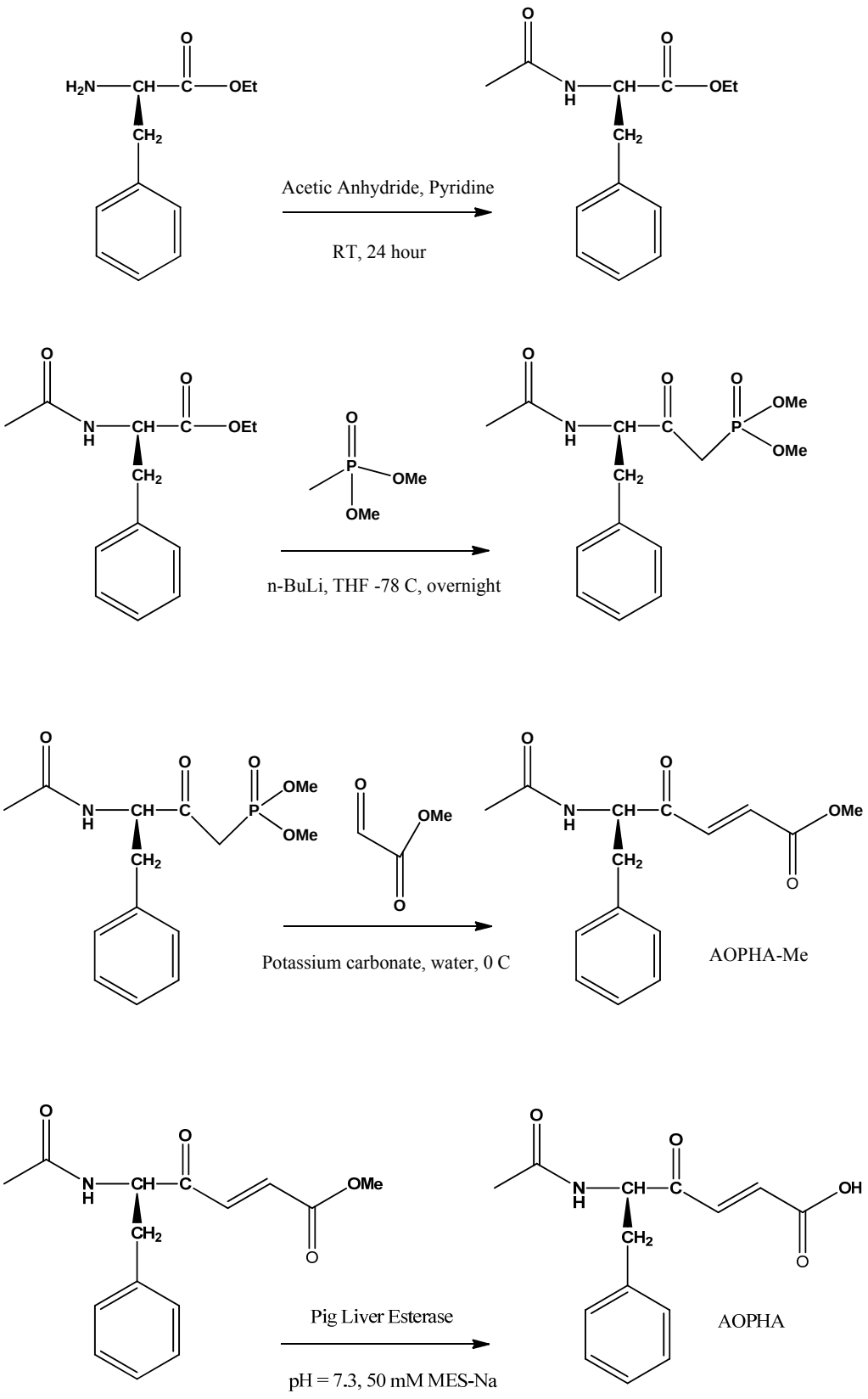

Figure 7. Synthesis of AOPHA and AOPHA-Me.

Recrystallization of PBA

PBA was recrystalized from boiling hexane. 2 g of PBA was added to approximately 50 mL of boiling hexane. The solution was then filtered and allowed to cool overnight. The white crystals were then collected by vacuum filtration and rinsed with cold hexane. The melting point was found to be 85°C.

Solid Phase Peptide Synthesis.

Glycine-extended SP (RPKPQQFFGLMG-COOH) was synthesized using a PS3 peptide synthesizer (Rainin Instrument, Woburn, MA) with *p*-benzyloxybenzyl alcohol resin as solid support. The peptide was cleaved from the resin with trifluoroacetic acid and purified by high-performance liquid chromatography (HPLC) on a C8 reverse phase column, and the sequence was analyzed by the Edman degradation method on a Porton 1090 sequencer. The molecular weight was analyzed by fast-atom bombardment mass spectrometry.

Synthesis of poly(cyclohexane-1,4-diyl acetone dimethylene ketal) (PCADK)

PCADK was synthesized and characterized following the procedure developed in the laboratory of Dr. Niren Murthy (Lee 2007; Kao 2009). Briefly, PCADK was synthesized in a 100 mL two-necked flask, connected to a short-path distilling head. The diols, 1,4-cyclohexanedimethanol (5 g, 34.86 mmol) and 1,5-pentanediol (0.908 mL, 8.72 mmol) were dissolved in 15 mL of distilled benzene and kept 100 °C. Re-crystallized *p*-toluenesulfonic acid and distilled 2,2-diethoxypropane (equal molar ratio to the two diols combined) was added to initiate the reaction. Additional doses of ketals (1 mL) and

benzene (4 mL) were subsequently added to the reaction 2 hours later, via a pressure equalizing funnel, to compensate for the 2,2-dimethoxypropane and benzene that had been distilled off. Two additional doses of 5 mL benzene were added to the reaction at hours 6 and 24 to decrease the viscosity of the reaction mixture. After 48 hours, the reaction was quenched by adding triethylamine (120 μL). The PCADK product was analyzed by ^{1}H-NMR and GPC. ^{1}H NMR ([2H]chloroform): δ 3.4 – 3.18 (m, 4H, CH2), δ 1.66 (s, 2H, CH), δ 1.85 – 0.93 (m, 8H, CH2), and δ 1.32 (s, 6H, CH3).

Formation and Characterization of Microparticles

Gel Permeation Chromatography (GPC) of PCADK

The molecular weight of PCADK was determined by gel permeation chromatography (GPC) using a Shimadzu system (Kyoto, Japan) equipped with a UV detector. Tetrahydrofuran was used as the mobile phase at a flow rate of 1 mL/min. Polystyrene standards (Peak Mw = 1,060, 2,970, 10,680 and 19,760) from Polymer Laboratories (Amherst, MA) were used to establish a molecular weight calibration curve.

Preparation and Characterization of AOPHA-ME Loaded PCADK Microparticles

AOPHA-Me was encapsulated into microparticles using a single oil-in-water emulsion, solvent evaporation method. Briefly, 50 mg of AOPHA-Me and 450 mg of PCADK were dissolved in 2 mL of dichloromethane. This solution was combined with 16 mL of 5 % poly(vinyl alcohol) (PVA)/phosphate buffer solution (pH 7.4) and the

mixture was homogenized in a PowerGen homogenizer at 21,500 rpm for 2 minutes. The resulting oil-in-water emulsion was added to 20 mL of 1 % PVA/phosphate buffer solution (pH 7.4) and stirred for 4 hours, evaporating the dichloromethane and forming particles. The resulting particles were washed twice in deionized water (with centrifugation at 10,000 rpm) to remove the PVA, and lyophilized. Typically these procedures yielded 400 mg of particles. SEM images of the AOPHA-Me-encapsulated PCADK microparticles (AOPHA-Me-PKMs) and blank PCADK microparticles showed typical particle sizes of 0.1-2.5 μm.

The encapsulation efficiency and loading of AOPHA-Me PKMs was analyzed by reverse phase HPLC. Briefly, 3-6 mg of AOPHA-Me PKMs were dissolved in 1 mL of 40 % acetonitrile/0.1% TFA solution. The resulting solution was then injected into a Shimadzu HPLC with a Prevail C18 Column using a 40% acetonitrile/0.1% TFA mobile phase at 1.0 mL/min with a PDA detector set from 190-300 nm. A standard curve of AOPHA-Me was generated to fit a least square linear regression.

Scanning Electron Microscopy (SEM)

SEM images were taken to analyze the morphology of the polyketal microparticles. Briefly, SEM samples were prepared by attaching lyophilized particles onto 12.7 mm diameter aluminum sample mounting stubs (Electron Microscopy Sciences, Hatifield, PA), using conductive double sided carbon discs (SPI Supplies, West Chester, PA). The samples were coated with a gold sputter coater (International Scientific Instruments, Prahran, Australia) for 1 minute under an argon atmosphere. The

SEM samples were subsequently analyzed using either a HITACHI S-800 or LEO-1530 scanning electron microscope (Tokyo, Japan).

In-vitro Release of AOPHA-ME PCADK Loaded-Microparticles

The *in-vitro* release of AOPHA-Me PKMs was analyzed by HPLC. First, a 10 mL suspension of AOPHA-Me PKMs (0.1 mg/mL) was made in either 50 mM pH 7.4 phosphate buffer or 50 mM pH 5.0 acetate buffer. The suspension was then incubated at 37°C in a shaker. At various times the suspension was centrifuged at 15,000 rpm and 1 mL was withdrawn. This aliquot was then centrifuged again at 15,000 rpm and 50 μL was withdrawn for analysis, and the remaining volume was returned to the original aliquot and was then returned to 37°C in the shaker.

Preparation and Characterization of AOPHA-ME PLGA Loaded-Microparticle

AOPHA-Me-encapsulated PLGA microparticles and blank PLGA microparticles were prepared and characterized in the same manner as PCADK microparticles.

Cell Culture Procedures and Assays

Cell Culture

RAW 264.7 cells were grown in DMEM supplemented with 10% (vol/vol) FBS, 100 U/ml penicillin, and 100 μg/ml streptomycin. Cells were maintained at 37°C in a humidified atmosphere containing 5% CO_2. Confluent cells were subcultured by scraping and plated at 10% confluence during each passage. For experiments, cells were

seeded in either 96-well plates or 12 cm^2 dishes and grown overnight to 70-80% confluence. At least two hours before each experiment, cell media was exchanged for unsupplemented DMEM. LPS, SP, SP-Gly or PBA were dissolved in PBS and diluted in unsupplemented DMEM. AOPHA-Me was dissolved in DMSO and diluted in unsupplemented DMEM such that the final concentration of DMSO was less than 0.1%.

ELISA Assay for TNF-α

The concentration of TNF-α present in the media of RAW 264.7 macrophages was determined using a mouse TNF-α ELSIA kit according to the instructions of the manufacturer. Briefly, the cell supernatant was incubated in a 96-well plate coated with anti-TNF-α antibodies. The cell supernatant was then washed away, and the bound TNF-α was incubated with another anti-TNF-α antibody conjugated to a molecule of biotin. Then avidin, a powerful biotin-binding protein, conjugated to horseradish peroxidase was added. The avidin-horseradish peroxidase binds to the biotin on the anti-TNF-α antibody. Then the horseradish peroxidase substrate tetramethylbenzidine is added, which undergoes a reaction which can be monitored spectroscopically at 450 nm. Results are given as relative TNF-α concentrations.

Griess Assay for Nitrite

Nitric oxide production was quantified by measurement of its oxidation product nitrite via the Griess reaction (Ding 1988). 90 μL of supernatant was mixed with 45 μL of 1% sulfanilamide in 10% HCl, incubated for 5-10 minutes in the dark, then mixed with 45 μL of 0.1% N-1-napthylethylenediamine dihydrochloride, then incubated for 5-10 minutes in the dark and then the absorbance was read at 550 nm by a microplate reader.

Western Blot Analysis for Signaling Pathway Proteins

RAW 264.7 cells were grown to 70-80% confluence in 12 cm^2 dishes, washed with PBS and extracted with a mixture of 2% SDS, 1mM PMSF, and 1:100 dilution of protease inhibitor cocktail. Lysed cells were scraped, transferred to microcentrifuge tubes, and sonicated for two, 15-second pulses at room temperature. Protein concentrations were determined using the Bio-Rad DC assay. Proteins were separated on 12.5% acrylamide SDS gels and transferred to PVDF membranes using a Trans-Blot Turbo system. Membranes were stained with Ponceau Red, and then incubated in block buffer for 1–2 hours. p38 MAPK, phospho-p38 MAPK, JNK or phospho-JNK antibodies were incubated separately with membranes in block buffer overnight at 4˚C. Immunopositive bands were detected using alkaline phosphatase-linked anti-rabbit secondary antibody, with development using BCIP/NBT as substrates. Blots were scanned on an HPscanjet 4400C scanner and band densities determined using UN-SCAN-IT software (version 5.1) from Silk Scientific, Inc. (Orem, UT). Two replicate blots were analyzed for each experiment. Antibodies used for the detection of phosphorylated forms of p38 and JNK only recognize these enzymes when they are dually phosphorylated at the key activation sites Thr180 and Tyr182 or Thr183 and Tyr185, respectively (Dérijard, Hibi et al. 1994; Raingeaud, Gupta et al. 1995).

Cell Viability

Cell viability of RAW 264.7 macrophages was determined by use of an MTT assay. The MTT assay was conducted in 96-well plates, with 20 uL of 5 mg/mL MTT in

PBS being added to each well of the plate. Living cells react with MTT to form formazan crystals. The plates were incubated for two hours, the supernatants were removed, and 200 uL of DMSO was added each to each well to dissolve the formazan crystals. The absorbance of the dissolved formazan crystals was read at 570 nm minus the absorbance at 670 nm.

Molecular Modeling

Autodock Vina was used for all docking in this study (Trott and Olson 2010). In general, parameters were kept at their default values. The size of the docking grid was 50 x 60 x 50, which encompasses the entire apoptosis signal-regulating kinase 1 (ASK1) structure and the grid spacing was set at 1.0. Ligand structures were prepared using ChemBio3D Ultra 12.0 and individual PDB files were prepared for docking using AutoDock Tools. The 2CLQ ASK1 kinase structure was obtained from the PDB. To prepare the structure for docking, the ligand and all water molecules were removed and charges and non-polar hydrogen atoms were added using AutoDock Tools.

Experimental arthritis in rats

Animals

Adult male, Sprague Dawley rats were purchased from Harlan Sprague Dawley, Inc. (Indianapolis, IN) and allowed to acclimate for at least 5 days in appropriate caging prior to experimentation. Animals were kept in the animal facility at Mercer University's School of Pharmacy in Atlanta, GA and received food and water *ad libitum*. All animal

experiments were approved by the Mercer University Institutional Animal Care and Use Committee (Macon, GA).

Adjuvant arthritis in rats

These experiments were carried out at Mercer University School of Pharmacy in collaboration with Dr. Stanley Pollack. Adjuvant arthritis was induced in rats using the procedure we had previously developed. Rats received a subplantar injection of 0.1 ml Freund's Complete Adjuvant (1 mg/ml *M. butyricum* in mineral oil) into the right hindpaw (Sunman 2003). The contralateral paw and control animals received subplantar injections of mineral oil only. Changes in hindpaw volume were determined plethysmographically by mercury displacement at various time points following injections.

Statistical analysis

Data were analyzed with a one-way way analysis of variance and followed by Tukey's post hoc test. Values of p less than 0.05 were considered significant for all calculations. Statistical analyses were performed using Statistix for Windows v8.1 and Microsoft Excel.

CHAPTER 3

RESULTS

Previous work in animals showed that AOPHA-Me and PBA possess potent anti-inflammatory properties. In animal models of acute and chronic inflammation, these compounds reduced edema via a non-COX inhibitory pathway (Ogonowski, May et al. 1997; Bauer, Sunman et al. 2007). AOPHA-Me, when dosed via intraperitoneal injection, completely inhibits edema resulting from carrageenan-induced acute inflammation in rats. In addition, PBA inhibits JNK and activates p38 MAPK in both ras transformed WB and human lung carcinoma cells (Matesic, Sidorova *et al*. 2011). Although designed and validated *in-vitro* as amidation inhibitors, the rapid anti-inflammatory response of AOPHA-Me in acute carragenina-induced inflammation in rats suggested that these inhibitors may in part draw their anti-inflammatory function from activities unrelated to amidation. To gain further understanding of their activities we investigated the effect of AOPHA-Me and PBA in RAW 264.7 macrophage cell culture on pro-inflammatory signaling pathways.

SP, SP-Gly AOPHA-Me and PBA do not alter RAW 264.7 Macrophage Viability

The effects of SP, SP-Gly, PBA and AOPHA-Me on RAW 264.7 macrophage viability were determined using MTT assays. None of these compounds had any significant effect on cell viability after 24 hours of incubation, as shown in Figure 8.

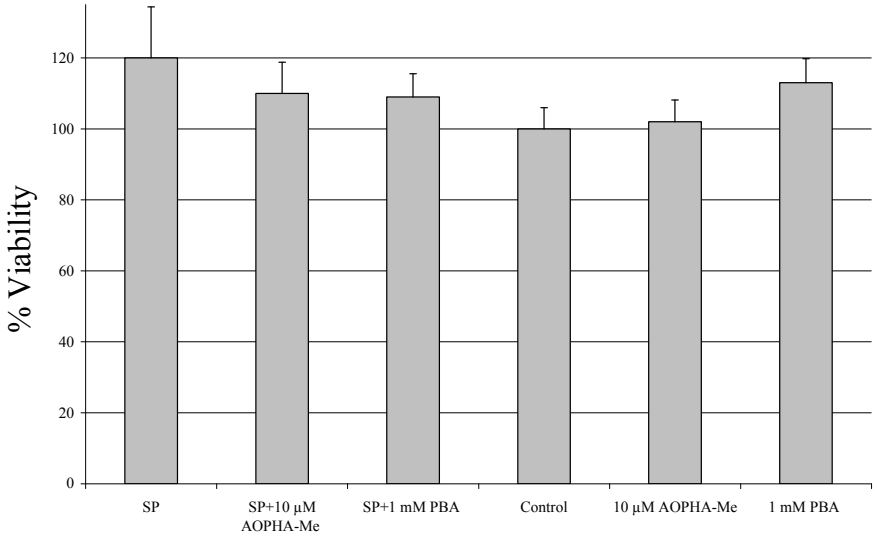

Figure 8. The effects of SP, PBA and AOPHA-Me on RAW 264.7 macrophage viability were determined using MTT assays. No compound had any significant effect on cell viability after 24 hours of incubation. n=4. Data were analyzed with a one-way way analysis of variance and followed by Tukey's post hoc test. Values of *p* less than 0.05 were considered significant for all calculations.

SP but not SP-Gly Stimulates TNF-α Production in RAW 264.7 Macrophages

We investigated the effects of SP and SP-Gly on TNF-α production by RAW 264.7 macrophages. As shown in Figure 9, incubation with SP for 24 hours stimulated TNF-α production in a dose-dependent manner for concentrations ranging from 1-100 μM. In contrast, SP-Gly at similar concentrations had no effect on TNF-α production, as shown in Figure 10. To determine the time course of TNF-α upregulation by SP in macrophages, RAW 264.7 macrophages were incubated with 1 μM SP or 10 μM SP for 2, 4, 8, 12, 16, 20 and 24 hours. As shown in Figure 11, an increase in TNF-α concentration was apparent after about 4 hours, and reached a maximum at about 20 hours.

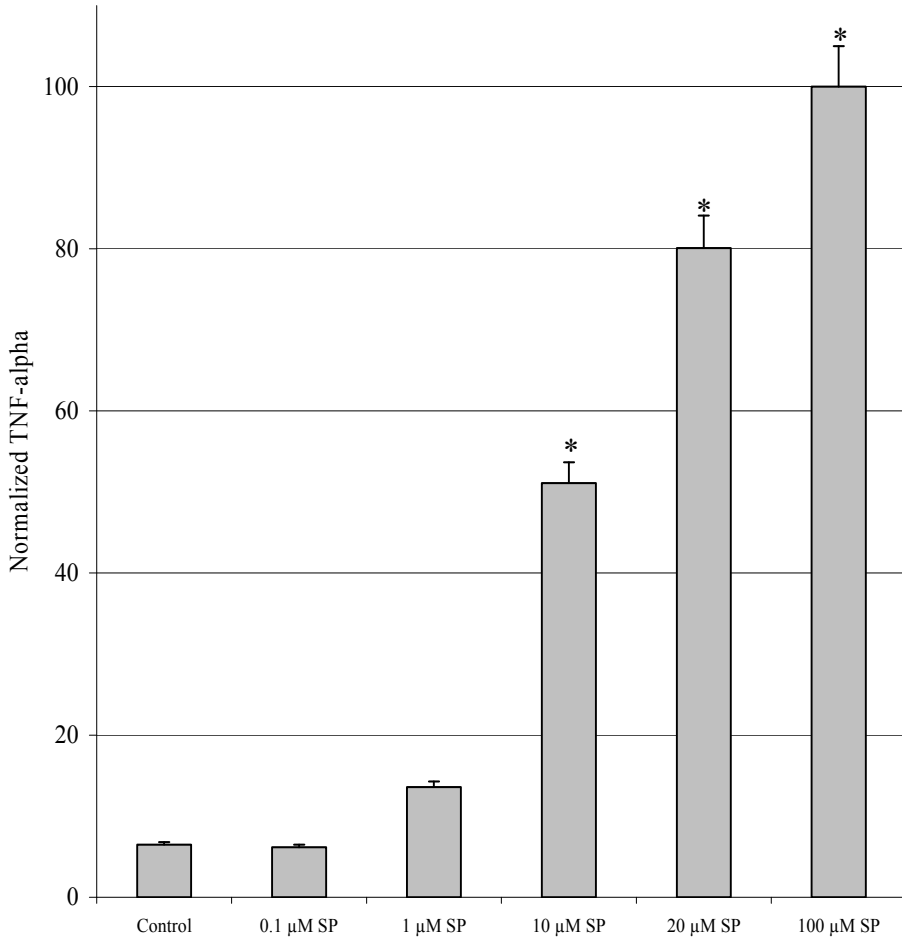

Figure 9. SP upregulates TNF-α in RAW 264.7 macrophages. Cells were incubated with 0.1-100 µM SP for 24 hours. The cell media was analyzed for TNF-α with an ELISA kit. n=4. Data were analyzed with a one-way way analysis of variance and followed by Tukey's post hoc test. Values of *p* less than 0.05 were considered significant for all calculations. * $p < 0.05$ versus control samples.

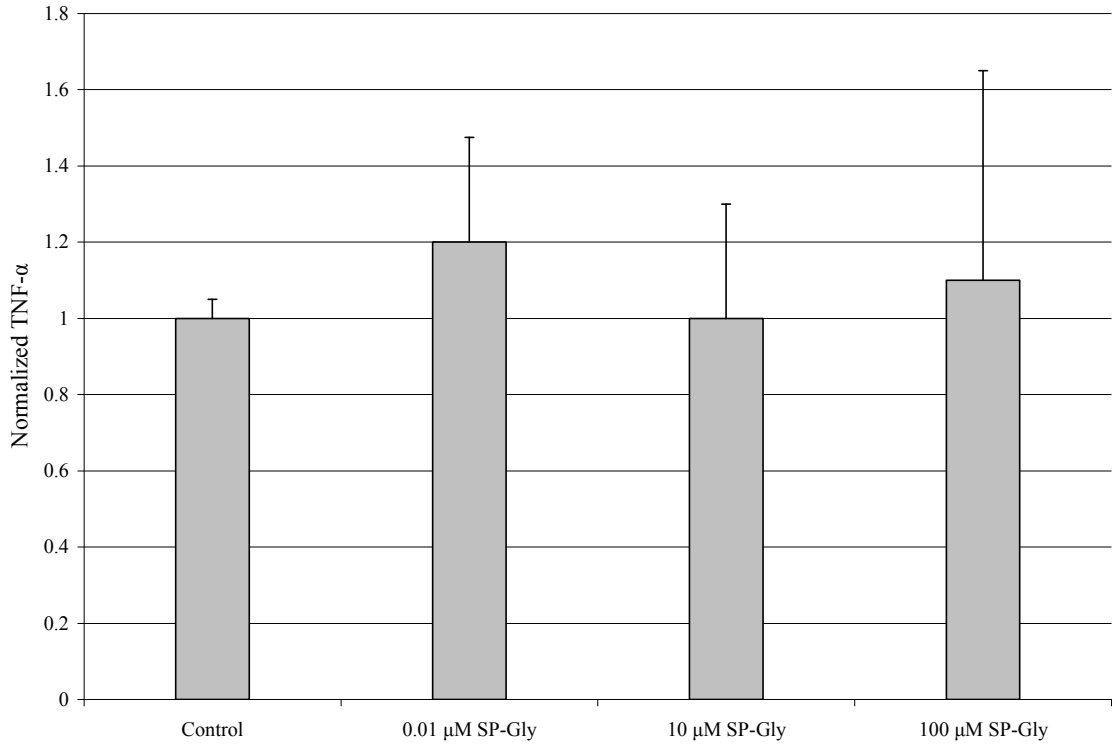

Figure 10. SP-Gly has no effect on TNF-α in RAW 264.7 macrophages. Cells were incubated with 0.01-100 μM SP-Gly for 24 hours. The cell media was analyzed for TNF-α with an ELISA kit. n=4. Data were analyzed with a one-way way analysis of variance and followed by Tukey's post hoc test. Values of p less than 0.05 were considered significant for all calculations. * $p < 0.05$ versus control samples.

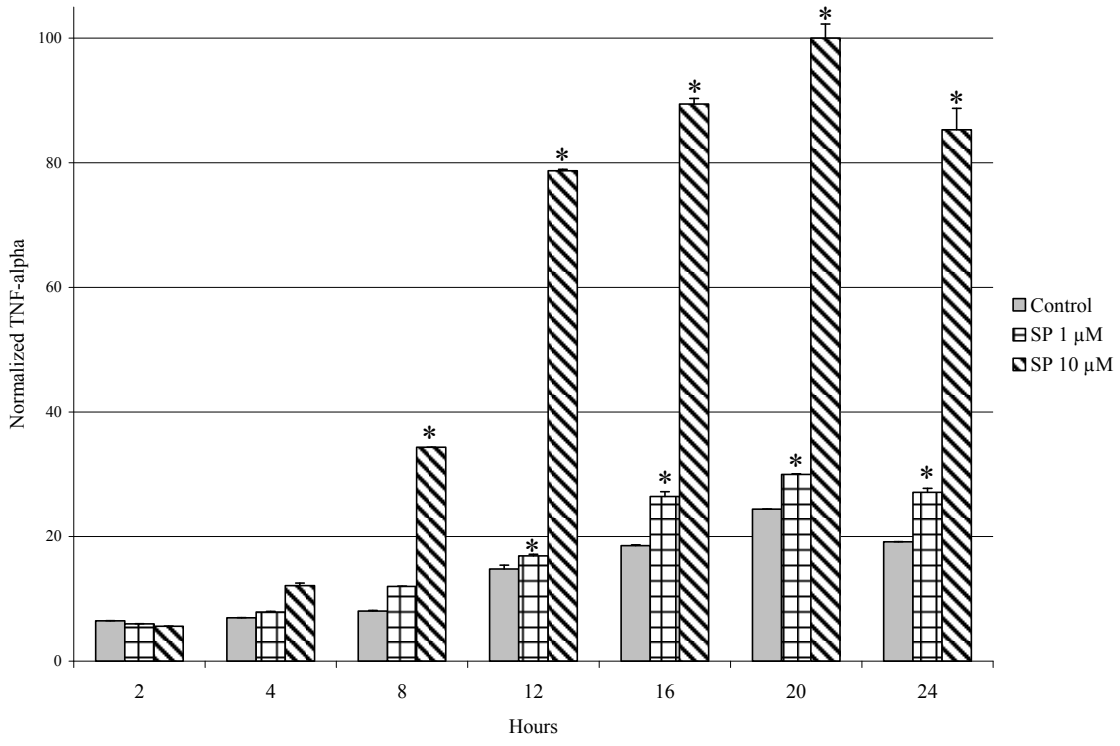

Figure 11. Time-dependent effect of SP on TNF-α expression in RAW 264.7 macrophages. Cells were incubated with 1 μM or 10 μM SP for 2, 4, 8, 12, 16, 20 and 24 hours. The cell media was analyzed for TNF-α with an ELISA kit. n=4. Data were analyzed with a one-way way analysis of variance and followed by Tukey's post hoc test. Values of *p* less than 0.05 were considered significant for all calculations. * $p < 0.05$ versus control samples.

Inhibition of SP-stimulated TNF-α Production in Macrophages

Next, we investigated the effects of 4-phenyl-3-butenoic acid (PBA) and 5-(Acetylamino)-4-oxo-6-phenyl-2-hexenoic acid methyl ester (AOPHA-Me) on SP-stimulation of TNF-α production by RAW 264.7 macrophages. As shown in Figure 12, co-incubation of 0.01-1 mM PBA with 20 μm SP for 24 hours reduced TNF-α expression by as much as 68%. It is apparent from Figure 12 that AOPHA-Me is more potent than PBA, since a reduction in TNF-α expression of 79% was obtained in the presence of only 10 μM AOPHA-Me.

AOPHA-Me and PBA Decrease Phosphorylation of JNK and p38 MAPK by SP in RAW 264.7 Macrophages

We next examined the effects of AOPHA-Me and PBA on JNK and p38 MAPK phosphorylation by SP. The procedure we used in this experiment is illustrated in Figure 13.

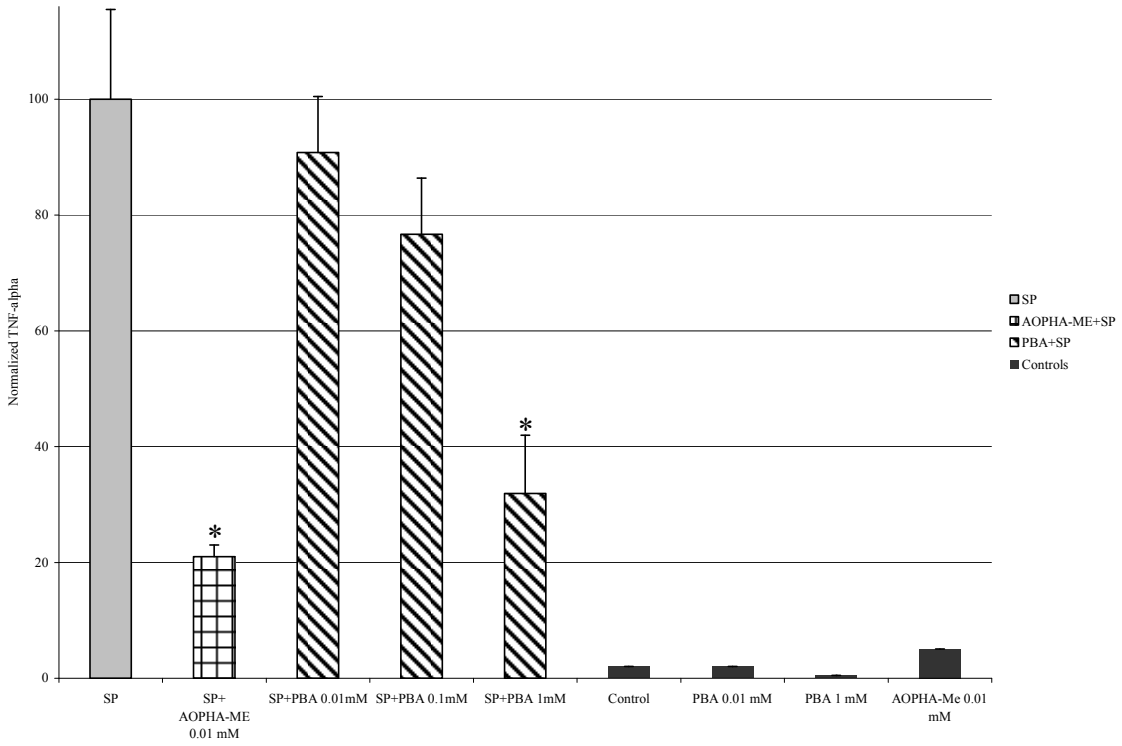

Figure 12. AOPHA-Me and PBA decrease SP-stimulation of TNF-α in RAW 264.7 macrophages. Cells were co-incubated with 20 μM SP and 0.01-1 mM PBA or 10 μM acrylate ester for 24 hours. The cell media was analyzed for TNF-α with an ELISA kit. n=4. Data were analyzed with a one-way way analysis of variance and followed by Tukey's post hoc test. Values of p less than 0.05 were considered significant for all calculations. * $p < 0.05$ versus SP samples.

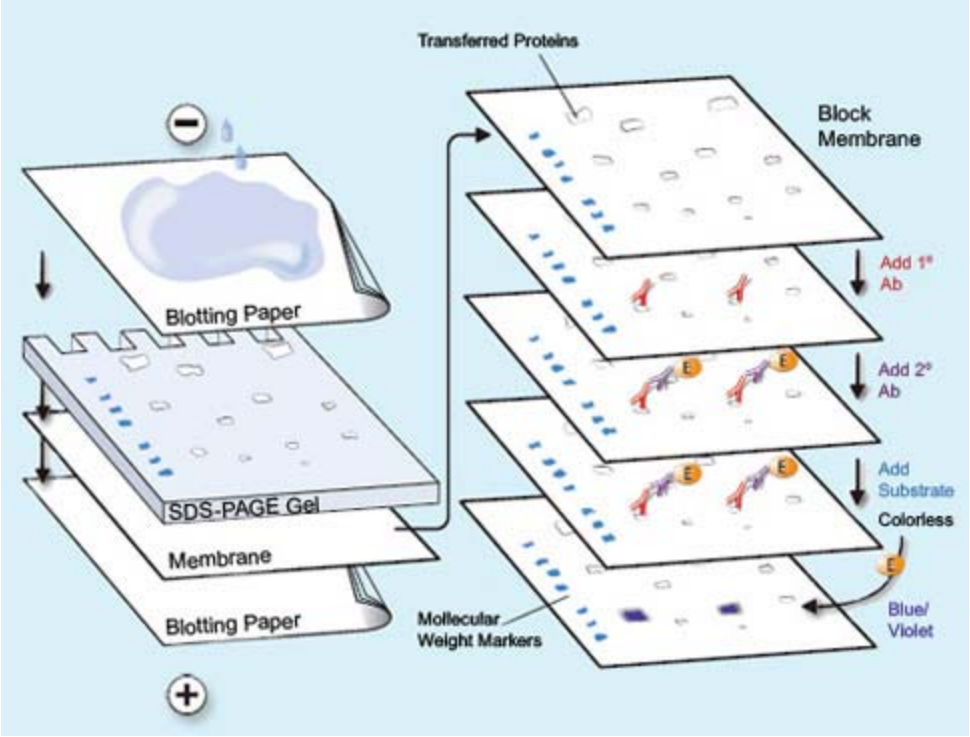

Figure 13. Illustration of Western Blot technique. Proteins from the cellular extract are separated using electrophoresis in a gel. The proteins are then transferred to a membrane via an electrical current. The membrane is then blocked by the addition of block buffer containing non-fat milk proteins. A primary antibody is then added which binds to the protein of interest. A secondary antibody, conjugated to alkaline phosphatase, is then added which binds the primary antibody. The alkaline phosphatase substrates BCIP and NBT are then added which undergo a color change and stain the membrane.

Figure 14 shows the effects of SP treatment on p38 MAPK phosphorylation in RAW 264.7 macrophages in the absence and presence of AOPHA-Me. It is apparent that treatment with 20 μM SP for 24 hours markedly increases phosphorylation of p38 MAPK. It has been shown that phosphorylation at both Thr180 and Tyr182 is required for activation of p38 MAPK (Raingeaud, Gupta *et al*. 1995), and the antibody we used for the detection of phosphorylated p38 MAPK is specific for the dually phosphorylated form of p38 MAPK. It is apparent that 10 μM AOPHA-Me markedly inhibits phosphorylation of p38 MAPK. As shown in Figure 15, densitometric scans of the blots in Figure 14 reveal a 15.6-fold increase in the immunoreactive band density of phospho-p38 MAPK in SP-stimulated cells which is inhibited by 94% in the presence of AOPHA-Me.

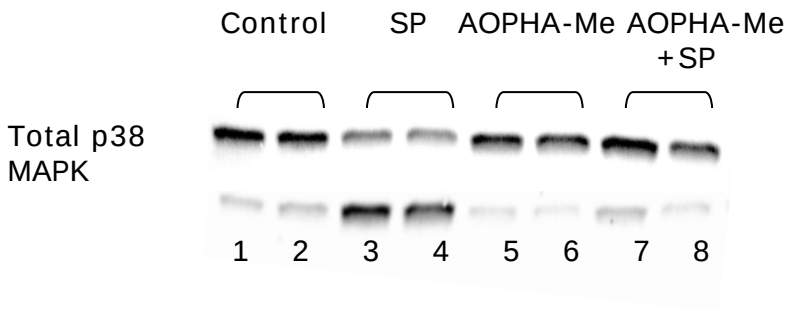

Figure 14. AOPHA-Me prevents SP-stimulated activation of p38 MAPK (Thr180/Tyr182 phosphorylation) in RAW 264.7 macrophages. Cells were either left untreated, treated with 20 μM SP, 10 μM AOPHA-Me, or co-incubated with 20 μM SP and 10 μM AOPHA-Me for 24 hours. Whole cell lysates were extracted for total protein for Western blot analysis as described in Materials and Methods. Identical treatments from replicate cultures are shown on each blot. Phospho-p38 MAPK antibodies used are specific for Thr180/Tyr182. Data were analyzed with a one-way way analysis of variance and followed by Tukey's post hoc test. Values of p less than 0.05 were considered significant for all calculations.

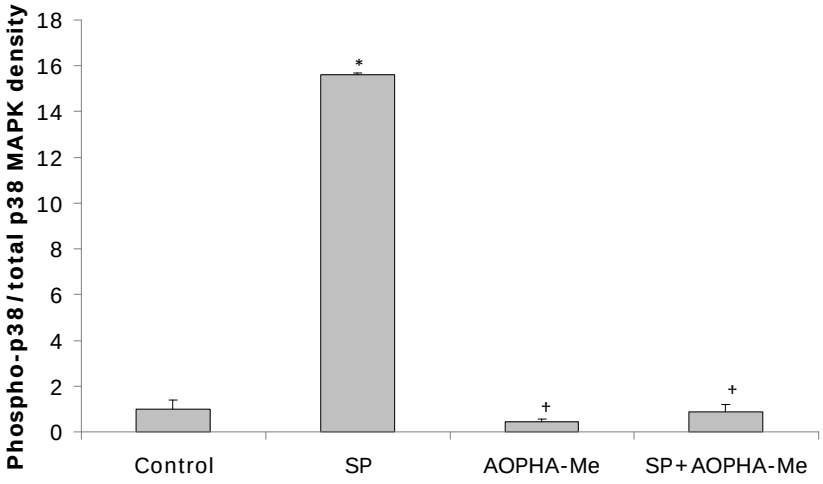

Figure 15. AOPHA-Me prevents SP-stimulated activation of p38 MAPK (Thr180/Tyr182 phosphorylation) in RAW 264.7 macrophages. Densitometric analysis of phospho-p38 and total p38 protein levels from Figure 14 reveal a 15.6-fold increase in the immunoreactive band density of phospho-p38 MAPK in SP-stimulated cells which is inhibited by 94% in the presence of AOPHA-Me. The denstometric quantification of bands in scanned blots are presented as the mean ±SD, and are representative of two independent experiments (asterisks indicate $p < 0.05$ compared to control, crosses indicate $p < 0.05$ compared to SP). Data were analyzed with a one-way way analysis of variance and followed by Tukey's post hoc test. Values of p less than 0.05 were considered significant for all calculations.

Figure 16 shows the effects of SP treatment on JNK phosphorylation in the absence and presence of AOPHA-Me. It is apparent that treatment with 20 μM SP for 24 hours increases phosphorylation of JNK. It has been shown that phosphorylation at both Thr183 and Tyr185 is required for activation of JNK (Dérijard, Hibi *et al*. 1994), and the antibody we used for the detection of phosphorylated JNK is specific for the dually phosphorylated form of JNK. It is apparent that 10 μM AOPHA-Me markedly inhibits phosphorylation of JNK. As shown in Figure 17, densitometric scans of the blots in Figure 16 reveal a 2.2-fold increase in the density of phospho-JNK in SP-stimulated cells and an inhibition of 63% in the presence of AOPHA-Me.

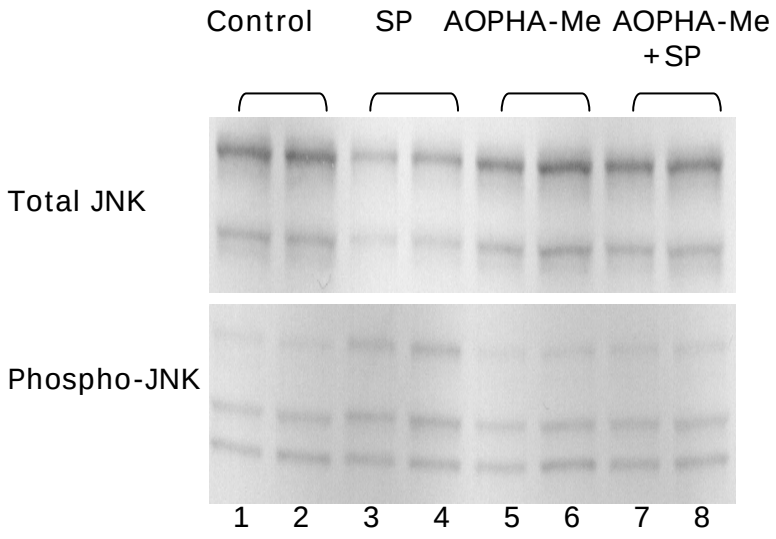

Figure 16. AOPHA-Me prevents SP-stimulated activation of JNK (Thr183/Tyr185 phosphorylation) in RAW 264.7 macrophages. Cells were either left untreated, treated with 20 μM SP, 10 μM AOPHA-Me, or co-incubated with 20 μM SP and 10 μM AOPHA-Me 24 hours. Whole cell lysates were extracted for total protein for Western blot analysis as described in Materials and Methods. Identical treatments from replicate cultures are shown on each blot. Phospho-JNK antibodies used are specific for Thr183/Tyr185. Data were analyzed with a one-way way analysis of variance and followed by Tukey's post hoc test. Values of p less than 0.05 were considered significant for all calculations.

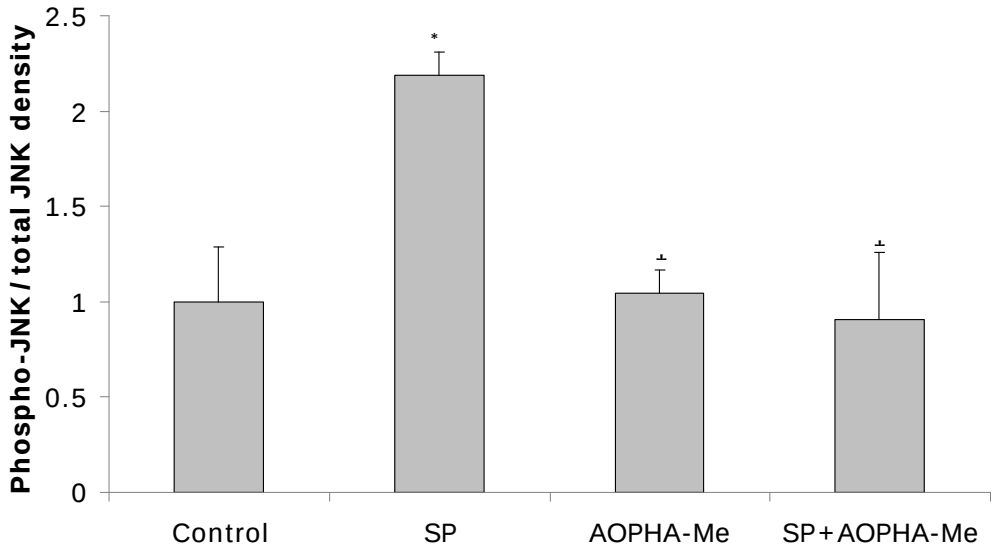

Figure 17. AOPHA-Me prevents SP-stimulated activation of JNK (Thr183/Tyr185 phosphorylation) in RAW 264.7 macrophages. Densitometric analysis of phospho-JNK and JNK protein levels from Figure 16 reveal a 2.2-fold increase in the density of phospho-JNK in SP-stimulated cells and an inhibition of 63% in the presence of AOPHA-Me. The denstometric quantification of bands in scanned blots are presented as the mean ±SD, and are representative of two independent experiments (asterisks indicate $p < 0.05$ compared to control, crosses indicate $p < 0.05$ compared to SP). Data were analyzed with a one-way way analysis of variance and followed by Tukey's post hoc test. Values of p less than 0.05 were considered significant for all calculations.

Figures 18-21 illustrate similar experiments on phosphorylation of p38 MAPK and JNK in the presence and absence of PBA. Once again, densitometric scans, Figures 20 and 21, of the blots from Figures 18 and 19 reveal that SP treatment gives rise to 9.3-fold and 2.9-fold increases in the densities of phosph-p38 MAPK and phospho-JNK, respectively, which are in turn inhibited by 84% and 91%, respectively, upon treatment with PBA.

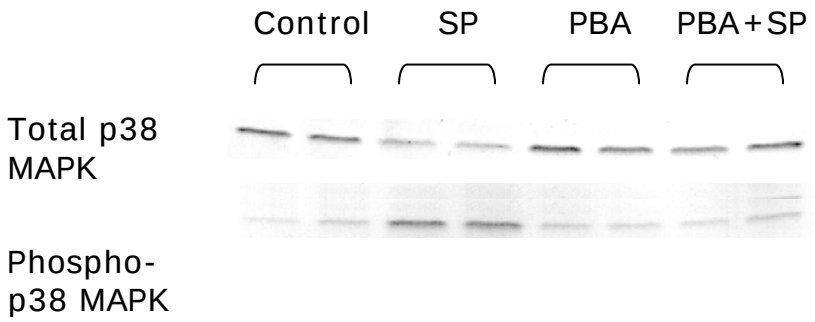

Figure 18. PBA prevents SP-stimulated activation of p38 MAPK (Thr180/Tyr182 phosphorylation) in RAW 264.7 macrophages. Cells were either left untreated, treated with 20 μM SP, 1mM PBA or co-incubated with 20 μM SP and 1 mM PBA for 24 hours. Whole cell lysates were extracted for total protein for Western blot analysis as described in Materials and Methods. Identical treatments from replicate cultures are shown on each blot. Phospho-p38 MAPK antibodies used are specific for Thr180/Tyr182. Data were analyzed with a one-way way analysis of variance and followed by Tukey's post hoc test. Values of *p* less than 0.05 were considered significant for all calculations.

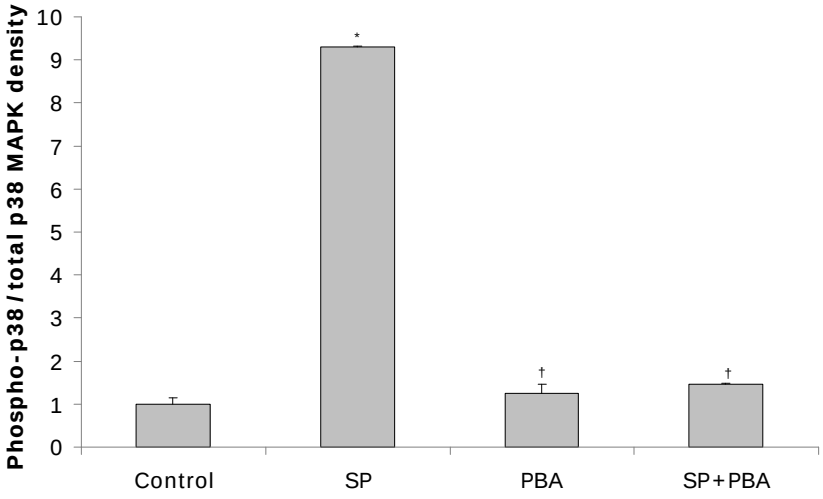

Figure 19. PBA prevents SP-stimulated activation of p38 MAPK (Thr180/Tyr182 phosphorylation) in RAW 264.7 macrophages. Densitometric analysis of phospho-p38 and total p38 protein levels from Figure 18 reveal a 9.3-fold increase in the immunoreactive band density of phospho-p38 MAPK in SP-stimulated cells which is inhibited by 84% in the presence of PBA. The denstometric quantification of bands in scanned blots are presented as the mean ±SD, and are representative of two independent experiments (asterisks indicate $p < 0.05$ compared to control, crosses indicate $p < 0.05$ compared to SP). Data were analyzed with a one-way way analysis of variance and followed by Tukey's post hoc test. Values of p less than 0.05 were considered significant for all calculations.

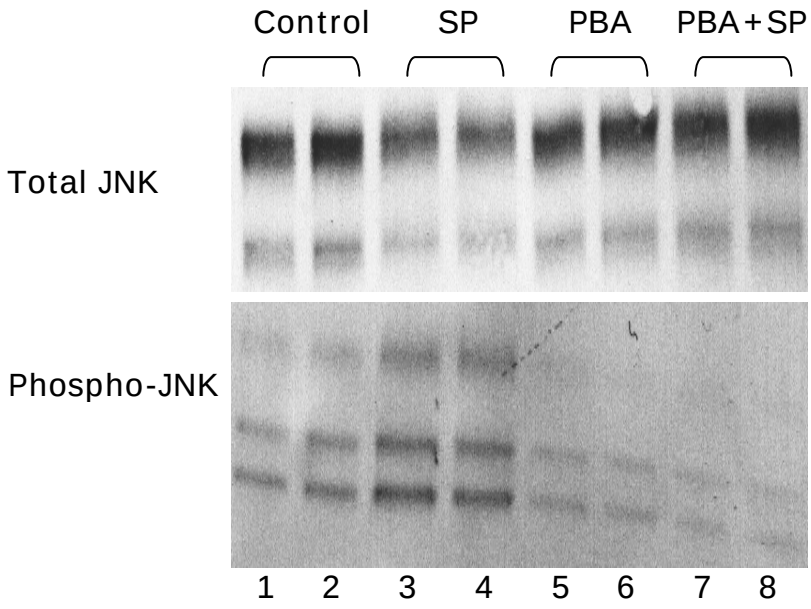

Figure 20. PBA prevents SP-stimulated activation of JNK (Thr183/Tyr185 phosphorylation) in RAW 264.7 macrophages. Cells were either left untreated, treated with 20 μM SP, 1mM PBA or co-incubated with 20 μM SP and 1 mM PBA for 24 hours. Whole cell lysates were extracted for total protein for Western blot analysis as described in Materials and Methods. Identical treatments from replicate cultures are shown on each blot. Phospho-JNK antibodies used are specific for Thr183/Tyr185. Data were analyzed with a one-way way analysis of variance and followed by Tukey's post hoc test. Values of *p* less than 0.05 were considered significant for all calculations.

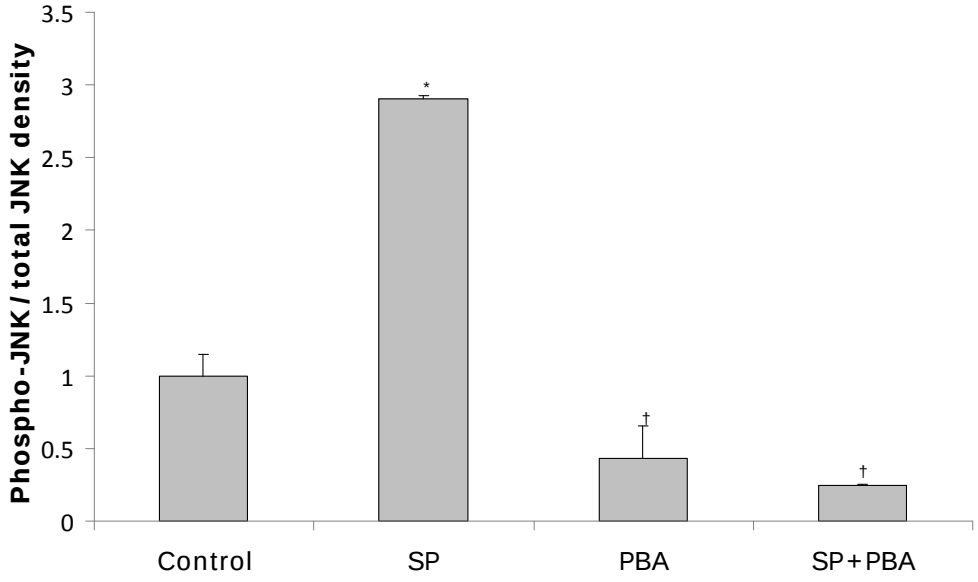

Figure 21. PBA prevents SP-stimulated activation of JNK (Thr183/Tyr185 phosphorylation) in RAW 264.7 macrophages. Densitometric analysis of phospho-JNK and total JNK protein levels from Figure 20 reveal a 2.9-fold increase in the immunoreactive band density of phospho-JNK in SP-stimulated cells which is inhibited by 91% in the presence of PBA. The denstometric quantification of bands in scanned blots are presented as the mean ±SD, and are representative of two independent experiments (asterisks indicate $p < 0.05$ compared to control, crosses indicate $p < 0.05$ compared to SP). Data were analyzed with a one-way way analysis of variance and followed by Tukey's post hoc test. Values of p less than 0.05 were considered significant for all calculations.

PBA Inhibits LPS Stimulation of TNF-α Production in Macrophages

We investigated the effect of PBA on LPS stimulation of TNF-α production by RAW 264.7 macrophages. As shown in Figure 22, treatment with 10 ng/mL LPS for 24 hours stimulated TNF-α production in RAW 264.7 macrophages, and co-incubation of 1 mM PBA with LPS abolished this stimulation of TNF-α production by RAW 264.7 macrophages.

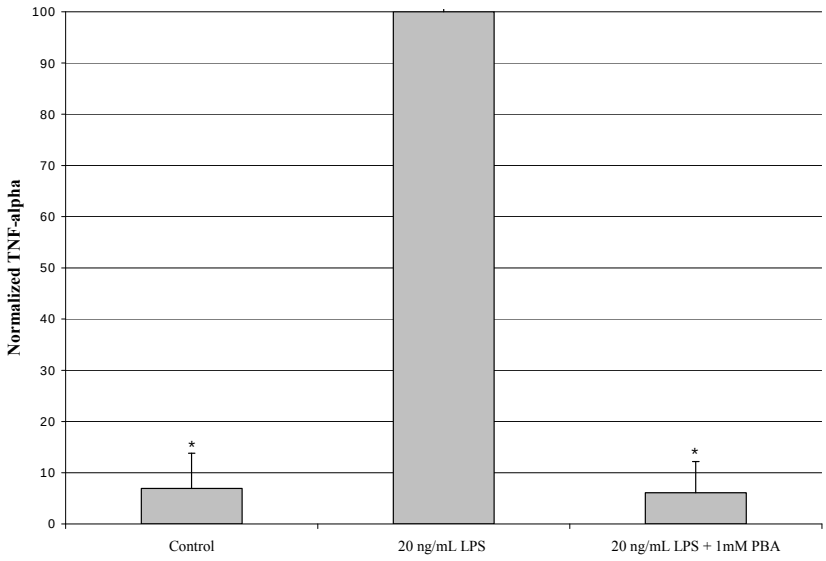

Figure 22. Co-incubation of 1 mM PBA with 10 ng/mL LPS for 24 hours abolished LPS stimulation of TNF-α production by RAW 264.7 macrophages. n=4. Data were analyzed with a one-way way analysis of variance and followed by Tukey's post hoc test. Values of p less than 0.05 were considered significant for all calculations. * $p < 0.05$ versus LPS.

Substance P does not Enhance LPS Stimulation of TNF-α

We investigated the effect of SP on LPS stimulation of TNF-α production by RAW 264.7 macrophages. As shown in Figure 23, treatment with 10 ng/mL LPS for 24 hours stimulated TNF-α production in RAW 264.7 macrophages, and co-incubation of 1-100 μM SP with LPS had no effect on the stimulation of TNF-α production by RAW 264.7 macrophages.

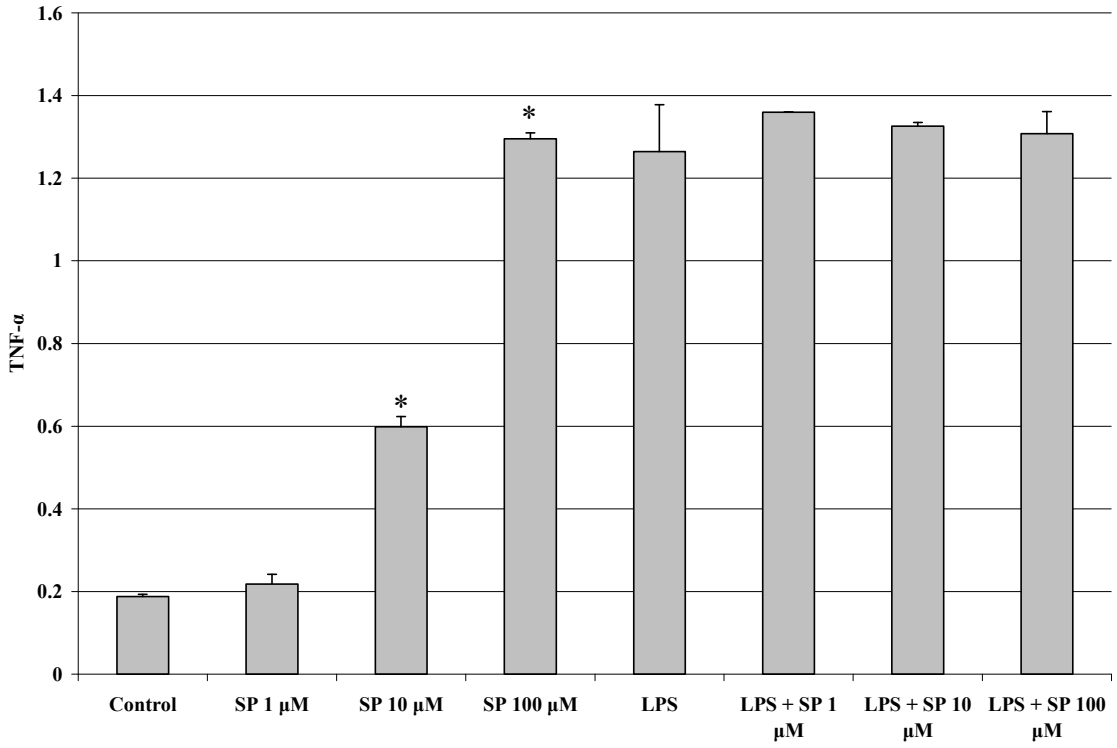

Figure 23. Co-incubation of 1-100 μM SP with 10 ng/mL LPS for 24 hours had no effect on LPS stimulation of TNF-α production by RAW 264.7 macrophages. n=4. Data were analyzed with a one-way way analysis of variance and followed by Tukey's post hoc test. Values of *p* less than 0.05 were considered significant for all calculations. * $p < 0.05$ versus control.

Substance P-Gly does not Enhance LPS Stimulation of TNF-α

We investigated the effect of SP-Gly on LPS stimulation of TNF-α production by RAW 264.7 macrophages. As shown in Figure 24, treatment with 10 ng/mL LPS for 24 hours stimulated TNF-α production in RAW 264.7 macrophages, and co-incubation of 1 μM SP-Gly with LPS had no effect on the stimulation of TNF-α production by RAW 264.7 macrophages.

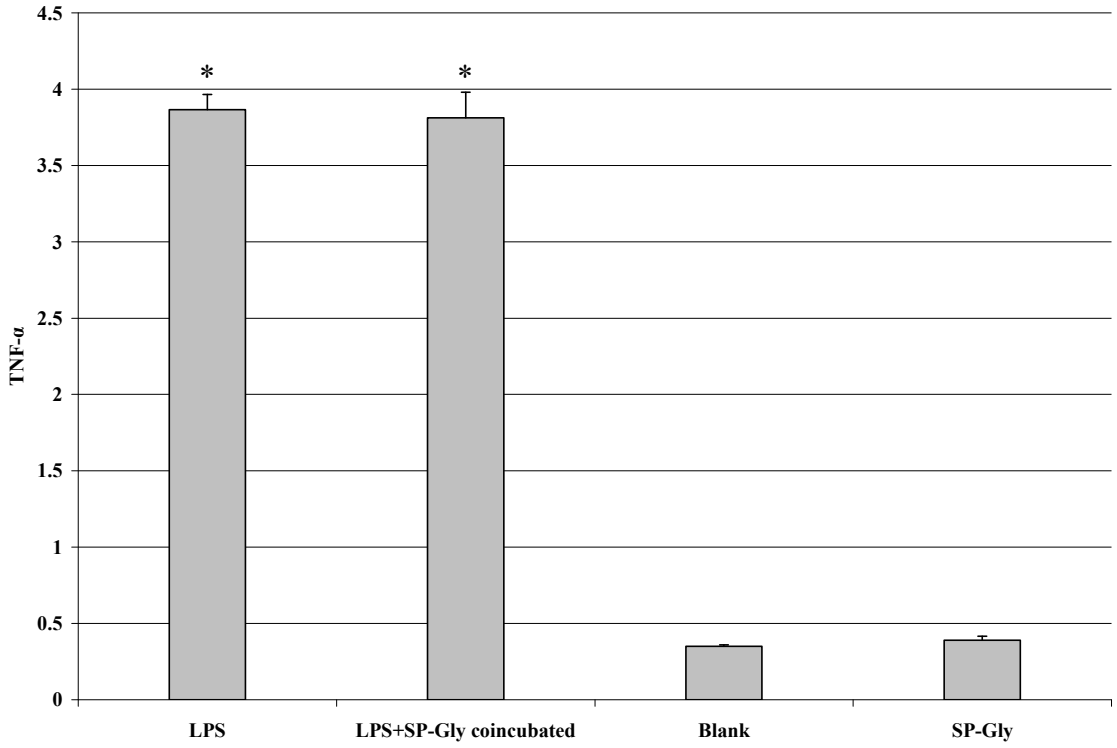

Figure 24. Co-incubation of 1 μM SP-Gly with 10 ng/mL LPS for 24 hours had no effect on LPS stimulation of TNF-α production by RAW 264.7 macrophages. n=4. Data were analyzed with a one-way way analysis of variance and followed by Tukey's post hoc test. Values of *p* less than 0.05 were considered significant for all calculations. * $p < 0.05$ versus control.

Substance P or Substance P-Gly do not Enhance LPS Stimulation of Nitrite

We investigated the effect of SP and SP-Gly on LPS stimulation of nitrite production by RAW 264.7 macrophages. As shown in Figure 25, treatment with 10 ng/mL LPS for 24 hours stimulated nitrite production in RAW 264.7 macrophages, and co-incubation of 100-1000 nM SP or SP-Gly with LPS had no effect on the stimulation of nitrite production by RAW 264.7 macrophages.

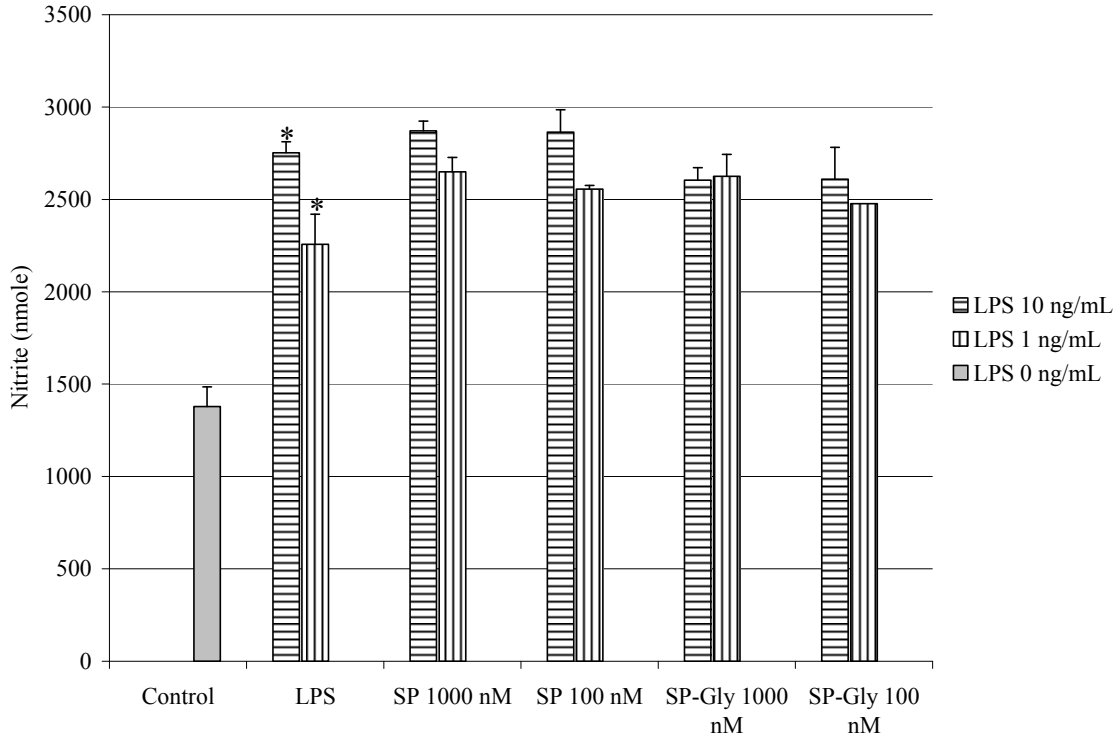

Figure 25. Co-incubation of 100-1000 nM SP or SP-Gly with 1 or 10 ng/mL LPS for 24 hours had no effect on LPS stimulation of nitrite production by RAW 264.7 macrophages. n=4. Data were analyzed with a one-way way analysis of variance and followed by Tukey's post hoc test. Values of p less than 0.05 were considered significant for all calculations. * $p < 0.05$ versus control.

AOPHA-Me and PBA Virtually Dock in the ATP Binding Site of ASK1

Bunkoczi et al (2007) have reported the crystal structure of apoptosis signal-regulating kinase 1 (ASK1) bound to the kinase inhibitor staurosporine, see Figure 25 for the structure of staurosporine. It has been demonstrated that inhibition of ASK1 results in decreased phosphorylation of JNK and p38 MAPK (Terao, Suzuki et al. 2012). We therefore used the molecular modeling software, AutoDock Vina, to investigate whether or not our inhibitors would overlap with the bound staurosporine when docked to the ATP binding site of ASK1. To first validate the use of AutoDock Vina for this purpose, we docked staurosporine and observed it to be faithfully recapitulated with the crystallographically-determined binding of staurosporine.

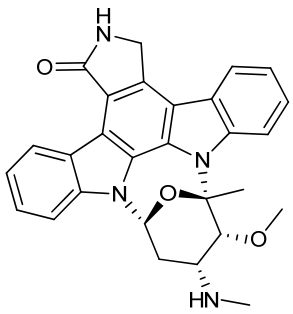

Figure 25. Molecular structure of staurosporine.

Our results are illustrated in Figure 26. In Figure 26A, it is evident that AOPHA-Me (yellow) and PBA (green) exhibit predicted overlap with both the virtually bound staurosporine (grey) and the crystallographically-determined binding of staurosporine (black). We calculate a docking energy of -7.0 kcal/mol for binding of AOPHA-Me to ASK1, a docking energy of -5.9 kcal/mol for binding of PBA to ASK1, and a binding docking of -6.9 kcal/mol for binding of ATP to ASK1. In addition, we

calculate a docking energy of -12.0 kcal/mol for the binding of staurosporine to ASK1, which is expected as staurosporine is known to bind more tightly than ATP to a number of kinases (Meggio, Deana et al. 1995). Note that, in Figure 26B, the phenyl ring of both AOPHA-Me and PBA packs against the hydrophobic side-chains of the ASK1 residues Leu686, Val694, Ala707, and Leu810. This is in agreement with the crystallographically-determined binding of staurosporine which was shown by Bunkoczi et al (2007) to also pack with its five-ring system against these hydrophobic residues of the binding pocket. It should be noted that in studies using MKK7, the MAPK kinase upstream of JNK, AOPHA-Me and PBA did not bind to the ATP-binding site of MKK7.

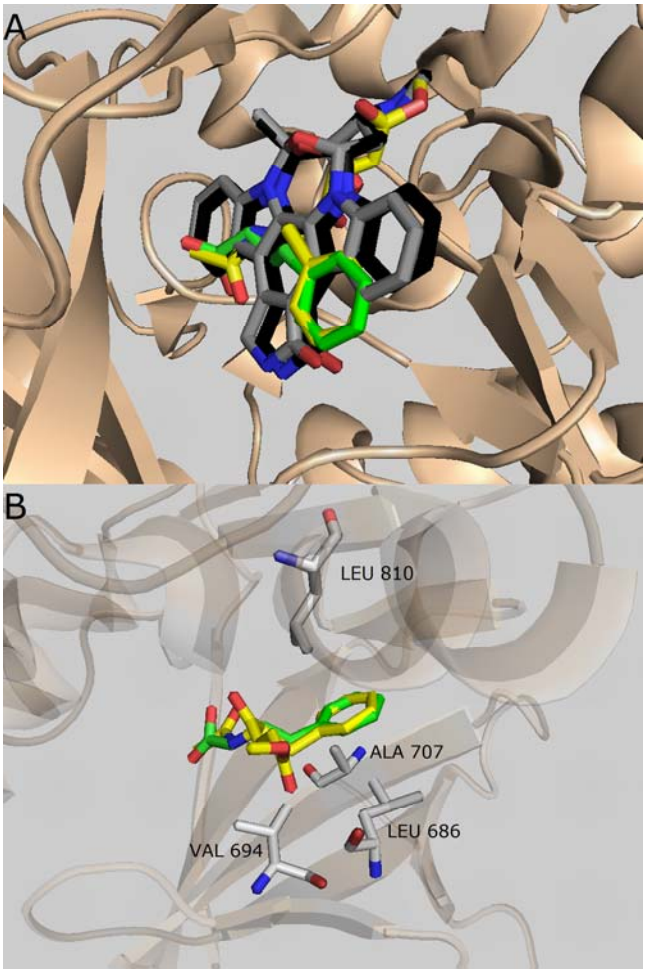

Figure 26. Docking of inhibitors into the ATP binding site of ASK1 using AutoDock Vina. A. Models of AOPHA-Me, PBA and staurosporine superimposed with the crystallographically-determined binding site of staurosporine. Crystallographic staurosporine, black; Virtual staurosporine, grey; AOPHA-Me, yellow; PBA, green. B. Superimposed models of AOPHA-Me, yellow, and PBA, green, shown with the main interacting residues of ASK1 in ball-and-stick representation. Note that the phenyl ring of both AOPHA-Me and PBA packs against the hydrophobic side-chains of the ASK1 residues Leu686, Val694, Ala707, and Leu810, in agreement with the crystallographically-determined binding of staurosporine (Bunkoczi, Salah et al. 2007).

Characterization of Inhibitor-Loaded Microparticles

In previous studies in this laboratory, we were unable to evaluate the efficacy of AOPHA-Me in a chronic model of inflammation in rats due to the low solubility of AOPHA-Me in various vehicles. In addition, some chronic experiments had to be terminated early because signs of toxicity were evident in the animals, presumably from the solvent used to deliver the AOPHA-Me. We therefore turned to the use of microparticles as a potential delivery method for AOPHA-Me in experimental chronic inflammation in rats. In order to utilize this approach we obviously had to first construct and characterize these particles before they could be used in the appropriate animal experiments. We used two different polymers to separately construct the particles. We used PCADK which is unique in that it is rapidly hydrolyzed by acid. We also used PLGA, a very commonly used polymer for microparticle formation with good biocompatibility properties.

Synthesis of PCADK and determination of Molecular Weight

PCADK was synthesized as described in Methods, and based on GPC analysis was determined to have a weight average molecular mass of 10191 and a number average molecular mass of 4968. A representative GPC spectrum for PCADK is shown in Figure 27.

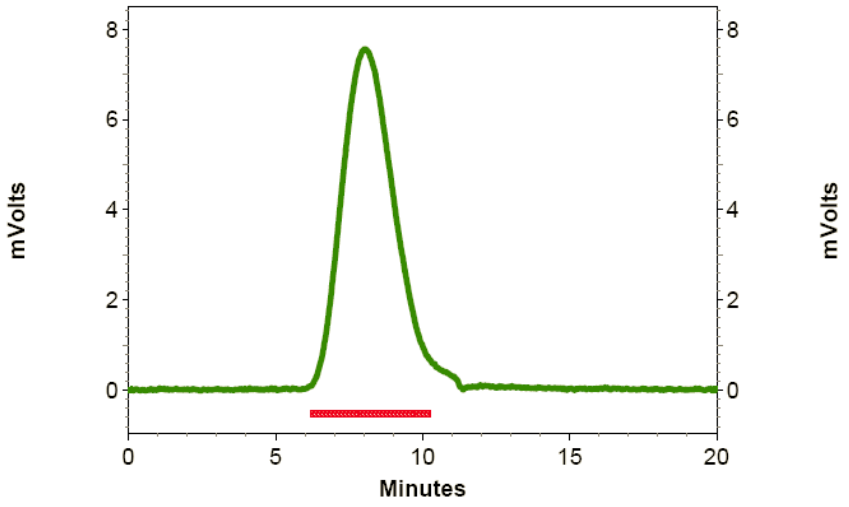

Figure 27. The GPC spectrum of PCADK. PCADK elutes from six to ten minutes. The bar indicates the area from which the molecular mass was calculated from a standard curve as described in Methods.

Preparation of AOPHA-Me-Loaded PCADK Particles

AOPHA-Me loaded PCADK particles were prepared as described in Methods. Scanning electron microscopy was performed to determine the particle shape and size. It is apparent from the Figure 28 that the particles were spheroids that ranged in diameter from 0.1 μm to 2.5 μm.

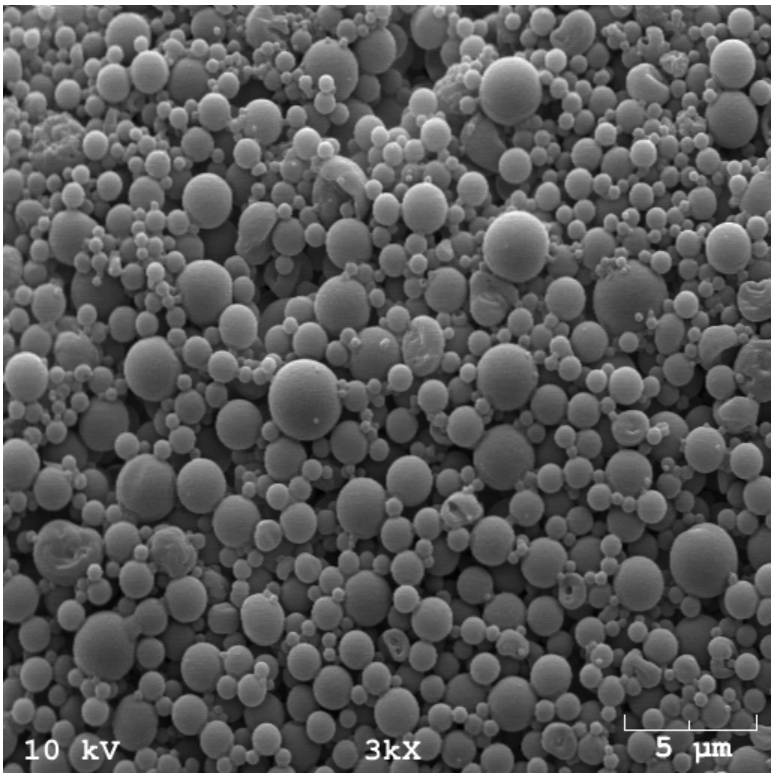

Figure 28. SEM image of PCADK particles.

Analysis of AOPHA-Me-Loaded PCADK particles

PCADK particles were dissolved in 40% acetonitrile containing 0.1% TFA. The solvent was analyzed for AOPHA-Me content using HPLC with a 40% acetonitrile solvent and a C18 column with a flow rate of 1 mL/min. AOPHA-Me from AOPHA-Me PCADK particles eluted at 9.3 minutes and several peaks from empty PCADK particles eluted at various times over 30 minutes as shown in Figure 29. A standard curve of pure AOPHA-Me was generated and it was found that PCADK particles contained 0.3% wt/wt of AOPHA-Me.

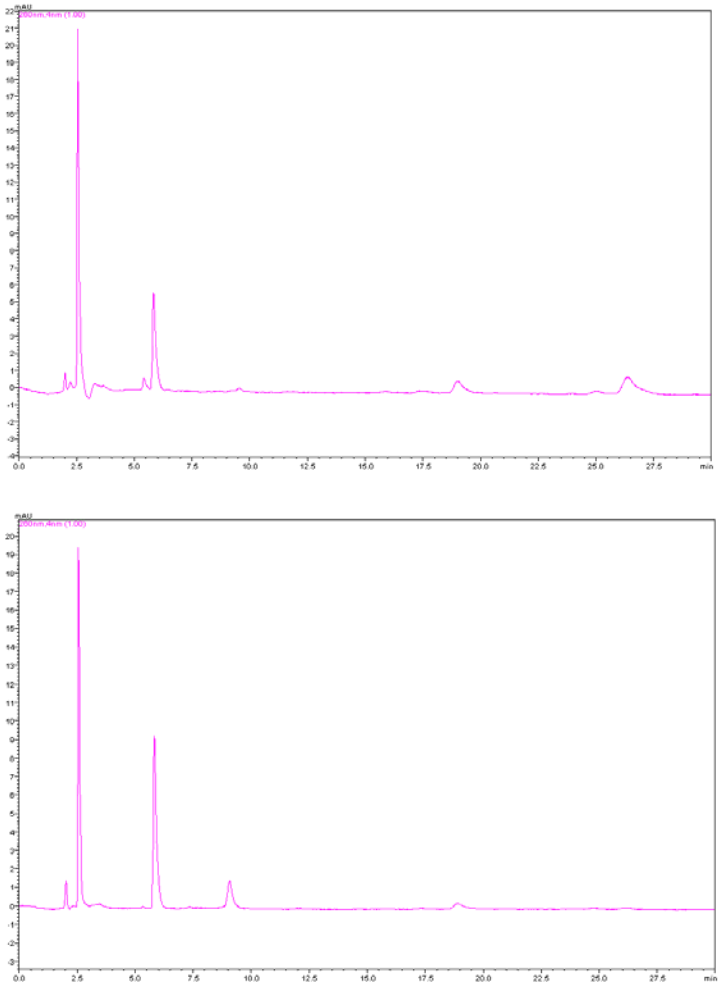

Figure 29. HPLC spectrum of empty PCADK particles (panel A) and AOPHA-Me particles (panel B). AOPHA-Me elutes at 9.3 minutes.

in-vitro Release of AOPHA-Me from PCADK Particles

PCADK particles were incubated in pH 7.4 and pH 5.0 buffers at 37 ˚C to mimic physiological temperature, as described in Materials and Methods. At the indicated times over the course of a week the buffer was analyzed via HPLC for AOPHA-Me. As shown in Figure 30, as expected, a rapid release of AOPHA-Me was observed at pH 5.0 while a

sustained release was obtained at pH 7.4.

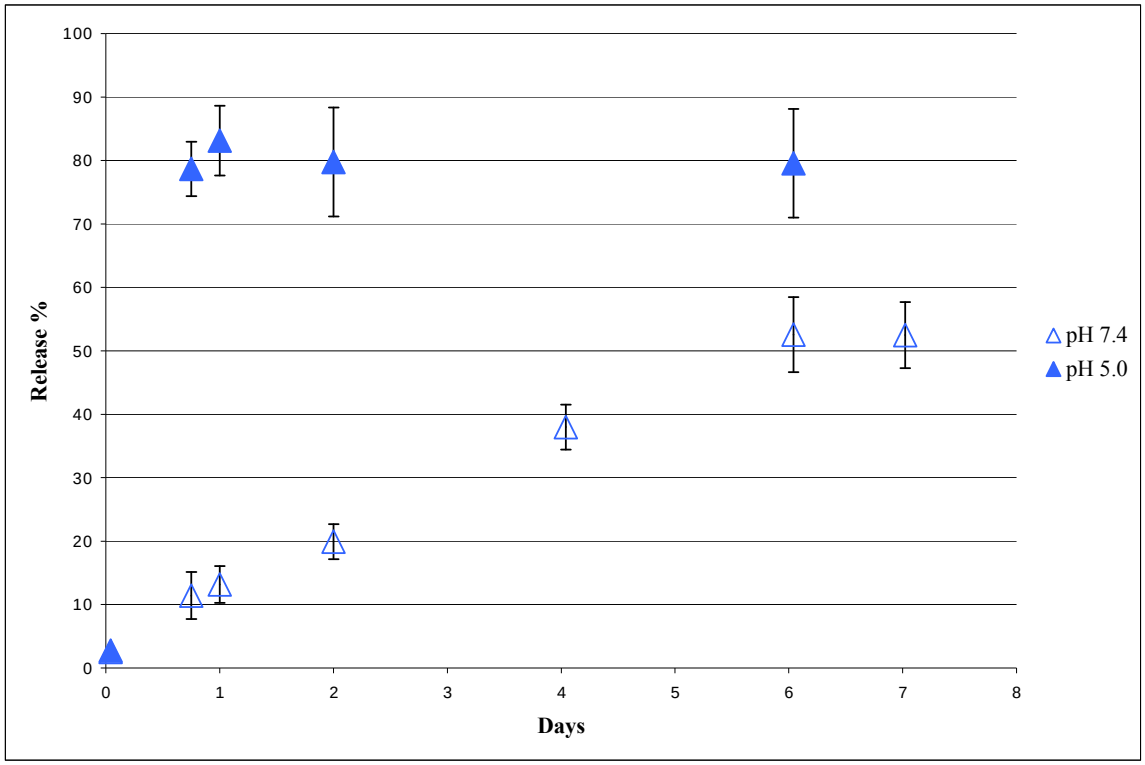

Figure 30. PCADK particles were incubated in pH 7.4 and pH 5.0 buffers as described in Methods. At the indicated times the buffer was analyzed via HPLC for AOPHA-Me. n=3

Preparation of PLGA Particles

PLGA particles were prepared as described in Materials and Methods. Scanning electron microscopy was performed to determine the particle shape and size, as shown in Figure 31. It is apparent from the Figure 31 that the particles were spheroids that ranged in diameter from 0.1 μm to 5.0 μm.

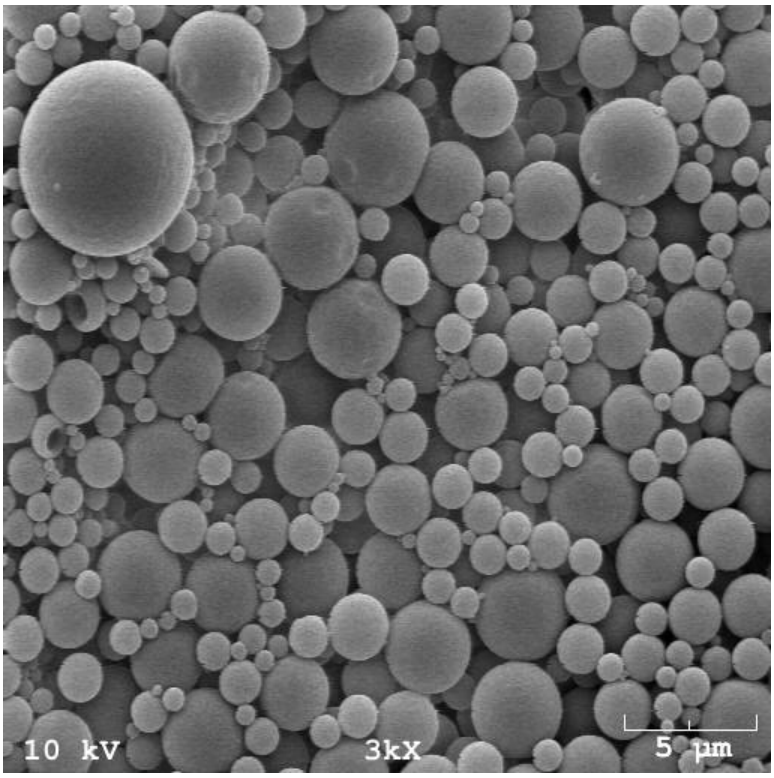

Figure 31. SEM image of PLGA particles.

Analysis of AOPHA-Me-Loaded PLGA Particles

PLGA particles were dissolved in 40% acetonitrile containing 0.1% TFA. The solvent was analyzed for AOPHA-Me content using HPLC, with a 40% acetonitrile solvent and a C8 column with a flow rate of 1 mL/min. AOPHA-Me from AOPHA-Me PLGA particles eluted at 5.9 minutes under the conditions used, as shown in Figure 32. Only one significant peak eluted from empty PLGA particles at 2.5 minutes, as shown in Figure 32. A standard curve of pure AOPHA-Me was generated and it was found that PLGA particles loaded with AOPHA-Me contained the inhibitor at 2% wt/wt.

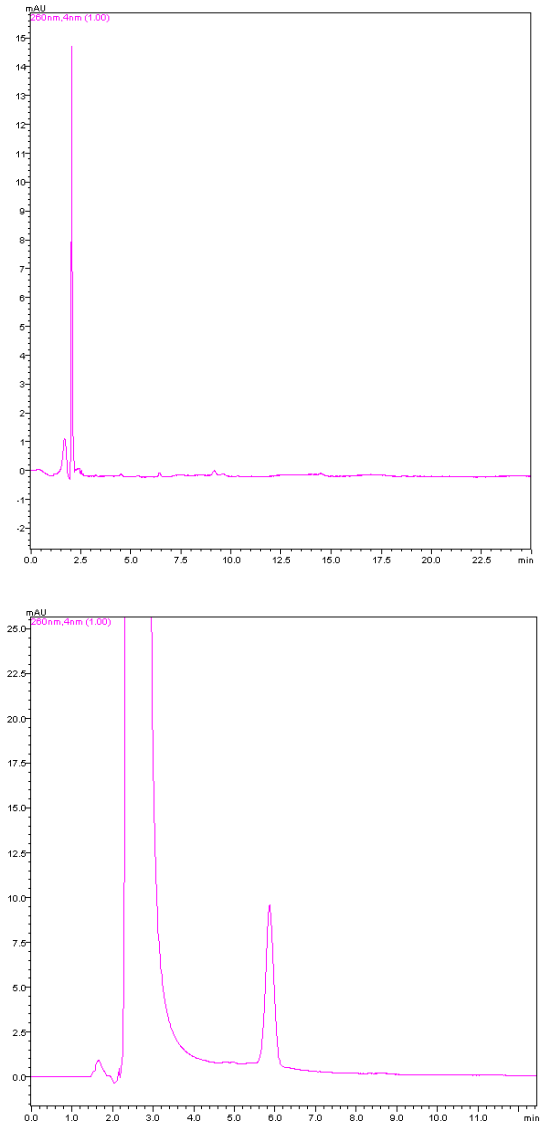

Figure 32. HPLC spectrum of empty PLGA particles (panel A) and AOPHA-Me PLGA particles (panel B). AOPHA-Me elutes at 5.9 minutes.

in-vitro release of AOPHA-Me-loaded PLGA particles

PLGA particles were incubated in pH 7.4 and pH 5.0 buffers at 37 ˚C to mimic physiological temperatures, as described in Materials and Methods. At the indicated times over the course of eight days the buffer was analyzed via HPLC for AOPHA-Me,

as described in Materials and Methods. As shown in Figure 33 a sustained release of AOPHA-Me from PLGA particles was observed at both pH 7.4 and 5.0.

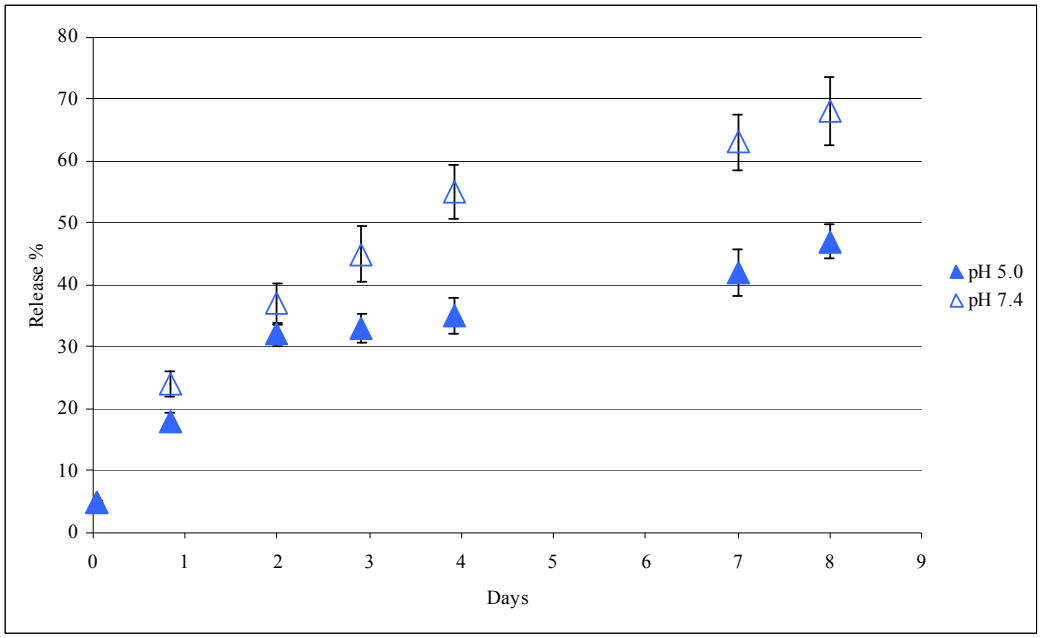

Figure 33. PLGA particles were incubated in pH 7.4 and pH 5.0 buffers as described in Methods. At the indicated times the buffer was analyzed via HPLC for AOPHA-Me. n=3.

Anti-inflammatory Activity of Microparticle-Encapsulated AOPHA-Me

Having constructed and characterized AOPHA-Me-loaded microparticles we then used them as a treatment in experimental arthritis in rats induced by FCA. Due to AOPHA-Me being insoluble in water this compound was previously dosed using organic solvents. It was found that multiple doses using organic solvents as a carrier caused skin necrosis and injections had to be stopped (Sunman 2003). AOPHA-Me-loaded

microparticles were suspended in sterile saline. No signs of toxicity were observed in these experiments, presumably because saline was used as vehicle instead of a solvent.

Adjuvant arthritis was induced, as described in Materials and Methods, in rats. AOPHA-Me-loaded PCADK particles were dosed as a saline suspension i.p. at 200 mg/kg during days 10-14 of the animal model of inflammation. On day 15 the volume of the hindpaws was measured via liquid displacement. As shown in Figure 34 rats that had received FCA developed swelling of both hindpaws and this was clearly evident from visual inspection and measurement of the rats. Treatment with AOPHA-Me-loaded PCADK particles resulted in a statistically significant reduction in the hindpaw volume of both hindpaws. It should be noted that treatment with empty PCADK particles resulted in a reduction in hindpaw volume, but the effect did not exhibit statistical significant.

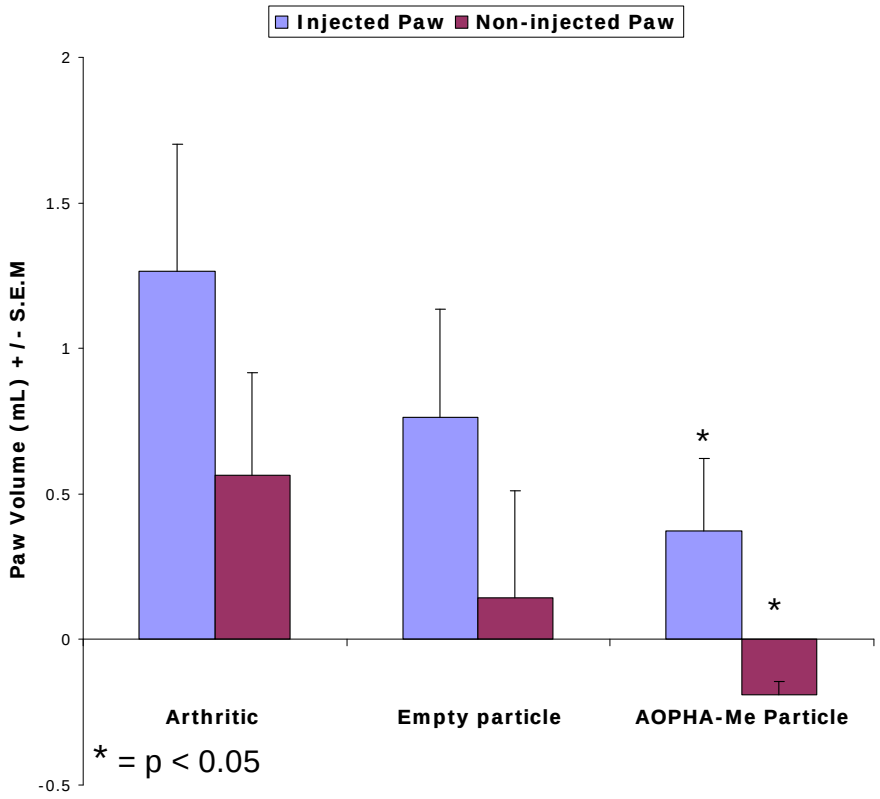

Figure 34. Effect of AOPHA-Me-loaded PCADK particles on adjuvant arthritis when dosed from days 10 to 14. Empty particles controls were treated with empty PCADK particles. Adjuvant arthritis was induced on day 0 as described under Methods. Volumes of injected and contralateral paws were measured at various time points through day 15. Change in paw volume was calculated as the difference between the volumes of arthritic control, empty particle control, or AOPHA-Me-loaded particle-treated hindpaws and volumes of nonarthritic control hindpaws. Data are presented as the mean S.E.M. for each group (n=6). Data were analyzed with a one-way way analysis of variance and followed by Tukey's post hoc test. Values of *p* less than 0.05 were considered significant for all calculations.

The effect of AOPHA-Me-loaded PLGA particles on adjuvant arthritis in rats was also investigated. Adjuvant arthritis was induced as described in Materials and Methods in rats. AOPHA-Me-loaded PLGA particles were dosed as a saline suspension i.p. at 200 mg/kg during days 10-14 of the animal model of inflammation. On day 15 the volume of the hindpaws was measured via liquid displacement. As shown in Figure 35 rats that had received FCA developed swelling of both hindpaws and this was clearly evident from visual inspection of the rats. However, as is evident from Figure 35 treatment with AOPHA-Me-loaded PLGA particles resulted in no statistically significant effect on hindpaw volume.

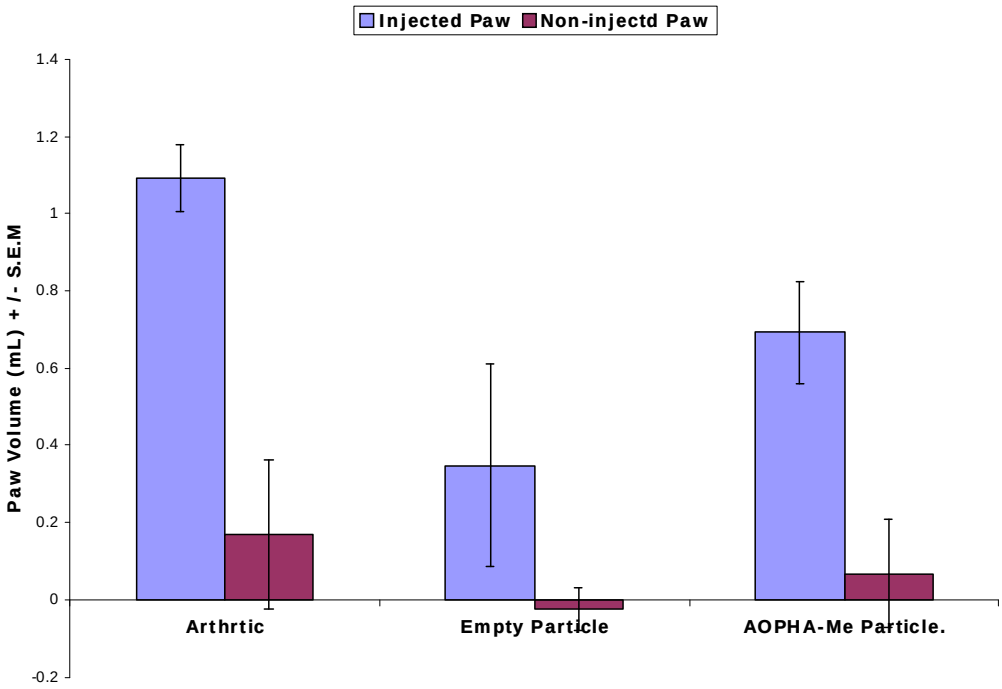

Figure 35. Effect of AOPHA-Me-loaded PLGA particles on adjuvant arthritis when dosed from days 10 to 14. Empty particles controls were treated with empty PLGA particles. Adjuvant arthritis was induced on day 0 as described under Methods. Volumes of injected and contralateral paws were measured at various time points through day 15. Change in paw volume was calculated as the difference between the volumes of arthritic control, empty particle control, or AOPHA-Me loaded particle-treated hindpaws and volumes of nonarthritic control hindpaws. Data are presented as the mean S.E.M. for each group (n=6). No group differed from the arthritic control group in a statistically significant manner. Data were analyzed with a one-way way analysis of variance and followed by Tukey's post hoc test.

.

CHAPTER 4

DISCUSSION

Protein kinases comprise a class of enzymes which modify the activities of other enzymes by the addition of phosphate groups to tyrosine, serine or threonine amino acid residues. Mitogen-activated protein kinases (MAPKs) comprise a family of serine/threonine protein kinases which transmit signals from cell surface receptors to the nucleus via a cascade of phosphorylation events, as shown in Figure 36 (Johnson and Lapadat 2002).

MAPKs themselves are activated by a cascade of intracellular phosphorylation events following stimulation from a wide variety of receptors and receptor ligands. Stimulating factors and their receptors that activate MAPKs include: hormones and growth factors that act through receptor tyrosine kinases; cytokine receptors; peptides such as SP and their G-protein coupled, seven-transmembrane receptors; and transforming growth factor-beta related polypeptides, acting through Ser-Thr kinase receptors.

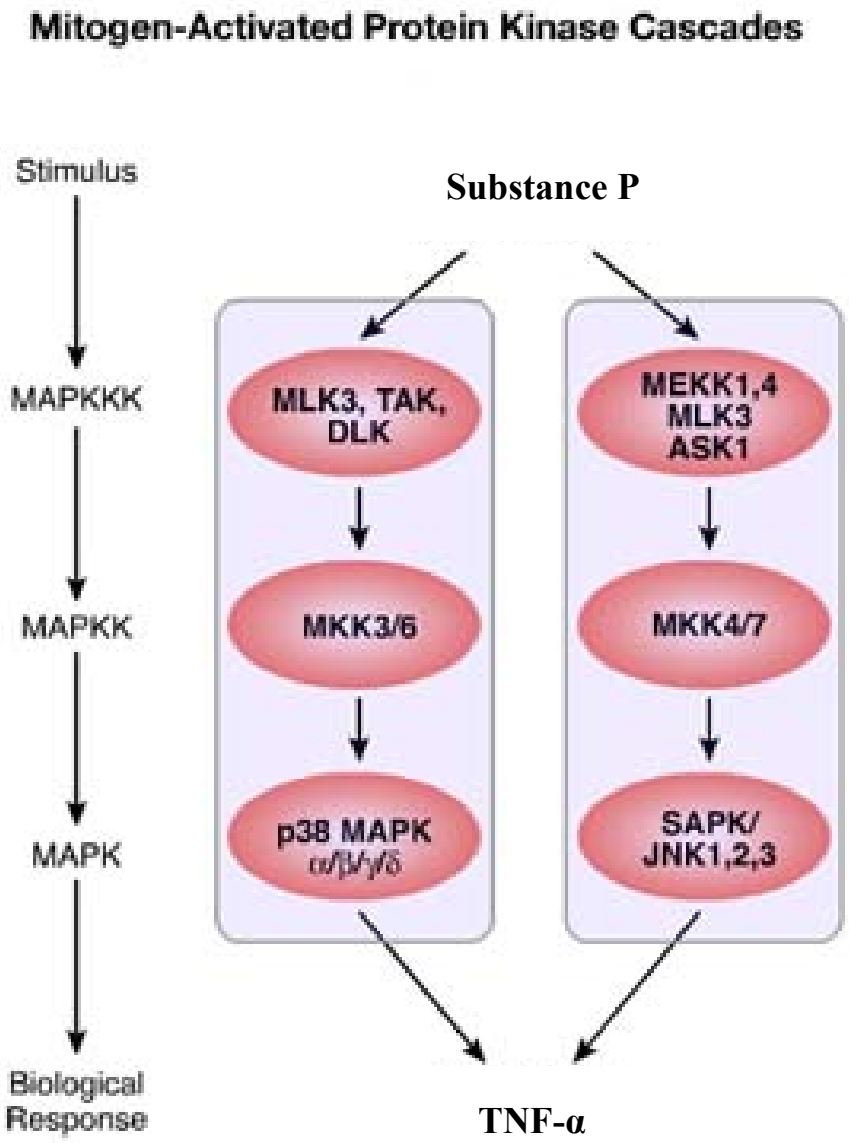

Figure 36. The MAPK signaling cascade as illustrated by Pocrnich (Pocrnich, Liu *et al*. 2009).

Each MAPK family is composed of three tiers of kinases that are sequentially phosphorylated by the preceding MAPK family member. First a MAP kinase kinase kinase phosphorylates a MAP kinase kinase, which then phosphorylates a MAP kinase. Phosphorylated MAPKs then activate several transcription factors such as NF-κB, AP-1, CREB, c-Jun, and STAT1; this leads to changes in gene expression affecting many aspects of cell function, such as upregulation of cytokines (Dong 2002). Other targets of MAPKs include additional kinases, phosphatases and cytoskeletal elements. Three families of mammalian MAPKs have been well characterized; the ERK, JNK, and p38 MAPK families. JNK and p38 MAPK are stress-activated MAPK families; while ERK is mainly activated by growth factors regulating cell growth.

NF-κB is the central transcription factor for expression of genes involved in inflammatory and immune responses, such as the cytokines (e.g. TNF-α, IL-6, IL-1β) and the chemokines (Hayden and Ghosh 2012). In mast cells, SP stimulates TNF-α via NF-κB activation by JNK and p38 MAPK, see Figure 36 (Azzolina, Guarneri et al. 2002; Azzolina, Bongiovanni et al. 2003). LPS stimulation of TNF-α in RAW 264.7 macrophages is controlled by ERK, JNK, p38 MAPK and NF-κB (Geppert, Whitehurst et al. 1994; Lee, Laydon et al. 1994; Swantek, Cobb et al. 1997).

The results presented in this dissertation support the conclusion that AOPHA-Me and PBA reduce SP-stimulated TNF-α production by preventing phosphorylation of JNK and p38 MAPK in RAW 264.7 macrophages. To demonstrate this, we first show that SP stimulates TNF-α expression in RAW 264.7 macrophages, as shown in Figures 8 and 10. This effect is both concentration dependent and reaches a maximal effect around 20-24 hours. We note that others have reported that SP stimulation results in TNF-α

upregulation in primary culture (Lee, Ho *et al*. 1994) but, to the best of our knowledge, our findings represent the first report on the effect of SP on TNF-α production in RAW 264.7 macrophages. Next, we report that both AOPHA-Me and PBA attenuate SP-stimulated TNF-α expression in RAW 264.7 macrophages, as shown in Figure 11. Compounds that can inhibit TNF-α signaling have been of particular interest in treating inflammatory diseases and indeed, we have shown that AOPHA-Me and PBA exhibit anti-inflammatory activity in rat models of both chronic and acute models of arthritis (Bauer, Sunman *et al*. 2007). We note that Sun *et al*. (2008) have reported that treatment with SP increased phosphorylation of p38, but not of JNK, in RAW 264.7 macrophages; however they used a much lower concentration of SP in their work. In addition, we report that PBA inhibits TNF-α upregulation by LPS in macrophages.

It has been shown that upregulation of cytokines, such as TNF-α, in immune cells is generally controlled by the MAPK pathways (Dong 2002) and it would thus be expected that inhibition of MAPK activity would result in inhibition of cytokine upregulation. Indeed, Azzolina *et al* (2002) have shown that SP upregulates TNF-α via activation of JNK and p38 MAPK in mast cells. Similarly, the link between JNK and p38 MAPK activation and TNF-α upregulation has also been demonstrated for LPS-activated RAW 264.7 macrophages (Swantek, Cobb et al. 1997; Ajizian, English et al. 1999). These findings support our conclusion that AOPHA-Me and PBA inhibition of TNF-α expression in SP-stimulated RAW 264.7 macrophages is a consequence of the inhibitory activities of AOPHA-Me and PBA on phosphorylation of JNK and p38 MAPK. In our view, it is also very likely that PBA inhibition of TNF-α upregulation by LPS in macrophages is due to inference in MAPK signaling. It has been well established

that LPS stimulation of TNF-α expression is MAPK dependent, and we have demonstrated that PBA inhibits MAPK signaling.

In contrast to our results with SP, we find that SP-Gly has no effect on TNF-α expression in RAW 264.7 macrophages, as shown in Figure 9. We had hypothesized that SP-Gly and SP would have similar activities, on the assumption that amidation of SP-Gly to SP would readily occur. It has long been assumed that the glycine-extended precursors of bioactive peptides have little or no bioactivity prior to amidation (Prigge, Mains *et al*. 2000). For example, SP-Gly-induced relaxation of rat aortic strips and stimulation of NO production in bovine endothelial cells is markedly reduced in the presence of inhibitors which prevent conversion of SP-Gly to SP (Oldham, Li et al. 1997; Abou-Mohamed, Huang et al. 2000). It has also been shown that injection of SP-Gly and carrageenan with an amidation inhibitor, N,N-diethyldithiocarbamate, in rat paws has no effect on edema, whereas injection of SP itself with carrageenan and the same inhibitor elicited a significant increase in edema (Gilligan, Lovato et al. 1994). It is therefore apparent that, at least under our experimental conditions, RAW 264.7 macrophages are unable to amidate exogenous SP-Gly to a degree that would stimulate TNF-α production.

If RAW 264.7 macrophages are unable to amidate exogenous SP-Gly it raises the question of how our inhibitors, designed as amidation inhibitors, inhibit SP activation of JNK and p38 MAPK. We found through the use of molecular modeling software Autodock Vina that AOPHA-Me and PBA are predicted to bind to the ATP binding site of apoptosis signal-regulating kinase 1 (ASK1), a member of the MAPKs upstream of both JNK and p38 MAPK, with energies of -7.0 kcal/mol and -5.9 kcal/mol respectively. This is in comparison to ATP binding to the ATP binding site of ASK1 with an energy of

-6.9 kcal/mol. Importantly, the phenyl ring of both AOPHA-Me and PBA packs against the hydrophobic side-chains of the ASK1 residues Leu686, Val694, Ala707, and Leu810. This is in agreement with the crystallographically-determined binding of staurosporine, a known ASK1 inhibitor, which was shown by Bunkoczi et al (2007) to also pack with its five-ring system against these hydrophobic residues of the binding pocket. Inhibition of ASK1 has been shown to inhibit the activation of JNK and p38 MAPK in pancreatic β cells and could therefore provide a plausible explanation for the effects of AOPHA-Me and PBA on MAPK signaling (Terao, Suzuki et al. 2012).

Nonsteroidal anti-inflammatory drugs (NSAIDs) and disease-modifying antirheumatic drugs (DMARDs) are the two most commonly used classes of drugs in treating rheumatoid arthritis and inflammation. The use of anti-inflammatory compounds dates to antiquity as willow bark was used by the ancient Greeks (400 BC) to relieve fever and inflammation. In the early 19^{th} century salicin was determined to be the active molecule in willow bark, and this discovery spurred development of anti-inflammatory drugs. The mechanism of action of NSAIDs was unknown Vane suggested in 1971 that aspirin-like drugs inhibit cyclooxygenase (COX), the enzyme responsible for the rate-limiting step of the biosynthesis of eicosanoids (Vane, 1971). It has been established that COX catalyzes the formation of the endoperoxides hydroperoxy endoperoxide prostaglandin G_2 and prostaglandin H2 from arachidonic acid. The endoperoxides are then converted to prostanoids such as thromboxane (TXA_2), prostacyclin (PGI_2) and prostaglandin E_2 (PGE_2) (Botting and Botting, 2004). COX exists as several isoforms, including COX-1, a constitutive isoform that is ubiquitously expressed in almost all

tissues, and COX-2 which is an inducible isoform that is upregulated during inflammation (Seibert *et al*., 1990).

Over the years NSAIDs have proven to have several therapeutic uses. First and foremost, they are used as analgesics for mild-to-moderate pain. The analgesic activity of NSAIDs is much less potent than that of opioids, so although NSAIDs do not possess the unwanted side effects of opioids on the central nervous system, NSAIDs cannot be substituted for opioids in cases of severe pain. NSAIDs also lower fever (i.e. they are anti-pyretics). The most common long-term use of NSAIDs is for the treatment of chronic inflammation in musculoskeletal disorders, such as rheumatoid arthritis, osteoarthritis, and ankylosing spondylitis.

The use of NSAIDs can give rise to serious side-effects due to non-selective inhibition of both COX-1 and COX-2. Of greatest concern is their ability to inflict gastric or intestinal ulceration which can result in anemia from blood loss. The inhibition of gastric prostaglandins (PGI_2 and PGE_2), which protect the gastic mucosa, can result in tissue damage and bleeding. These eicosanoids inhibit stomach acid secretion, promote mucosal blood flow and enhance the production of cytoprotective mucus.

The prostanoid, TXA_2 promotes platelet aggregation and is therefore essential for proper functioning of these cells. Aspirin, the prototypical NSAID, is an irreversible inhibitor of COX, and it inhibits biosynthesis of TXA_2 by activated platelets. Because platelets lack a nucleus, aspirin-inhibited platelets cannot resynthesize COX so new platelets are required to replace the COX activity that was been lost upon aspirin treatment.

NSAIDs also impair renal function by inhibiting vasodilatory prostaglandins. This leads to restricted renal blood flow and glomerular filtration. Hypertension and kidney edema can also result from retention of water and salt. Chronic use of NSAIDs can sometimes result in renal papillary necrosis due to decreased blood flow (i.e. analgesic nephropathy) (De Broe and Elseviers 1998).

In recent years, selective COX-2 inhibitors (Celebrex, Vioxx, and Bextra) were developed with the goal of retaining anti-inflammatory activity while minimizing gastric or intestinal side-effects. The rationale here is that by selectively inhibiting the COX-2 inducible isoform, the COX-1 constitutive isoform can continue to function and protect against ulceration. In addition, unlike aspirin, selective COX-2 inhibitors do not impede platelet aggregation (Patrignani, Sciulli *et al*. 1999). The COX isoforms are largely homologous, but they do possess several key differences in their structures; it is these differences that permit the design of selective COX-2 inhibitors. COX-1 has an isoleucine at position 523 while COX-2 has a slightly smaller valine at position 523. The smaller valine in COX-2 allows a drug to gain access to a hydrophobic side pocket which is otherwise blocked by the isoleucine in COX-1 (Wong *et al*., 1997). Celebrex and Vioxx both occupy this pocket in COX-2 with a phenysulfonamide or phenylmethylsulfone function group, respectively (Gierse *et al*., 1999; Price and Jorgensen, 2000; Walker *et al*., 2001; Hood *et al*., 2003). In addition, COX-2 contains a flexible leucine at position 503 while COX-1 contains a significantly bulkier phenylalanine amino acid residue. Position 503 is near the active site of COX and the additional flexibility afforded by the leucine in COX-2 contributes to inhibitor binding (Marnett, Rowlinson *et al*. 1999).

It has been well established that COX-2 selective inhibitors indeed exhibit less gastrointestinal toxicity and are better tolerated than non-selective NSAIDs (Degner, 2004). Selective COX-2 inhibitors have also been shown to possess equipotent activity in treating osteoarthritis and rheumatoid arthritis patients. Unfortunately, use of selective COX-2 inhibitors has been found to increase the risk of myocardial infarction and stroke (Bombardier *et al*., 2000; Bresalier *et al*., 2005).

The mechanism of this increased cardiovascular risk appears to be related to the inhibition of PGI_2 production that results in alteration of the balance between PGI_2 and TXA_2 (Grosser, Fries *et al*. 2006). TXA_2 is produced by COX-1 in activated platelets and promotes aggregation of these cells (Patrignani, Sciulli *et al*. 1999). PGI_2 is a vasodilator that inhibits platelet activation and is synthesized downstream of both COX-1 and COX-2 by blood vessels in vascular smooth muscle cells and endothelial cells (Belton, Byrne *et al*. 2000). Therefore, selective inhibition of COX-2 leads to a change in the balance between PGI_2 and TXA_2 since production of PGI_2 is inhibited but production of TXA_2 is unaffected. PGI_2 receptor-deficient mice have an increased risk of blot clot formation (i.e. thrombosis) when subjected to appropriate stimuli (Murata *et al*., 1997). In addition, COX-2 deficient mice ($COX\text{-}1^{+/-}$ $COX\text{-}2^{-/-}$) have a high incidence of mortality due to spontaneous thrombosis (Riehl, 2010). Elevated levels of plasminogen activator inhibitor 1 (PAI-1), an inhibitor of fibrinolysis, give rise to a decreased occlusion time in the carotid artery thrombosis model for COX-2 deficient mice. Elevated levels of PAI-1 are associated with decreased PGI_2 production, and this was observed in COX-2 deficient mice.

The risk of myocardial infarction and stroke has led the FDA and European Medicines Agency to withdraw Vioxx and Bextra from the market in the USA and Europe. Both agencies have required that warnings be placed on Celebrex. In addition, the FDA has placed a similar warning on all traditional NSAIDs.

NSAIDs do not halt the progression of diseases such as rheumatoid arthritis. Although they relieve pain, swelling and improve a patient's quality of life, joint destruction continues to progress, eventually leading to loss of joint function. DMARDs differ from NSAIDs in that treatment with DMARDs can actually halt rheumatoid disease progression and joint destruction (Saag, 2008). There are two classes of DMARDs: the "traditional DMARDs" are mainly small molecules that were originally developed for other therapeutic purposes, and the "biological DMARDs" are a class of recombinant proteins which have well-defined functions related to interrupting pro-inflammatory signaling molecules. Some of these -- methotrexate (MTX) -- are immunosuppressant drugs. The mechanism of action of these traditional DMARDs is still not clearly understood, but is thought to be related to a depression of immune system function (Rath, Sander et al. 2011).

MTX is considered to be the "gold-standard" of treatment for rheumatoid arthritis. If monotherapy with MTX fails, treatment will often continue with a combination of MTX and another DMRD. Although the biological action of MTX is known to be inhibition of dihydrofolate reductase, it is not entirely clear how it functions as a DMRD. MTX has been found to raise the concentration of adenosine at sites of cellular injury (Cronstein, 1993). Treatment of mice with MTX was found to be correlated with a reduction in the accumulation of leukocytes in inflamed air pouches, thereby reducing the

inflammatory response. This reduction in leukocyte accumulation was eliminated upon administration of a selective adenosine A2 receptor antagonist, which thereby counteracts the effects of the increased adenosine concentration.

The most commonly prescribed biological DMARDs are TNF-α inhibitors (Singh, 2012). Two classes of TNF-α inhibitors are currently on the market. The first class is comprised of recombinant monoclonal antibodies against TNF-α. The second class is exemplified by Enbrel, a soluble TNF-α receptor fused to the IgG1 antibody. Inhibition of TNF-α signaling suppresses the immune system thereby mitigating the inflammatory response.

The use of DMARDs can give rise to many unwanted and potentially deadly side-effects. In particular, DMARDs can act as immunosuppressant agents, leading to infection or a worsening of existing infections. The risk of contracting tuberculosis, or the possibility that a patient already has a latent case of tuberculosis are particular concerns in the use of biological DMARDs (Roth, 2012). The FDA now requires drug manufacturers to include a black box warning on biological TNF-α inhibitors because of this risk of infection.

Besides the side-effects of biological DMARDs, there are other issues that may complicate their use. Biological DMARDs are proteins and therefore cannot be taken orally because they would be destroyed by the digestive system. They must be administered by subcutaneous injection. In addition, biological DMARDs are very expensive. For example, a yearly regiment of Enbrel can cost approximately $20,000. Although the combination of MTX and a biological TNF-α inhibitor is the preferred treatment in cases where monotherapy with MTX fails, it has been determined that triple

therapy with MTX and two traditional DMARDs, sulfasalazine and hydroxychloroquine, is just as effective as Enbrel-MTX therapy but much less expensive (O'Dell, 2012).

Because of the severe side-effects of current DMARDs and selective COX-2 inhibitors there is a great need to develop new anti-inflammatory drugs. In addition, not all patients experience remission of their disease using current treatment regiments; therefore, new therapies targeting different metabolic pathways are needed. Small molecule inhibitors of non-receptor protein kinases, which participate in intracellular signaling cascades, are of current interest for the treatment for inflammatory conditions (Cohen and Fleischmann 2010). For example, several small molecule Janus kinase (JAK) inhibitors have proceeded through phase II or phase III clinical trials for the treatment of rheumatoid arthritis, irritable bowl syndrome, and psoriasis (Garber 2011; Fleischmann, Kremer et al. 2012). In addition, Xeljanz, a small molecule JAK inhibitor, was recently approved by the FDA for clinical treatment of rheumatoid arthritis. Inhibition of the JAK pathway prevents the activation of several transcription factors and thereby impedes upregulation of a number of pro-inflammatory cytokines such as TNF-α and IL-6 (Quintás-Cardama, Vaddi *et al*. 2010).

There are four JAK isoforms, JAK1, JAK2, JAK3 and TYK2. All members of the JAK family are upstream in the signaling cascade of pro-inflammatory pathways (Rawlings, Rosler *et al*. 2004). Over 60 cytokines signal through receptors that require JAKs for activity. Mice deficient in JAK1 and JAK2 undergo embryonic death while JAK3 knockout mice develop immunodeficiency disorders (Nosaka, Van Deursen et al. 1995; Parganas, Wang et al. 1998; Rodig, Meraz et al. 1998). Xeljanz inhibits JAK1, JAK2 and JAK3, but treatment with Xeljanz avoids deadly complications such as death

and immunosuppression because it only partially inhibits these kinases (Garber 2011). However, Xeljanz carries a black box warning informing patients that treatment with Xeljanz carries an increased risk for infection, cancers and lymphoma.

Three other JAK inhibitors are currently being tested in clinical trials. In contrast to Xeljanz these inhibitors each are selective for JAK isoforms. LY3009104 inhibits JAK1 and JAK2, VX-509 inhibits JAK3 and GLPG0634 inhibits JAK1. These compounds are expected to have different therapeutic windows, and avoid some of the side-effects that a non-selective JAK inhibitor such as Xeljanz carries.

Previous work in our laboratory has shown that AOPHA-Me is an anti-inflammatory agent in acute carragenina-induced inflammation in rats. We have now demonstrated that AOPHA-Me when encapsulated in PCADK particles displays anti-inflammatory activity in chronic FCA-induced inflammation in rats. Of note is that when AOPHA was encapsulated in PLGA particles no anti-inflammatory effect was observed even though a greater amount of AOPHA-Me was successfully encapsulated in the particles. As confirmed by our *in-vitro* release results, PCADK particles have the unique property of being rapidly degraded in the presence of acid compared to PLGA particles. We therefore conclude that the anti-inflammatory activity of AOPHA-Me-loaded PCADK particles is due, in part, to the acid-labile properties of PCADK polymer.

Also of note was that we observed that empty PCADK and PLGA particles reduced the symptoms of edema in the model but not in a statistically significant manner. It has been found that injection of mineral oil alone affords protection against the inflammatory response of injected FCA in rats (Zhang 1999). The authors hypothesized

that the mineral oil can affect the balance of immune cell response in the host leading to protection against FCA. Similarly, we hypothesize that empty microparticles could also affect host immune cell response.

In summary we have demonstrated that the anti-inflammatory compounds AOPHA-Me and PBA interrupt TNF-α upregulation in RAW 264.7 macrophages by SP. In addition, we have also shown that these compounds inhibit the phosphorylation and thereby activation of JNK and p38 MAPK by SP. Molecular modeling predictions are consistent with the view that our compounds bind to the ATP-binding site of MAPKs upstream of JNK and p38 MAPK, which would thereby inhibit JNK and p38 MAPK phosphorylation. We have also shown that AOPHA-Me, when encapsulated in PCADK microparticles, is an effective treatment for edema induced by FCA in rats.

AOPHA and PBA were designed and confirmed to be amidation inhibitors. Our results suggest that the inhibition of both TNF-α signaling and MAPK activation by these compounds is unrelated to their activity as amidation inhibitors. It is conceivable that this dual action of inhibiting PAM and MAPKs may be of some advantage in enhancing the anti-inflammatory activity of a therapeutic molecule. Pro-inflammatory amidated peptide hormones such as SP activate MAPK signaling. Thus, inhibition of amidation and MAPK signaling would be expected to further inhibit pro-inflammatory signals from peptide hormones than an amidation inhibitor alone. It is hopeful that future studies will help elucidate the relative advantages of inhibiting amidation and/or MAPK signaling in the design of the next generation of anti-inflammatory drugs.

PART 2:

IDENTIFICATION OF THE STEREOCHEMICAL DEPENDENCE OF *MYO*-INOSITOL-1,2,3,4,5,6-HEXAKISPHOSPHATE INHIBITION TO EARLY-STAGE LOBLOLLY PINE SOMATIC EMBRYO GROWTH

CHAPTER 5

INTRODUCTION

Planting and harvesting of Loblolly pine (LP, *Pinus tadea*) dominates the forestry industry in the southern USA, with over one billion seedlings planted per year (Schultz 1999). LP belongs to the gymnosperms, which are vascular plants whose seeds are not contained by a fruiting body. Somatic embryogenesis (SE), the technique of asexually generating plant embryos in tissue culture, holds great promise for the clonal reproduction of high value trees such as LP produced from breeding and genetic engineering programs.

Reproduction in gymnosperms

Reproduction in plants proceeds by the process called the alternation of generations where a multicellular diploid body, the sporophyte, produces spores by meiosis which develop into a multicellular haploid body, the gametophyte, by mitotic division (Goldberg, de Paiva *et al*. 1994). The gendered gametophyte then produces gametes, either sperm or eggs, by mitosis. The sperm and egg then combine to produce a diploid embryo which by mitotic division matures to become a new sporophyte, thus completing the cycle. This is in contrast to animals, where a diploid organism directly produces haploid gametes by meiosis. In pines, the tree is the dominant sporophyte life stage. In pines, the gametophyte life stage exists only for reproduction and is contained within the cones of the sporophyte. The sporophyte produces two types of spores, microspores and megaspores, which are produced by the microsporangia and

megasporangia, respectively (Reiser and Fischer 1993). These reproductive organs are housed in separate cones on the same tree. The microspores develop into pollen. The pollen is released by the tree and brought to the ovule of either the same or a different tree by either winds or insects where it develops into the male gametophyte. The male gametophyte then produces sperm. The macrospore is retained by the pine within cones and develops into a female gametophyte (FG) which produces two to six eggs. The eggs are fertilized when the female gametophyte takes in the sperm of the male gametophyte via a structure called a pollen tube which is grown by the male gametophyte.

Only one embryo typically survives embryogenesis to full development. After fertilization, this embryo grows inside the FG which is encompassed by the seed. The embryo passes through three stages of development, proembryogensis, early embryogenesis and then late embryogenesis. Figure 37 shows a classification system, developed by Pullman and Webb (1994), where LP embryogenesis is subdivided into nine distinct stages based on morphological characteristics of the embryo.

Proembryogensis, which is equivalent to stage 1, involves the initial cell divisions after fertilization but before formation of the embryo. The proembryo is divided into four tiers of cells with each tier being composed of four cells (Owens 2006). One of these tiers develops into the embryo proper and another becomes the suspensor system. The suspensor system provides functions such as, physically supporting the embryo inside the FG, producing growth hormones and facilitating nutrient transfer from the egg and FG. The embryo is nourished by the egg cytoplasm during this stage. During early and late embryogenesis the embryo's nourishment is supplied by the FG.

Early embryogenesis, occurs during stages 2-4, and involves suspensor elongation and formation of the root meristem. The undifferentiated embryonic cell mass also continues to grow. During early embryogensis, the embryo and suspensor system are an intertwined mass of tubular and isodiametric cells.

Late embryogenesis, includes stages 5-9, and involves the formation of the polar meristems of the root and shoot via differentiation in the embryonic mass. At stage 9 the suspensor system undergoes programmed cell death. Following seed dispersal, the dormant embryo will germinate and form a seedling.

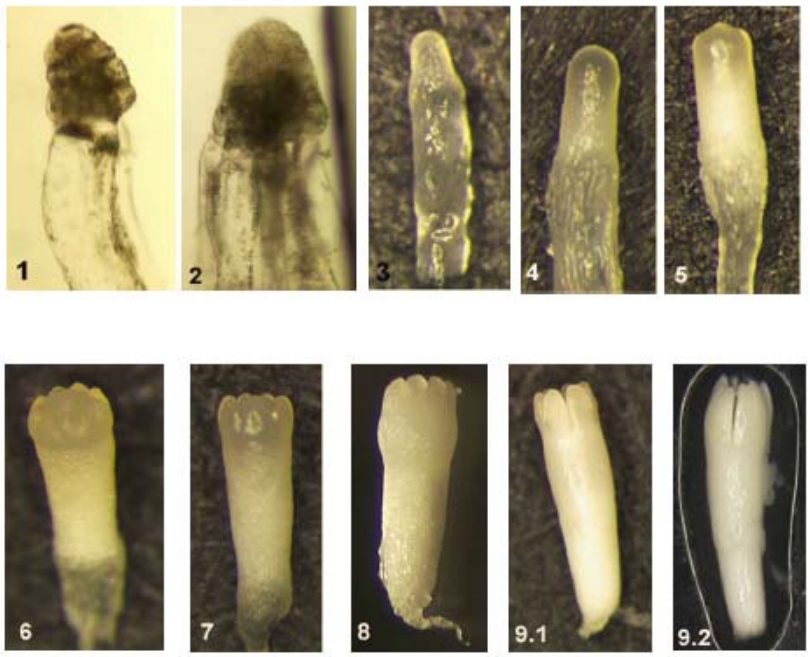

Figure 37. Zygotic embryos of Loblolly pine, stages 1 through 9.2, modified from (Cairney and Pullman 2007).

Somatic Embryogenesis

SE is a tissue culture technique where a plant is clonally propagated from an embryonic cell line which was cloned from either zygotic embryos or FGs. It also refers to the development of the somatic embryo, as illustrated in Figure 38. Somatic embryogenesis is initiated from a dissected seed when either the zygotic embryo or FG is placed in tissue culture medium containing plant growth regulators, such as auxin and cytokinin. These regulators induce the plant tissue to proliferate into a tissue mass containing multiple somatic embryos (Cairney and Pullman 2007). These stage 1 and 2 somatic embryos are then induced to multiply in either liquid or solid culture. The somatic embryos are clones of each other. During the development and maturation phase, which encompasses stages 3-7, somatic embryos are induced to develop into stage 8 and 9 embryos capable of germination. Maturation of somatic embryos is typically achieved on a semi-solid medium over 3 to 6 weeks. Perhaps the most important distinction between zygotic and somatic embryogenesis is that the somatic embryo is grown in the absence of the FG. Thus all of the nutrients and chemical messengers supplied by the FG would be absent in somatic embryogenesis and must be supplied by the tissue culture medium.

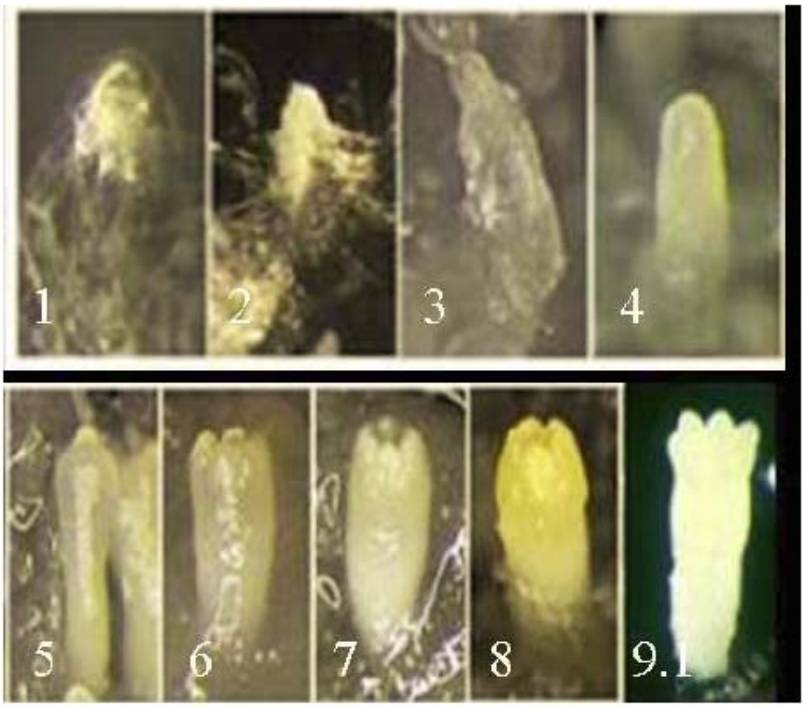

Figure 38. Somatic embryos of Loblolly pine, stages 1 through 9.1 modified from (Cairney and Pullman 2007).

Usefulness of SE in LP clonal forestry

Wood is used as a raw material in products such as paper and building materials in addition to a myriad of individual consumer products such as furniture. It is also used as an energy source, notably within a paper mill where the unused portion of the tree is incinerated. Different industries desire various properties from trees such as faster growth, resistance to disease and insects and modification of the lignin content. These traits can be selected by breeding programs or genetic engineering and superior trees are propagated by control of pollination, plant cutting, and micro-propagation. Somatic embryogenesis can also be used to mass produce clones of superior trees. Although commercially successful in trees such as Eucalyptus and Poplus, somatic embryogenesis has not been as successful for LP. This is not due to a single factor but rather low culture initiation and survival, low somatic embryo germination and loss of desired genotypes over time all contribute to difficulty in LP SE.

myo-Inositol-1,2,3,4,5,6-Hexakisphosphate

myo-inositol-1,2,3,4,5,6-hexakisphosphate (*myo*-$InsP_6$), also called phytic acid, is one of the isomers $InsP_6$. All have six phosphate groups attached to six carbon groups. Figure 39 illustrates the structures of $InsP_6$ and its isomers. *myo*-$InsP_6$ is ubiquitous in plant and animal cells (Abel, Anderson *et al*. 2001). It serves as a source of phosphate and inositol storage in plants (Raboy 2003). *myo*-$InsP_6$ has been found to possess anti-cancer activity in human cell lines such as colon carcinoma HT-29 cells (Sakamoto, Venkatraman *et al*. 1993), erythroleukemia K562 cells (Shamsuddin, Baten *et al*. 1992), prostate carcinoma DU145 cells (Singh, Agarwal *et al*. 2003), and cervical carcinoma

HeLa cells (Ferry, Matsuda *et al*. 2002) and in animal models of pulmonary neoplasia (Wattenberg 1995), colon cancer (Challa, Rao *et al*. 1997) and skin tumors (Gupta, Singh *et al*. 2003).

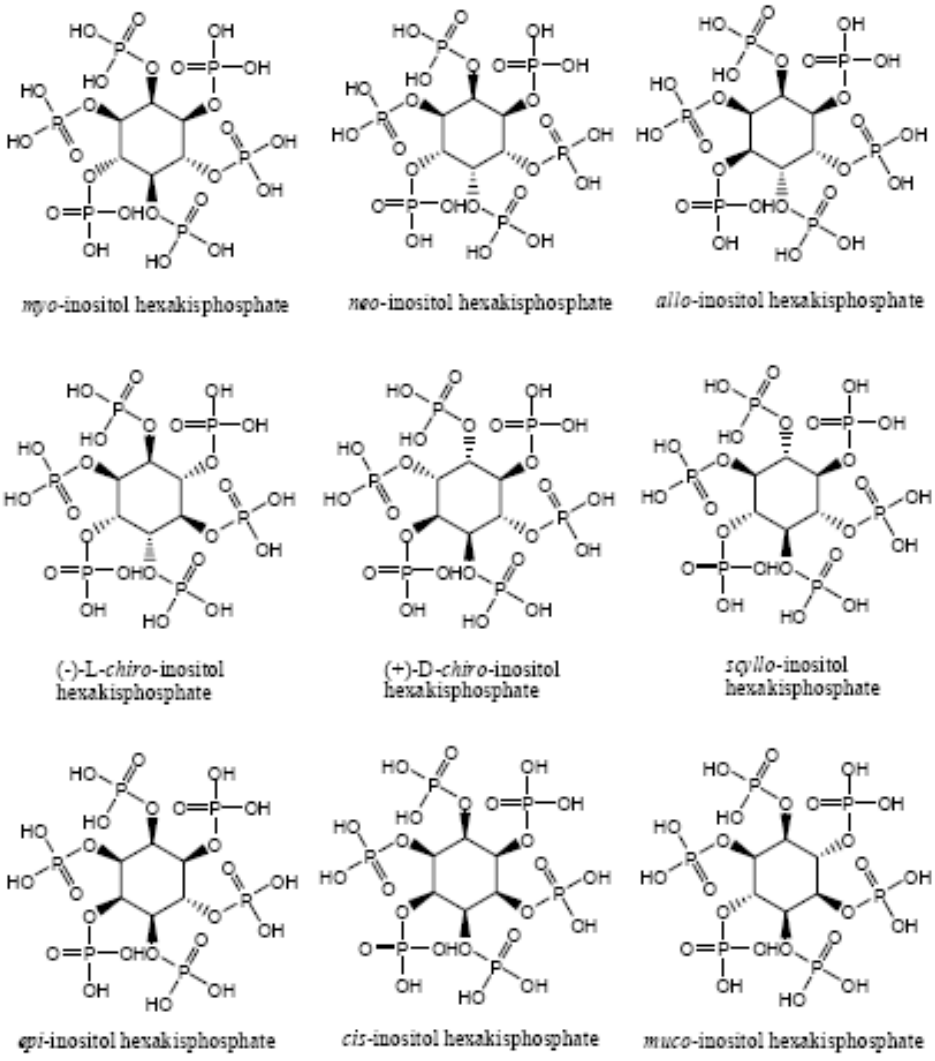

Figure 39. Stereoisomers of inositol hexakisphosphate.

When dosed with inositol, *myo*-$InsP_6$ was found to improve the effect of chemotherapy when given as an adjunct treatment in human colon cancer patients (Druzijanic, Juricic *et al*. 2004). Treatment also improved patients' quality of life by the

diminishing side effects of chemotherapy such as nausea, vomiting, and alopecia. It also prevented the loss of white blood cells and platelets. In addition, *myo*-$InsP_6$ treatment in lung cancer was found to increase the regression rate of dysplastic lesions (Lam, McWilliams *et al*. 2006). Conversely, when used as an adjuvant treatment with chemotherapy for breast cancer, *myo*-$InsP_6$ and inositol was found to have no effect on tumor markers (Bacic, Druzijanic *et al*. 2010). However, the patients' quality of life was markedly improved by treatment with *myo*-$InsP_6$ and inositol.

myo-$InsP_6$ is a chelating agent and due to its attraction for cations such as calcium, magnesium, iron, and zinc it has been historically classified as an anti-nutrient. However it has been shown to have benefits when taken as a dietary supplement where it has been shown to posses activity preventing kidney stone formation in rats (Grases, Garcia-Gonzalez *et al*. 1998) and lowering serum cholesterol in rats (Jariwalla, Sabin *et al*. 1990). In addition there is evidence it serves as a co-factor in DNA repair (Hanakahi, Bartlet-Jones *et al*. 2000) and in yeast it is involved in mRNA export from the nucleus to the cytosol (York, Odom *et al*. 1999).

Isomers of $InsP_6$

While *myo*-InsP6 is ubiquitous, the other stereoisomers of $InsP_6$ are rarely found in nature. *scyllo*-, *neo*-, and D-*chiro*-$InsP_6$ have been isolated from soil (Cosgrove 1980). However, only *neo*- and D-*chiro*-$InsP_6$ have ever been found in an organism. *neo*- and D-*chiro*-$InsP_6$ have been found only in human intestinal amoebae and velvet mesquite leaves, respectively (L'Annunziata and Fuller 1971; Martin, Laussmann et al. 2000). *muco*-$InsP_6$ was also reported as being detected in velvet mesquite leaves but this finding

has been criticized on analytical grounds (L'Annunziata and Fuller 1971; Cosgrove 1980). The remaining four inositol stereoisomers (*allo*, L-*chiro*, *cis*, and *epi*) do not appear to occur in nature in their phosphorylated forms.

CHAPTER 6

MATERIALS AND METHODS

Materials

Phytic acid dodecasodium salt hydrate from rice was obtained from Sigma (St Louis, MO). *muco*-inositol hexakisphosphate (*muco*-$InsP_6$) was a generous gift by Dr. Alan Richardson from the collection of the late Dr. Dennis Cosgrove. There is some uncertainty as to the barium stoichiometry in this *muco*-$InsP_6$ material, and due to the very limited quantity available to us we were unable to carry out any experiments to resolve this uncertainty. The range of *muco*-$InsP_6$ concentrations tested was such that even if the barium stoichiometry in the sample was as low as zero or as high as six, the tested concentrations spanned the range over which $InsP_6$ itself exhibits inhibitory activity.

Preparation of maintenance and multiplication media (1133 and 1250)

Media components and concentrations (1133 and 1250) are listed in Table 1. Both media were prepared by mixing all the reagents with the exception of abscisic acid and glutamine, adjusting the pH to 5.7 with 1N KOH and autoclaving the resulting mixture in the absence (1133) or the presence (1250) of Gelrite using the liquid cycle (highest temperature of 121 °C). Abscisic acid and glutamine were filter-sterilized through a 0.2 μm syringe filter (Pall, East Hills, NY) and then added to the autoclaved media mixture. Two ml of the subsequent media mixture was poured into each well of a 24-well Costar #3526 cluster plate (Corning, Corning, NY).

Table 1. Media ingredients of media 1133 and 1250.

Components	Media and components (mg/l)	
	1133	**1250**
NH_4NO_3	603.8	603.8
KNO_3	909.9	909.9
KH_2PO_4	136.1	136.1
$Ca(NO_3)_2 \bullet 4H_2O$	236.2	236.2
$MgSO_4 \bullet 7H_2O$	246.5	246.5
$Mg(NO_3)_2 \bullet 6H_2O$	256.5	256.5
$MgCl_2 \bullet 6H_2O$	101.7	101.7
KI	4.15	4.15
H_3BO_3	15.5	15.5
$MnSO_4 \bullet H_2O$	10.5	10.5
$ZnSO_4 \bullet 7H_2O$	14.4	14.4
$Na_2MoO_4 \bullet 2H_2O$	0.125	0.125
$CuSO_4 \bullet 5H_2O$	0.125	0.125
$CoCl_2 \bullet 6H_2O$	0.125	0.125
$FeSO_4 \bullet 7H_2O$	6.95	9.95
Na_2EDTA	9.33	9.33
Sucrose	30,000	30,000
Myo-inositol	1,000	1,000
Casamino acids	500	500
L-Glutamineb	450	450
Thiamine _HCl	1	1
Pyridoxine HCl	0.5	0.5
Nicotinic acid	0.5	0.5
Glycine	2	2
MES	–	250
Biotin	–	0.05
Folic acid	–	0.5
2,4-D	1.1	1.1
BAP	0.45	0.45
Kinetin	0.43	0.43
Abscisic acid	1.3	1.3
Gelrite	–	2500
pH	5.7	5.7

Embryogenic Cell Culture Maintenance

Embryogenic cultures were maintained as described in Pullman, Johnson *et al*. (2003). Cultures were stored in 250-ml Erlenmeyer flasks incubated in the dark at 20 to 22°C. Every seven days, the contents of the culture flask were poured into sterile centrifuge tubes and settled by gravity for 20 min. The old liquid media was decanted, settled cell volumes were measured to monitor the cell growth, and cells were resuspended in media 1133 at a density of 1 ml settled cells/9 ml medium (5 ml of settled

cells/45 ml of media 1133). The cultures were rotated at 90-100 rpm and maintained with weekly transfers at the same ratio of cells to medium.

Early-stage somatic embryogenic multiplication bioassay

The staging system illustrated in Figure 40 was used to evaluate morphological development in zygotic and somatic embryos. Somatic embryos at stage 2 were isolated by forceps from suspension culture and placed on 2 mL of multiplication medium 1250 contained in 24-well plates. *myo*- $InsP_6$ and *muco*-$InsP_6$ stock solutions were adjusted to pH 5.7 using MES buffer and sterilized with a 0.2 μm syringe filter. 50 microliters of sterile solution was topically applied to each stage 2 somatic embryos. Embryos were grown in the dark at 23-25 ^{o}C and after four to seven weeks the diameter of the embryogenic tissue was measured with a dissecting microscope using a calibrated eyepiece reticle. Typically a single embryo, approximately 1 mm in size, grows into a mass of multiple embryos about 5-9 mm in diameter depending on culture genotype, medium contents, and time.

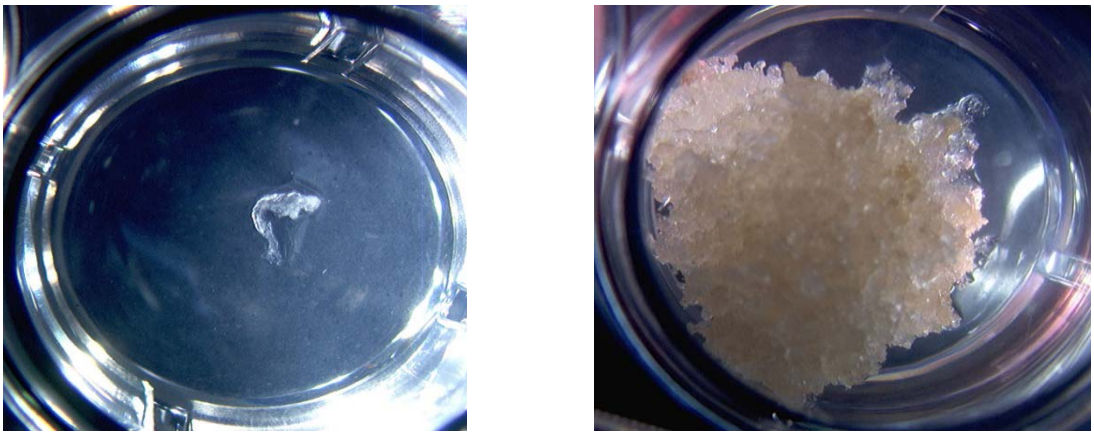

Figure 40. Illustration of early-stage somatic embryo growth bioassay. A single stage 2 embryo is placed in on 2 mL of multiplication medium 1250 contained in 24-well plates. In 4-6 weeks, the single embryo will multiply into a colony of embryos 5-9 mm in diameter.

Statistical analysis

All the data were evaluated by multifactor analysis of variance. The significant differences between means of each treatment were determined by the multiple range test at 95% level of significance. Both analyses were performed using Statgraphics Plus Version 4.0 (Manugistics, Rockville, MD).

CHAPTER 7

RESULTS

In previous work, we have shown that extracts from early-stage FGs stimulate growth and multiplication of early-stage somatic embryos, whereas water extracts from late-stage FGs contain substance(s) inhibitory to early-stage somatic embryo growth (De Silva, Bostwick *et al*. 2008). The early-stage stimulator was isolated and determined to be citric acid on the basis of NMR and mass spectrometry. Topical application of citric acid to LP somatic embryos was found to be stimulatory to early-stage growth. In addition, the amount of citric acid isolated from FGs (65 nmoles per stage 2-3 FG) was found to be in good correlation with the amount of citric acid (25-50 nmoles) that stimulates early-stage embryo growth.

As shown by us, identical exact mass and fragmentation patterns obtained from high resolution exact mass measurement and MS/MS analysis under negative mode clearly identified a purified inhibitor of early-stage LP somatic embryo growth from late-stage FG tissue as one of the isomers of inositol-1,2,3,4,5,6-hexakisphosphate (Wu, Cameron Sullards et al. 2012). The active molecule was then identified as *myo*-inositol hexakisphosphate on the basis of ^{1}H-, ^{31}P- and ^{13}C-NMR, ^{1}H-^{1}H COSY, ^{1}H-^{31}P HSQC and ^{1}H-^{13}C HSQC, when compared to an authentic standard of *myo*-InsP_6.

Concentration dependence of bioactivity on *myo*-InsP_6

Bioassays were carried out to confirm that the *myo*-InsP_6 authentic standard inhibits the early-stage somatic embryo growth. Results for five genotypes (51, 222, 433, 279,

132) tested at none and five concentrations of *myo*-$InsP_6$ are averaged and shown in Figure 41. The *myo*-$InsP_6$ standard at five concentrations was found to inhibit somatic embryo growth in a statistically significant manner. Furthermore, inhibition corresponding to the concentration of *myo*-$InsP_6$ actually isolated from female gametophytes (0.32 μM in the bioassay well) was the most significant. An additional two genotypes were tested at none and 0.32 μM. All seven genotypes tested showed reduced growth in the bioassay with application of $InsP_6$ at 0.32 μM; differences were statistically significant at P = 0.05.

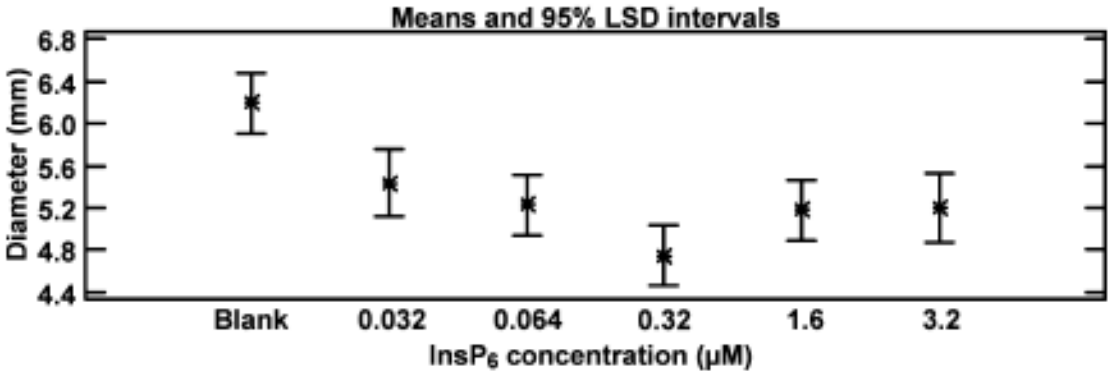

Figure 41. Bioassay results averaged for five genotypes (51, 222, 433, 279, 132) tested at different concentrations of *myo*-$InsP_6$ standard. Means of five genotypes are shown along with 95% least significant difference (LSD) intervals for each concentration of *myo*-$InsP_6$ tested.

muco-IP6 does not inhibit early-stage somatic embryo growth

Bioassays were carried out to test whether or not *muco*-$InsP_6$, a stereoisomer of *myo*-$InsP_6$, also inhibits early-stage embryo growth. Results for one genotype (652) tested at none and six concentrations of *muco*-$InsP_6$ are shown in Table 2. It is evident from the data that *muco*-$InsP_6$ at six concentrations does not inhibit somatic embryo growth.

Table 2. Effect of *muco*-InsP6 on early-stage somatic embryo growth.

muco-$InsP_6$ concentration ($\mu g\ ml^{-1}$)	Diameter (mm)	Calculated *muco*-$InsP_6$ concentration range (μM)[1]
0	6.8 ± 0.3	0
6.7	5.7 ± 0.4	0.023–0.052
41	6.4 ± 0.4	0.14–0.32
50	6.4 ± 0.4	0.17–0.39
67	6.5 ± 0.4	0.23–0.52
92	6.3 ± 0.4	0.32–0.71
670	6.0 ± 0.4	2.3–5.2

Diameter values are followed by their standard error. No treatment was statistically different from any other group, ANOVA $p > 0.05$.

[1] Calculated *muco*-$InsP_6$ molar concentration ranges for barium stoichiometry from zero to six (see 'Materials and Methods' section).

CHAPTER 8

DISCUSSION

Clonal forestry is beset by many challenges. Tree plantations require extensive tracts of land to be dedicated to only growing trees and years of growing time are required before the trees can be harvested. The trees can also be lost to a variety of natural disasters such as fire, disease and storms before they are harvested.

Tree plantations of elite tree genotypes allow rapid growth and harvesting of wood. Other advantages of clonal propagation of trees via SE include the consistent production of the same genotype, the ability to quickly plant new genotypes according to changes in the environment, and the ability to better control the genetic diversity of a tree plantation. However, only 12% of wood consumption comes from genetically modified tree plantations. Most commercial forestry operations utilize wild trees or come from basic seed collections (Gupta, Pullman et al. 1993; Merkle and Dean 2000)

It should be possible to double the biomass harvested of clonally propagated trees compared to a conventional tree plantation (Ragauskas, Williams *et al*. 2006). Among the many advantageous traits that can be introduced into clonally propagated trees include disease and pest resistance, tolerance for drought and cold conditions, increased nitrogen acquisition, a reduction in root systems, and increased cellulose content that is more easily processed.

Currently, somatic embryos of LP do not fully develop. Depending on the specific genotype, varying levels of success in LP SE have been achieved. However, no genotype consistently develops past stage 9.1 (see Figure 38). It is also not uncommon to

face low initiation rates, low culture survival, low maturation rates and low germination, as well as low or no embryo production. To overcome these obstacles it is necessary to further understand the molecular biology of SE and identify signaling molecules that affect SE.

In previous work, we have shown that extracts from early-stage FGs stimulate growth and multiplication of early-stage somatic embryos, whereas water extracts from late-stage FGs contain substance(s) inhibitory to early-stage somatic embryo growth (De Silva, Bostwick *et al*. 2008). The early-stage stimulator was isolated and determined to be citric acid on the basis of NMR and mass spectrometry. Topical application of citric acid to LP somatic embryos was found to be stimulatory to early-stage growth. In addition, the amount of citric acid isolated from FGs (65 nmoles per stage 2-3 FG) was found to be in good correlation with the amount of citric acid (25-50 nmoles) that stimulates early-stage embryo growth.

As shown by us, identical exact mass and fragmentation patterns obtained from high resolution exact mass measurement and MS/MS analysis under negative mode clearly identified a purified inhibitor of early-stage LP somatic embryo growth from late-stage FG tissue as one of the isomers of inositol-1,2,3,4,5,6-hexakisphosphate (Wu, Cameron Sullards et al. 2012). The active molecule was then identified as *myo*-inositol hexakisphosphate on the basis of ^{1}H-, ^{31}P- and ^{13}C-NMR, ^{1}H-^{1}H COSY, ^{1}H-^{31}P HSQC and ^{1}H-^{13}C HSQC, when compared to an authentic standard of *myo*-InsP_6.

myo-InsP6 is ubiquitous and the most abundant inositol phosphate derivative in eukaryotic cells. It is known for its anticancer activity in reducing the proliferation of malignant cells (Shamsuddin, Baten et al. 1992; Shamsuddin, Yang et al. 1995; Ferry,

Matsuda et al. 2002). Additionally, *myo*-InsP6 increases differentiation of malignant cells leading to reversion to the normal phenotype with decreased production of tumor markers (Shamsuddin, Vucenik *et al*. 2005). Some evidence has begun to emerge that *myo*-InsP6 may also function as a signaling molecule in plant cells. Lemtiri-Chlieh *et al*. (2000) reported that the plant stress hormone, abscisic acid, increases *myo*-InsP6 in intact guard cells of *Solanum tuberosum* and that InsP6 inhibits the inward rectifying K^+ current of *S. tuberosum* and *Vicia faba* guard cell protoplasts in a Ca^{2+}-dependent manner. Subsequently (Lemtiri-Chlieh, MacRobbie *et al*. 2003), they showed by laser uncaging of *myo*-InsP6, in *V. faba* guard cell protoplasts loaded with calcium-sensitive dye, that InsP6 causes release of Ca^{2+} from internal stores. It should also be noted that Tan *et al.* (2007) have recently reported that InsP6 is a cofactor in the transport inhibitor response 1 protein that senses and becomes activated by the phytohormone auxin. However, reduction of proliferation in plant cells by *myo*-InsP6 has not been reported to date, and many aspects of the function of *myo*-InsP6 in plants have remained undefined (Turner, Papházy et al. 2002; Raboy 2003). Our findings constitute the first report that InsP6 inhibits cell proliferation in plants.

Is it possible that inhibition of somatic embryo growth in plants by *myo*-InsP6 and *myo*-InsP6's anticancer activity occur via similar mechanisms? In cancer cell lines, *myo*-$InsP_6$ has been found to both suppresses and enhances various signaling pathways, resulting in a reduction in cancer cell proliferation. It enhances protein kinase C δ (PKCδ) activity, and inhibits ERK, p38 MAPK, protein kinase B (PKB) and phosphatidylinositide 3-kinases (PI3K) (Huang, Ma et al. 1997; Vucenik, Ramakrishna et

al. 2005; Gu, Raina et al. 2010). However, plants do not express PKC δ or PKB but they do express ERK, p38 MAPK and PI3K (Munnik and Testerink 2009).

The effect of the inhibition of ERK and p38 MAPK signaling has not been investigated in plant embryos. However, bovine blastocyst formation was blocked when both ERK and p38 MAPK signaling was inhibited (Madan, Calder *et al*. 2005). It has been found that the ERKs are activated during pollen embryogenesis for several plant species (Coronado, González-Melendi *et al*. 2002). In addition, cork oak (*Quercus suber* L.) has been found to display activated ERKs during early proembryo development (Ramírez, Testillano *et al*. 2004). Based on these results it is possible that inhibition of MAPK signaling may contribute to the effect of *myo*-$InsP_6$ on LP early-stage somatic embryo growth.

In JB6 epidermal cells, it has been shown that *myo*-InsP6 inhibits epidermal growth factor-induced phosphatidylinositol-3 kinase (PtdIns 3-kinase), thereby impairing epidermal growth factor- or phorbol ester-induced cell transformation and activator protein 1 activation (Huang, Ma *et al*. 1997). PtdIns 3-kinases are widely distributed in eukaryotic cells, and they are involved in a number of cellular processes, including activation of intracellular signaling molecules such as rac, ras, rab, mitogen-activated protein kinase, protein kinase B⁄Akt(Vanhaesebroeck and Waterfield 1999), protein kinase C and JNK⁄p38 kinase (Leevers, Vanhaesebroeck et al. 1999; Meijer and Munnik 2003; Amin, Mansfield et al. 2007). Turning to plants, PtdIns 3-kinase homologs have been cloned in soybean (Hong and Verma 1994), Arabidopsis thaliana (Welters, Takegawa *et al*. 1994) and Brassica napus ((Das, Hussain *et al*. 2005), and expression of antisense PtdIns 3-kinase AtVPS34 mRNA results in severe inhibition in growth and

development of second-generation transformed plants. Recently, both PtdIns 3-kinase and PtdIns 4-kinase activities have been observed during the induction of somatic embryogenesis in Coffea arabica (Ek-Ramos, Palma *et al*. 2003), and the products of both kinase activities were detected in the somatic-embryo extracts. Moreover, growth of these somatic embryos was inhibited when a kinase inhibitor was included in the induction medium during the first differentiated stage (Ek-Ramos, Palma *et al*. 2003). Taken together, these facts are not inconsistent with the notion that inhibition of PtdIns kinase may be a common feature of *myo*-$InsP_6$'s activity as an inhibitor of somatic embryo growth in plants and as an anticancer agent, but at this point the evidence must be regarded as circumstantial. In this regard, we have carried out a BLAST database search on an expressed sequence tag library of LP somatic embryos (Cairney, Zheng *et al*. 2006), and we have identified one singleton (Gene Bank number DR688191) that shows 83% identity in amino acid sequence to that of PtdIns 3-kinase AtVPS34. Clearly, additional studies will be needed to fully elucidate the mechanisms by which *myo*-InsP6, (and perhaps other inositol phosphates as well) regulate cellular growth and development in plants. Such studies could well lead to significant improvements in the technology of somatic embryogenesis in plants.

muco-$InsP_6$ does not inhibit early-stage somatic embryo growth, demonstrating that inhibition by *myo*-$InsP_6$ is stereospecific. Because *muco*-$InsP_6$ does not inhibit early-stage embryonic growth it is clear that the inhibitory effect of *myo*-InsP6 is not based on a change in media osmolality or due to the addition of a highly charged species to the plant cell media. Little work has been done with *muco*-$InsP_6$ so it is unknown if *muco*-$InsP_6$ inhibits or fails to inhibit any enzymes or has an effect on cancer cell growth.

It would be expected that if inhibition of somatic embryo growth in plants by *myo*-$InsP_6$ and anticancer activity of *myo*-$InsP_6$ occur via similar mechanisms then *muco*-$InsP_6$ would also fail to possess anticancer activity. It is known that *myo*-$InsP_6$ interacts with iron during iron transport through the cytosol or cellular organelles, such that *myo*-$InsP_6$ inhibits hydroxyl radical catalysis by iron (Hawkins, Poyner *et al*. 1993). The 1, 2, 3 (axial-equatorial-axial) phosphate grouping in *myo*-$InsP_6$ is crucial for this activity. *muco*-$InsP_6$ does not have a 1, 2, 3 (axial-equatorial-axial) phosphate grouping which would presumably diminish its ability to interact with iron relative to *myo*-$InsP_6$. $InsP_5$ isomers which lack this phosphate group show diminished iron binding capacity (Hawkins, Poyner *et al*. 1993). If the ability of *myo*-$InsP_6$ to bind iron contributes to the inhibition of somatic embryo growth that property would be absent in experiments using *muco*-InsP6 which would explain the observed stereochemical dependency. It is also possible that the specific stereochemistry of *myo*-$InsP_6$ allows it to act as an enzyme inhibitor while *muco*-$InsP_6$ cannot act as an enzyme inhibitor.

Future studies will further examine the natural products of FGs from stage 9.1. In preliminary work it was found that complete extracts of stage 9.1 FGs stimulated SE germination. Isolation of the natural product(s) responsible for the enhanced germination is possible via separation of the complete stage 9.1 extract by chromatography followed by germination bioassays. The isolated compound(s) can then be identified from NMR and mass spectrometry analysis.

REFERENCES

Abel, K., R. A. Anderson and S. B. Shears (2001). "Phosphatidylinositol and inositol phosphate metabolism." Journal of Cell Science **114**(12): 2207-2208.

Abou-Mohamed, G. A., J. Huang, C. D. Oldham, T. A. Taylor, L. Jin, R. B. Caldwell, S. W. May and R. W. Caldwell (2000). "Vascular and endothelial actions of inhibitors of substance P amidation." J. Cardiovasc. Pharmacol. **35**(6): 871-880.

Ajizian, S. J., B. K. English and E. A. Meals (1999). "Specific Inhibitors of p38 and Extracellular Signal-Regulated Kinase Mitogen-Activated Protein Kinase Pathways Block Inducible Nitric Oxide Synthase and Tumor Necrosis Factor Accumulation in Murine Macrophages Stimulated with Lipopolysaccharide and Interferon-gamma." Journal of Infectious Diseases **179**(4): 939-944.

Amin, M. A., P. J. Mansfield, A. Pakozdi, P. L. Campbell, S. Ahmed, R. J. Martinez and A. E. Koch (2007). "Interleukin-18 induces angiogenic factors in rheumatoid arthritis synovial tissue fibroblasts via distinct signaling pathways." Arthritis Rheum **56**(6): 1787-1797.

Auerbach, R., R. Lewis, B. Shinners, L. Kubai and N. Akhtar (2003). "Angiogenesis assays: a critical overview." Clin Chem **49**(1): 32-40.

Azzolina, A., A. Bongiovanni and N. Lampiasi (2003). "Substance P induces TNF-alpha and IL-6 production through NF kappa B in peritoneal mast cells." Biochim Biophys Acta **1643**(1-3): 75-83.

Azzolina, A., P. Guarneri and N. Lampiasi (2002). "Involvement of p38 and JNK MAPKs pathways in Substance P-induced production of TNF-alpha by peritoneal mast cells." Cytokine **18**(2): 72-80.

Bacic, I., N. Druzijanic, R. Karlo, I. Skific and S. Jagic (2010). "Efficacy of IP6 + inositol in the treatment of breast cancer patients receiving chemotherapy: prospective, randomized, pilot clinical study." Journal of Experimental & Clinical Cancer Research **29**(1): 12.

Baud, V. and M. Karin (2001). "Signal transduction by tumor necrosis factor and its relatives." Trends Cell Biol **11**(9): 372-377.

Bauer, J. D., J. A. Sunman, M. S. Foster, J. R. Thompson, A. A. Ogonowski, S. J. Cutler, S. W. May and S. H. Pollock (2007). "Anti-Inflammatory Effects of 4-Phenyl-3-butenoic Acid and 5-(Acetylamino)-4-oxo-6-phenyl-2-hexenoic Acid Methyl Ester, Potential Inhibitors of Neuropeptide Bioactivation." Journal of Pharmacology and Experimental Therapeutics **320**(3): 1171-1177.

Belton, O., D. Byrne, D. Kearney, A. Leahy and D. J. Fitzgerald (2000). "Cyclooxygenase-1 and -2–Dependent Prostacyclin Formation in Patients With Atherosclerosis." Circulation **102**(8): 840-845.

Beutler, B. (2004). "Inferences, questions and possibilities in Toll-like receptor signalling." Nature **430**(6996): 257-263.

Bradbury, A. F., J. Mistry, B. A. Roos and D. G. Smyth (1990). "4-Phenyl-3-butenoic acid, an in vivo inhibitor of peptidylglycine hydroxylase (peptide amidating enzyme)." Eur J Biochem **189**(2): 363-368.

Brandt, J., H. Haibel, D. Cornely, W. Golder, J. Gonzalez, J. Reddig, W. Thriene, J. Sieper and J. Braun (2000). "Successful treatment of active ankylosing spondylitis with the anti-tumor necrosis factor alpha monoclonal antibody infliximab." Arthritis Rheum. **43**(6): 1346-1352.

Buckley, C. D., D. Pilling, J. M. Lord, A. N. Akbar, D. Scheel-Toellner and M. Salmon (2001). "Fibroblasts regulate the switch from acute resolving to chronic persistent inflammation." Trends in Immunology **22**(4): 199-204.

Bunkoczi, G., E. Salah, P. Filippakopoulos, O. Fedorov, S. Muller, F. Sobott, S. A. Parker, H. Zhang, W. Min, B. E. Turk and S. Knapp (2007). "Structural and functional characterization of the human protein kinase ASK1." Structure **15**(10): 1215-1226.

By, T., D. L. Scott, F. Wolfe and T. W. Huizinga (2010). "The Lancet Seminar: Rheumatoid arthritis." The Lancet **376**(9746): 1094-1108.

Cairney, J. and G. S. Pullman (2007). "The cellular and molecular biology of conifer embryogenesis." New Phytol **176**(3): 511-536.

Cairney, J., L. Zheng, A. Cowels, J. Hsiao, V. Zismann, J. Liu, S. Ouyang, F. Thibaud-Nissen, J. Hamilton, K. Childs, G. S. Pullman, Y. Zhang, T. Oh and C. R. Buell (2006). "Expressed sequence tags from loblolly pine embryos reveal similarities with angiosperm embryogenesis." Plant Mol Biol **62**(4-5): 485-501.

Carter, M. S. and J. E. Krause (1990). "Structure, expression, and some regulatory mechanisms of the rat preprotachykinin gene encoding substance P, neurokinin A, neuropeptide K, and neuropeptide gamma." J Neurosci **10**(7): 2203-2214.

Challa, A., D. R. Rao and B. S. Reddy (1997). "Interactive suppression of aberrant crypt foci induced by azoxymethane in rat colon by phytic acid and green tea." Carcinogenesis **18**(10): 2023-2026.

Chang, M. M., S. E. Leeman and H. D. Niall (1971). "Amino-acid sequence of substance P." Nat New Biol **232**(29): 86-87.

Cheng, Y. J., G. Imperatore, C. J. Caspersen, E. W. Gregg, A. L. Albright and C. G. Helmick (2012). "Prevalence of diagnosed arthritis and arthritis-attributable activity limitation among adults with and without diagnosed diabetes: United States, 2008-2010." Diabetes Care **35**(8): 1686-1691.

Cohen, S. and R. Fleischmann (2010). "Kinase inhibitors: a new approach to rheumatoid arthritis treatment." Curr. Opin. Rheumatol. **22**(3): 330-335.

Coronado, M. J., P. González-Melendi, J. M. Seguí, C. Ramírez, I. Bárány, P. S. Testillano and M. C. Risueño (2002). "MAPKs entry into the nucleus at specific interchromatin domains in plant differentiation and proliferation processes." Journal of Structural Biology **140**(1–3): 200-213.

Cosgrove, D. (1980). Inositol Phosphates: Their Chemistry, Biochemistry and Physiology. Amsterdam, Elsevier Scientific.

Das, S., A. Hussain, C. Bock, W. A. Keller and F. Georges (2005). "Cloning of Brassica napus phospholipase C2 (BnPLC2), phosphatidylinositol 3-kinase (BnVPS34) and phosphatidylinositol synthase1 (BnPtdIns S1)--comparative analysis of the effect of abiotic stresses on the expression of phosphatidylinositol signal transduction-related genes in B. napus." Planta **220**(5): 777-784.

De Broe, M. E. and M. M. Elseviers (1998). "Analgesic Nephropathy." New England Journal of Medicine **338**(7): 446-452.

De Silva, V., D. Bostwick, K. L. Burns, C. D. Oldham, A. Skryabina, M. C. Sullards, D. Wu, Y. Zhang, S. W. May and G. S. Pullman (2008). "Isolation and characterization of a molecule stimulatory to growth of somatic embryos from early stage female gametophyte tissue of loblolly pine." Plant Cell Rep **27**(4): 633-646.

Dérijard, B., M. Hibi, I. H. Wu, T. Barrett, B. Su, T. Deng, M. Karin and R. J. Davis (1994). "JNK1: a protein kinase stimulated by UV light and Ha-Ras that binds and phosphorylates the c-Jun activation domain." Cell **76**(6): 1025.

Derkx, B., J. Taminiau, S. Radema, A. Stronkhorst, C. Wortel, G. Tytgat and S. van Deventer (1993). "Tumour-necrosis-factor antibody treatment in Crohn's disease." The Lancet **342**(8864): 173-174.

Dixon, W., K. Hyrich, K. Watson, M. Lunt, J. Galloway, A. Ustianowski and D. Symmons (2010). "Drug-specific risk of tuberculosis in patients with rheumatoid arthritis treated with anti-TNF therapy: results from the British Society for Rheumatology Biologics Register (BSRBR)." Annals of the rheumatic diseases **69**(3): 522-528.

Dong, C. (2002). "MAP kinases in the immune response." Annu. Rev. Immunol. **20**: 55.

Donnerer, J., R. Schuligoi and C. Stein (1992). "Increased content and transport of substance P and calcitonin gene-related peptide in sensory nerves innervating inflamed tissue: evidence for a regulatory function of nerve growth factor in vivo." Neuroscience **49**(3): 693-698.

Druzijanic, N., J. Juricic, Z. Perko and D. Kraljevic (2004). IP6+ Inositol as adjuvant to chemotherapy of colon cancer: our clinical experience. Anticancer Research, INT INST ANTICANCER RESEARCH EDITORIAL OFFICE 1ST KM KAPANDRITIOU-KALAMOU RD KAPANDRITI, PO BOX 22, ATHENS 19014, GREECE.

Eipper, B. A., A. C. Myers and R. E. Mains (1985). "Peptidyl-glycine alpha-amidation activity in tissues and serum of the adult rat." Endocrinology **116**(6): 2497-2504.

Ek-Ramos, M. J., R. D. Palma and S. Hernández‐Sotomayor (2003). "Changes in phosphatidylinositol and phosphatidylinositol monophosphate kinase activities during the induction of somatic embryogenesis in Coffea arabica." Physiologia Plantarum **119**(2): 270-277.

Fearon, D. T. and R. M. Locksley (1996). "The Instructive Role of Innate Immunity in the Acquired Immune Response." Science **272**(5258): 50-54.

Feng, J., J. Shi, S. R. Sirimanne, C. E. Mounier-Lee and S. W. May (2000). "Kinetic and stereochemical studies on novel inactivators of C-terminal amidation." Biochem J **350 Pt 2**: 521-530.

Ferry, S., M. Matsuda, H. Yoshida and M. Hirata (2002). "Inositol hexakisphosphate blocks tumor cell growth by activating apoptotic machinery as well as by inhibiting the Akt/NFkappaB-mediated cell survival pathway." Carcinogenesis **23**(12): 2031-2041.

Fleischmann, R., J. Kremer, J. Cush, H. Schulze-Koops, C. A. Connell, J. D. Bradley, D. Gruben, G. V. Wallenstein, S. H. Zwillich and K. S. Kanik (2012). "Placebo-controlled trial of tofacitinib monotherapy in rheumatoid arthritis." The New England Journal Of Medicine **367**(6): 495-507.

Garber, K. (2011). "Pfizer's JAK inhibitor sails through phase 3 in rheumatoid arthritis." Nat. Biotechnol. **29**(6): 467-468.

Geppert, T. D., C. E. Whitehurst, P. Thompson and B. Beutler (1994). "Lipopolysaccharide signals activation of tumor necrosis factor biosynthesis through the ras/raf-1/MEK/MAPK pathway." Mol Med **1**(1): 93-103.

Gilligan, J. P., S. J. Lovato, M. D. Erion and A. Y. Jeng (1994). "Modulation of carrageenan-induced hind paw edema by substance P." Inflammation **18**(3): 285-292.

Goldberg, R. B., G. de Paiva and R. Yadegari (1994). "Plant embryogenesis: zygote to seed." Science **266**(5185): 605-614.

Grases, F., R. Garcia-Gonzalez, J. J. Torres and A. Llobera (1998). "Effects of phytic acid on renal stone formation in rats." Scand J Urol Nephrol **32**(4): 261-265.

Greaves, M. W. and R. A. Sabroe (1996). "Histamine: the quintessential mediator." J Dermatol **23**(11): 735-740.

Grosser, T., S. Fries and G. A. FitzGerald (2006). "Biological basis for the cardiovascular consequences of COX-2 inhibition: therapeutic challenges and opportunities." The Journal of Clinical Investigation **116**(1): 4-15.

Gu, M., K. Raina, C. Agarwal and R. Agarwal (2010). "Inositol hexaphosphate downregulates both constitutive and ligand‐induced mitogenic and cell survival signaling, and causes caspase‐mediated apoptotic death of human prostate carcinoma PC‐3 cells." Molecular carcinogenesis **49**(1): 1-12.

Gupta, K. P., J. Singh and R. Bharathi (2003). "Suppression of DMBA-induced mouse skin tumor development by inositol hexaphosphate and its mode of action." Nutr Cancer **46**(1): 66-72.

Gupta, P. K., G. Pullman, R. Timmis, M. Kreitinger, W. C. Carlson, J. Grob and E. Welty (1993). "Forestry in the 21st century: the biotechnology of somatic embryogenesis." Bio/technology **11**.

Hanakahi, L. A., M. Bartlet-Jones, C. Chappell, D. Pappin and S. C. West (2000). "Binding of inositol phosphate to DNA-PK and stimulation of double-strand break repair." Cell **102**(6): 721-729.

Hawkins, P. T., D. R. Poyner, T. R. Jackson, A. J. Letcher, D. A. Lander and R. F. Irvine (1993). "Inhibition of iron-catalysed hydroxyl radical formation by inositol polyphosphates: a possible physiological function for myo-inositol hexakisphosphate." Biochem. J **294**: 929-934.

Hayden, M. S. and S. Ghosh (2012). "NF-kappaB, the first quarter-century: remarkable progress and outstanding questions." Genes Dev **26**(3): 203-234.

Hong, Z. and D. P. Verma (1994). "A phosphatidylinositol 3-kinase is induced during soybean nodule organogenesis and is associated with membrane proliferation." Proc Natl Acad Sci U S A **91**(20): 9617-9621.

Hsieh, C., S. Macatonia, C. Tripp, S. Wolf, A. O'Garra and K. Murphy (1993). "Development of TH1 CD4+ T cells through IL-12 produced by Listeria-induced macrophages." Science **260**(5107): 547-549.

Huang, C., W.-Y. Ma, S. S. Hecht and Z. Dong (1997). "Inositol hexaphosphate inhibits cell transformation and activator protein 1 activation by targeting phosphatidylinositol-3′ kinase." Cancer research **57**(14): 2873-2878.

Jariwalla, R., R. Sabin, S. Lawson and Z. Herman (1990). "Lowering of serum cholesterol and triglycerides and modulation of divalent cations by dietary phytate." Journal of Applied Nutrition **42**(1): 18-28.

Johnson, G. L. and R. Lapadat (2002). "Mitogen-Activated Protein Kinase Pathways Mediated by ERK, JNK, and p38 Protein Kinases." Science **298**(5600): 1911-1912.

Johnston, A., J. E. Gudjonsson, H. Sigmundsdottir, B. Runar Ludviksson and H. Valdimarsson (2005). "The anti-inflammatory action of methotrexate is not mediated by lymphocyte apoptosis, but by the suppression of activation and adhesion molecules." Clinical Immunology **114**(2): 154-163.

Kangawa, K., N. Minamino, A. Fukuda and H. Matsuo (1983). "Neuromedin K: a novel mammalian tachykinin identified in porcine spinal cord." Biochem Biophys Res Commun **114**(2): 533-540.

Kar, S., S. J. Gibson, R. G. Rees, W. G. Jura, D. A. Brewerton and J. M. Polak (1991). "Increased calcitonin gene-related peptide (CGRP), substance P, and enkephalin immunoreactivities in dorsal spinal cord and loss of CGRP-immunoreactive motoneurons in arthritic rats depend on intact peripheral nerve supply." J Mol Neurosci **3**(1): 7-18.

Katopodis, A. G. and S. W. May (1990). "Novel substrates and inhibitors of peptidylglycine alpha-amidating monooxygenase." Biochemistry **29**(19): 4541-4548.

Katopodis, A. G., D. Ping and S. W. May (1990). "A novel enzyme from bovine neurointermediate pituitary catalyzes dealkylation of α-hydroxyglycine derivatives, thereby functioning sequentially with peptidylglycine α-amidating monooxygenase in peptide amidation." Biochemistry **29**(26): 6115-6120.

Katopodis, A. G., D. Ping, C. E. Smith and S. W. May (1991). "Functional and structural characterization of peptidylamidoglycolate lyase, the enzyme catalyzing the second step in peptide amidation." Biochemistry **30**(25): 6189-6194.

L'Annunziata, M. F. and W. H. Fuller (1971). "Soil and Plant Relationships of Inositol Phosphate Stereoisomers; the Identification of D-Chiro- and Muco-Inositol Phosphates in a Desert Soil and Plant System1." Soil Sci. Soc. Am. J. **35**(4): 587-595.

Lam, S., A. McWilliams, J. LeRiche, C. MacAulay, L. Wattenberg and E. Szabo (2006). "A phase I study of myo-inositol for lung cancer chemoprevention." Cancer Epidemiol Biomarkers Prev **15**(8): 1526-1531.

Leask, A., A. Holmes and D. J. Abraham (2002). "Connective tissue growth factor: a new and important player in the pathogenesis of fibrosis." Curr Rheumatol Rep **4**(2): 136-142.

Lee, H. R., W. Z. Ho and S. D. Douglas (1994). "Substance P augments tumor necrosis factor release in human monocyte-derived macrophages." Clin Diagn Lab Immunol **1**(4): 419-423.

Lee, J. C., J. T. Laydon, P. C. McDonnell, T. F. Gallagher, S. Kumar, D. Green, D. McNulty, M. J. Blumenthal, J. R. Keys, S. W. Land vatter, J. E. Strickler, M. M. McLaughlin, I. R. Siemens, S. M. Fisher, G. P. Livi, J. R. White, J. L. Adams and P. R. Young (1994). "A protein kinase involved in the regulation of inflammatory cytokine biosynthesis." Nature **372**(6508): 739-746.

Lee, S., S. C. Yang, M. J. Heffernan, W. R. Taylor and N. Murthy (2007). "Polyketal microparticles: a new delivery vehicle for superoxide dismutase." Bioconjug Chem **18**(1): 4-7.

Leevers, S. J., B. Vanhaesebroeck and M. D. Waterfield (1999). "Signalling through phosphoinositide 3-kinases: the lipids take centre stage." Current opinion in cell biology **11**(2): 219-225.

Lemtiri-Chlieh, F., E. A. MacRobbie and C. A. Brearley (2000). "Inositol hexakisphosphate is a physiological signal regulating the K+-inward rectifying conductance in guard cells." Proc Natl Acad Sci U S A **97**(15): 8687-8692.

Lemtiri-Chlieh, F., E. A. C. MacRobbie, A. A. R. Webb, N. F. Manison, C. Brownlee, J. N. Skepper, J. Chen, G. D. Prestwich and C. A. Brearley (2003). "Inositol hexakisphosphate mobilizes an endomembrane store of calcium in guard cells." Proceedings of the National Academy of Sciences **100**(17): 10091-10095.

Lieb, K., B. L. Fiebich, M. Berger, J. Bauer and K. Schultz-Osthoff (1997). "The neuropeptide substance P activates transcription factor NF-κB and κB-dependent gene expression in human astrocytoma cells." J. Immunol. **159**(10): 4952-4958.

Liles, W. C. and W. C. Van Voorhis (1995). "Review: nomenclature and biologic significance of cytokines involved in inflammation and the host immune response." J Infect Dis **172**(6): 1573-1580.

Macatonia, S. E., C.-S. Hsieh, K. M. Murphy and A. O'Garra (1993). "Dendritic cells and macrophages are required for Th1 development of CD4+ T cells from αβ TCR transgenic mice: IL-12 substitution for macrophages to stimulate IFN-γ production is IFN-γ-dependent." International Immunology **5**(9): 1119-1128.

Madan, P., M. D. Calder and A. J. Watson (2005). "Mitogen-activated protein kinase (MAPK) blockade of bovine preimplantation embryogenesis requires inhibition of both

p38 and extracellular signal-regulated kinase (ERK) pathways." Reproduction **130**(1): 41-51.

Maini, R. N., M. J. Elliott, E. M. Brennan, R. O. Williams, C. Q. Chu, E. W. A. Paleolog, P. J. Charles, P. C. Taylor and M. Feldmann (1995). "Monoclonal anti-TNFα Antibody as a Probe of Pathogenesis and Therapy of Rheumatoid Disease." Immunological Reviews **144**(1): 195-223.

Marnett, L. J., S. W. Rowlinson, D. C. Goodwin, A. S. Kalgutkar and C. A. Lanzo (1999). "Arachidonic Acid Oxygenation by COX-1 and COX-2: MECHANISMS OF CATALYSIS AND INHIBITION." Journal of Biological Chemistry **274**(33): 22903-22906.

Martin, J. B., T. Laussmann, T. Bakker-Grunwald, G. Vogel and G. Klein (2000). "neo-inositol polyphosphates in the amoeba Entamoeba histolytica." J Biol Chem **275**(14): 10134-10140.

Matesic, D. F., T. S. Sidorova, T. J. Burns, A. M. Bell, P. L. Tran, R. J. Ruch and S. W. May (2011). "p38 MAPK activation, JNK inhibition, neoplastic growth inhibition, and increased gap junction communication in human lung carcinoma and Ras-transformed cells by 4-phenyl-3-butenoic acid." J Cell Biochem **113**(1): 269-281.

Meggio, F., A. D. Deana, M. Ruzzene, A. M. Brunati, L. Cesaro, B. Guerra, T. Meyer, H. Mett, D. Fabbro and P. Furet (1995). "Different susceptibility of protein kinases to staurosporine inhibition." European Journal of Biochemistry **234**(1): 317-322.

Meijer, H. J. and T. Munnik (2003). "Phospholipid-based signaling in plants." Annual Review of Plant Biology **54**(1): 265-306.

Merkle, S. A. and J. F. Dean (2000). "Forest tree biotechnology." Current Opinion in Biotechnology **11**(3): 298-302.

Munnik, T. and C. Testerink (2009). "Plant phospholipid signaling:“in a nutshell”." Journal of lipid research **50**(Supplement): S260-S265.

Nawa, H., H. Kotani and S. Nakanishi (1984). "Tissue-specific generation of two preprotachykinin mRNAs from one gene by alternative RNA splicing." Nature **312**(5996): 729-734.

Nosaka, T., J. M. Van Deursen, R. A. Tripp, W. E. Thierfelder, B. A. Witthuhn, A. P. McMickle, P. C. Doherty, G. C. Grosveld and J. N. Ihle (1995). "Defective lymphoid development in mice lacking Jak3." SCIENCE-NEW YORK THEN WASHINGTON-: 800-800.

O'Connor, T. M., J. O'Connell, D. I. O'Brien, T. Goode, C. P. Bredin and F. Shanahan (2004). "The role of substance P in inflammatory disease." J Cell Physiol **201**(2): 167-180.

Ogonowski, A. A., S. W. May, A. B. Moore, L. T. Barrett, C. L. O'Bryant and S. H. Pollock (1997). "Antiinflammatory and Analgesic Activity of an Inhibitor of Neuropeptide Amidation." Journal of Pharmacology and Experimental Therapeutics **280**(2): 846-853.

Oldham, C. D., C. Li, J. Feng, R. O. Scott, W. Z. Wang, A. B. Moore, P. R. Girard, J. Huang, R. B. Caldwell, R. W. Caldwell and S. W. May (1997). "Amidative peptide processing and vascular function." Am J Physiol **273**(6 Pt 1): C1908-1914.

Owens, J. (2006). The Reproductive Biology of the Lodgepole Pine.
Page, N. M., N. J. Bell, S. M. Gardiner, I. T. Manyonda, K. J. Brayley, P. G. Strange and

P. J. Lowry (2003). "Characterization of the endokinins: Human tachykinins with cardiovascular activity." Proceedings of the National Academy of Sciences **100**(10): 6245-6250.

Parganas, E., D. Wang, D. Stravopodis, D. J. Topham, J.-C. Marine, S. Teglund, E. F. Vanin, S. Bodner, O. R. Colamonici, J. M. van Deursen, G. Grosveld and J. N. Ihle (1998). "Jak2 Is Essential for Signaling through a Variety of Cytokine Receptors." Cell **93**(3): 385-395.

Patrignani, P., M. G. Sciulli, S. Manarini, G. Santini, C. Cerletti and V. Evangelista (1999). "COX-2 is not involved in thromboxane biosynthesis by activated human platelets." J Physiol Pharmacol **50**(4): 661-667.

Pennefather, J. N., A. Lecci, M. L. Candenas, E. Patak, F. M. Pinto and C. A. Maggi (2004). "Tachykinins and tachykinin receptors: a growing family." Life Sciences **74**(12): 1445-1463.

Pocrnich, C. E., H. Liu, M. Feng, T. Peng, Q. Feng and C. M. Hutnik (2009). "p38 mitogen-activated protein kinase protects human retinal pigment epithelial cells exposed to oxidative stress." Can J Ophthalmol **44**(4): 431-436.

Prigge, S. T., R. E. Mains, B. A. Eipper and L. M. Amzel (2000). "New insights into copper monooxygenases and peptide amidation: structure, mechanism and function." Cell Mol Life Sci **57**(8-9): 1236-1259.

Pullman, G. S., S. Johnson, G. Peter, J. Cairney and N. Xu (2003). "Improving loblolly pine somatic embryo maturation: comparison of somatic and zygotic embryo morphology, germination, and gene expression." Plant Cell Reports **21**(8): 747-758.

Pullman, G. S. a. W. (1994). An Embryo Staging System for Comparison of Zygotic and Somatic Embryo Development. TAPPI R&D Division Biological Sciences. Minneapolis, MN: Technical Association of the Pulp and Paper Industry Press.

Quintás-Cardama, A., K. Vaddi, P. Liu, T. Manshouri, J. Li, P. A. Scherle, E. Caulder, X. Wen, Y. Li, P. Waeltz, M. Rupar, T. Burn, Y. Lo, J. Kelley, M. Covington, S. Shepard, J. D. Rodgers, P. Haley, H. Kantarjian, J. S. Fridman and S. Verstovsek (2010). "Preclinical characterization of the selective JAK1/2 inhibitor INCB018424: therapeutic implications for the treatment of myeloproliferative neoplasms." Blood **115**(15): 3109-3117.

Raboy, V. (2003). "myo-Inositol-1,2,3,4,5,6-hexakisphosphate." Phytochemistry **64**(6): 1033-1043.

Ragauskas, A. J., C. K. Williams, B. H. Davison, G. Britovsek, J. Cairney, C. A. Eckert, W. J. Frederick, J. P. Hallett, D. J. Leak and C. L. Liotta (2006). "The path forward for biofuels and biomaterials." science **311**(5760): 484-489.

Raingeaud, J., S. Gupta, J. S. Rogers, M. Dickens, J. Han, R. J. Ulevitch and R. J. Davis (1995). "Pro-inflammatory cytokines and environmental stress cause p38 mitogen-activated protein kinase activation by dual phosphorylation on tyrosine and threonine." Journal of Biological Chemistry **270**(13): 7420-7426.

Raman, M., W. Chen and M. H. Cobb (2007). "Differential regulation and properties of MAPKs." Oncogene **26**(22): 3100-3112.

Ramírez, C., P. S. Testillano, B. Pintos, M. A. Moreno-Risueño, M. A. Bueno and M. C. Risueño (2004). "Changes in pectins and MAPKs related to cell development during early microspore embryogenesis in Quercus suber L." European Journal of Cell Biology **83**(5): 213-225.

Rath, T., O. Sander and A. Rubbert (2011). "Conventional disease-modifying antirheumatic drugs to treat rheumatoid arthritis." Drug Development Research **72**(8): 657-663.

Rawlings, J. S., K. M. Rosler and D. A. Harrison (2004). "The JAK/STAT signaling pathway." Journal of Cell Science **117**(8): 1281-1283.

Reiser, L. and R. L. Fischer (1993). "The Ovule and the Embryo Sac." The Plant Cell Online **5**(10): 1291-1301.

Rodig, S. J., M. A. Meraz, J. M. White, P. A. Lampe, J. K. Riley, C. D. Arthur, K. L. King, K. C. F. Sheehan, L. Yin, D. Pennica, E. M. Johnson Jr and R. D. Schreiber (1998). "Disruption of the Jak1 Gene Demonstrates Obligatory and Nonredundant Roles of the Jaks in Cytokine-Induced Biologic Responses." Cell **93**(3): 373-383.

Sakamoto, K., G. Venkatraman and A. M. Shamsuddin (1993). "Growth inhibition and differentiation of HT-29 cells in vitro by inositol hexaphosphate (phytic acid)." Carcinogenesis **14**(9): 1815-1819.

Schultz, R. (1999). "Loblolly -- the pine for the twenty-first century." New Forests **17**(1-3): 71-88.

Serhan, C. N., N. Chiang and T. E. Van Dyke (2008). "Resolving inflammation: dual anti-inflammatory and pro-resolution lipid mediators." Nat Rev Immunol **8**(5): 349-361.

Shacter, E. and S. A. Weitzman (2002). "Chronic inflammation and cancer." Oncology (Williston Park) **16**(2): 217-226, 229; discussion 230-212.

Shamsuddin, A., I. Vucenik and K. Cole (2005). "IP6: a novel anti-cancer agent." Life Sci **61**: 343 - 554.

Shamsuddin, A., G.-Y. Yang and I. Vucenik (1995). "Novel anti-cancer functions of IP6: growth inhibition and differentiation of human mammary cancer cell lines in vitro." Anticancer Res **16**: 3287 - 1996.

Shamsuddin, A. M., A. Baten and N. D. Lalwani (1992). "Effects of inositol hexaphosphate on growth and differentiation in K-562 erythroleukemia cell line." Cancer letters **64**(3): 195-202.

Singh, G. and G. Triadafilopoulos (1999). "Epidemiology of NSAID induced gastrointestinal complications." The Journal of rheumatology. Supplement **56**: 18.

Singh, R. P., C. Agarwal and R. Agarwal (2003). "Inositol hexaphosphate inhibits growth, and induces G1 arrest and apoptotic death of prostate carcinoma DU145 cells: modulation of CDKI-CDK-cyclin and pRb-related protein-E2F complexes." Carcinogenesis **24**(3): 555-563.

Sun, J., R. D. Ramnath, L. Zhi, R. Tamizhselvi and M. Bhatia (2008). "Substance P enhances NF-κB transactivation and chemokine response in murine macrophages via ERK1/2 and p38 MAPK signaling pathways." Am. J. Physiol. **294**(6, Pt. 1): C1586-C1596.

Sunman, J. A. (2003). Inhibitors of neuropeptide synthesis: pharmacological effects and mechanisms in inflammation and tumorigenic cells. Copyright (C) 2013 American Chemical Society (ACS). All Rights Reserved.

Swantek, J. L., M. H. Cobb and T. D. Geppert (1997). "Jun N-terminal kinase/stress-activated protein kinase (JNK/SAPK) is required for lipopolysaccharide stimulation of tumor necrosis factor alpha (TNF-alpha) translation: glucocorticoids inhibit TNF-alpha translation by blocking JNK/SAPK." Mol Cell Biol **17**(11): 6274-6282.

Szekanecz, Z., M. M. Halloran, M. V. Volin, J. M. Woods, R. M. Strieter, G. Kenneth Haines, 3rd, S. L. Kunkel, M. D. Burdick and A. E. Koch (2000). "Temporal expression of inflammatory cytokines and chemokines in rat adjuvant-induced arthritis." Arthritis Rheum **43**(6): 1266-1277.

Tan, X., L. I. Calderon-Villalobos, M. Sharon, C. Zheng, C. V. Robinson, M. Estelle and N. Zheng (2007). "Mechanism of auxin perception by the TIR1 ubiquitin ligase." Nature **446**(7136): 640-645.

Tatemoto, K., J. M. Lundberg, H. Jornvall and V. Mutt (1985). "Neuropeptide K: isolation, structure and biological activities of a novel brain tachykinin." Biochem Biophys Res Commun **128**(2): 947-953.

Terao, Y., H. Suzuki, M. Yoshikawa, H. Yashiro, S. Takekawa, Y. Fujitani, K. Okada, Y. Inoue, Y. Yamamoto and H. Nakagawa (2012). "Design and biological evaluation of imidazo [1, 2-*a*] pyridines as novel and potent ASK1 inhibitors." Bioorganic & medicinal chemistry letters.

Trott, O. and A. J. Olson (2010). "AutoDock Vina: Improving the speed and accuracy of docking with a new scoring function, efficient optimization, and multithreading." Journal of Computational Chemistry **31**(2): 455-461.

Turner, B. L., M. J. Papházy, P. M. Haygarth and I. D. Mckelvie (2002). "Inositol phosphates in the environment." Philosophical Transactions of the Royal Society of London. Series B: Biological Sciences **357**(1420): 449-469.

Van, E. W. (1990). "Heat-shock proteins in autoimmune arthritis: a critical contribution based on the adjuvant arthritis model." APMIS **98**(5): 383-394.

Vanhaesebroeck, B. and M. D. Waterfield (1999). "Signaling by distinct classes of phosphoinositide 3-kinases." Exp Cell Res **253**(1): 239-254.

Vucenik, I., G. Ramakrishna, K. Tantivejkul, L. M. Anderson and D. Ramljak (2005). "Inositol hexaphosphate (IP6) blocks proliferation of human breast cancer cells through a PKCδ-dependent increase in p27Kip1 and decrease in retinoblastoma protein (pRb) phosphorylation." Breast cancer research and treatment **91**(1): 35-45.

Waksman, B. H. (2002). "Immune regulation in adjuvant disease and other arthritis models: relevance to pathogenesis of chronic arthritis." Scand J Immunol **56**(1): 12-34.

Wattenberg, L. (1995). "Chalcones, myo-inositol and other novel inhibitors of pulmonary carcinogenesis." J Cell Biochem Suppl **22**: 162-168.

Welters, P., K. Takegawa, S. D. Emr and M. J. Chrispeels (1994). "AtVPS34, a phosphatidylinositol 3-kinase of Arabidopsis thaliana, is an essential protein with

homology to a calcium-dependent lipid binding domain." Proceedings of the National Academy of Sciences **91**(24): 11398-11402.

Wu, D., M. Cameron Sullards, C. D. Oldham, L. Gelbaum, J. Lucrezi, G. S. Pullman and S. W. May (2012). "Myo‐inositol hexakisphosphate, isolated from female gametophyte tissue of loblolly pine, inhibits growth of early‐stage somatic embryos." New Phytologist **193**(2): 313-326.

York, J. D., A. R. Odom, R. Murphy, E. B. Ives and S. R. Wente (1999). "A Phospholipase C-Dependent Inositol Polyphosphate Kinase Pathway Required for Efficient Messenger RNA Export." Science **285**(5424): 96-100.

Yun, H. Y., R. C. Johnson, R. E. Mains and B. A. Eipper (1993). "Topological switching of the COOH-terminal domain of peptidylglycine alpha-amidating monooxygenase by alternative RNA splicing." Arch Biochem Biophys **301**(1): 77-84.

Zhang, Y., L. Lu, C. Furlonger, G. E. Wu and C. J. Paige (2000). "Hemokinin is a hematopoietic-specific tachykinin that regulates B lymphopoiesis." Nat Immunol **1**(5): 392-397.